

**CHARACTERIZATION, MODELING AND MAPPING
OF CANAL SEEPAGE
FROM GROUND WATER ELEVATION RESPONSES**

by

Cephas B. Holder

A thesis submitted in partial fulfillment
of the requirements for the degree of
Master of Science in Geographic Information Science
in the Department of Geosciences
Idaho State University

May 2009

Photocopy and Use Authorization

In presenting this thesis in partial fulfillment of the requirements for an advanced degree at Idaho State University, I agree that the Library shall make it freely available for inspection. I further state that permission for extensive copying of my thesis for scholarly purposes may be granted by the Dean of the Graduate School, Dean of my academic division, or by the University Librarian. It is understood that any copying or publication of this thesis for financial gain shall not be allowed without my written permission.

Signature _____

Date _____

Committee Approval

To the Graduate Faculty:

The members of the committee appointed to examine the thesis of CEPHAS B. HOLDER find it satisfactory and recommend that it be accepted.

Major Advisor _____

Dr. John A. Welhan

Committee Member _____

Dr. Daniel P. Ames

Committee Member _____

(Non-voting)

Mr. Steven T. Howser

Graduate Faculty Representative _____

Dr. Chikashi Sato

Acknowledgements

I would like to thank Steve Howser who was instrumental in introducing me to the historical well data and initiating the idea of trying to make use of this data, and for his support and encouragement throughout the study. I would like to thank the Board of Directors of the Aberdeen-Springfield Canal Company (ASCC) for their support of the study. Also I deeply appreciate the help of the ASCC staff for their willing support in familiarizing me with the system and their timely assistance and rescues when needed.

Next, I would like to thank the members of my advisory committee for their insights and guidance in completing this project. Special thanks to John Welhan and Steve Howser for their knowledge of statistics and the study area. Here I must also thank the various professors, staff, students and others around the ISU campus for their encouragement and well wishes.

Finally, I would like to thank the members of my Globally Positioned Siblings and other numerous family members of the Greatly Interesting Society for their support and for being the orientation in space and time for my life's purposes. In closing I would like to reintroduce the oldest and yet most current applications of GPS and GIS which tells us where we've been, where we are, where we're headed and how to fine tune our direction on that journey. In those acronyms G stands for God.

Thanks again to all who helped!

TABLE OF CONTENTS

Photocopy and Use Authorization	i
Title Page	ii
Committee Approval.....	iii
Acknowledgements.....	iv
TABLE OF CONTENTS.....	v
LIST OF FIGURES	viii
LIST OF TABLES	xi
Abstract.....	xii
Dedication.....	xiii
Chapter 1 INTRODUCTION	1
1.1. Background.....	1
1.2. Problem Identification	3
1.3. Study Area.....	4
1.3.1. Geohydrology.....	6
1.3.2. Soils of the Area.....	6
1.3.3. Canal System and Wells.....	7
1.4. Objectives and Scope.....	9
Chapter 2 THEORY AND APPROACH.....	10
2.1. Theory and Concepts	11
2.1.1. Surface and Ground Water Dynamics.....	11
2.1.2. Darcy's Law.....	12
2.1.3. Rationale for the Study	13

2.2. Practical Applications	15
Chapter 3 MATERIALS, METHODS AND RESULTS.....	16
3.1. Historic Well Data and GPS Measurements	18
3.1.1 Locations of Canals and Wells.....	19
3.1.2 Distances between Wells and Canals.....	22
3.1.3 Well Water Levels.....	24
3.1.4 Average Annual Response Hydrograph Analysis	24
3.1.5 Analysis of Shallow versus Deep Well Responses	26
3.1.6 Canal Water Levels.....	35
3.2. Data Modeling and Calculations.....	37
3.2.1 Estimating Ground Water Elevations for Gradient Calculations.....	37
3.2.2 Evaluating Uncertainty of Kriged Ground Water Level Estimates	39
3.2.3 Horizontal Hydraulic Gradient Calculations at Any Canal Location	53
3.2.4 Calculating a Seepage Index.....	54
3.2.5 Ranking Relative Seepage Loss.....	55
3.2.6 Sensitivity Analysis of Kriged Water Levels	55
Chapter 4 RESULTS AND DISCUSSION.....	58
4.1. Horizontal Hydraulic Gradient Calculations at Canal Reaches.....	58
4.2. Calculating a Relative Seepage Index.....	70
4.3. Mapping Relative Seepage Loss	70
4.4. Model Adaptability and Applicability.....	74
4.5. Relationship of Relative Seepage Ranking and Soil Permeability	75
Chapter 5 CONCLUSIONS and RECOMMENDATIONS.....	78

LITERATURE CITED.....	82
APPENDIX A – Water Balance	86
1. Theory and Concepts of system water balance.....	86
2. Evapotranspiration	87
3. Seepage Losses.	88
APPENDIX B - Methods of Quantifying and Modeling Seepage.....	89
1. Measurements	89
2. Data Analysis	90
3. Modeling.....	91
4. Artificial Neural Networks.....	92
APPENDIX C - Management of Seepage Loss	94
1. Conveyance Losses in the Study Area	94
2. Use of Geographic Information Science.....	95
3. Canal Design Optimization.....	96
4. Canal Maintenance and Modernization	97

LIST OF FIGURES

Figure 1.	Index map showing extent of Snake Plain Aquifer that underlies the study area.....	5
Figure 2.	Soil permeability types of Bingham County soils in the study area derived from Soil Survey Geographic (SSURGO) Data Base.....	7
Figure 3.	Seepage study area in relation to canal system, wells, check structures (adjustable water level control points) and American Falls Reservoir. Background is Bingham County Digital Ortho Image Compressed County Mosaic.....	8
Figure 4.	Cross-sectional diagram of how Darcy’s Law was applied to the canal system. See text for definition of symbols.....	13
Figure 5.	Relative location of wells and canal system in the study area.....	20
Figure 6.	Wells with historic water level data in early period 1944-49 (58 locations) and late period 1957-92 (6 locations).	21
Figure 7.	Summary of temporal coverage in the 58 historic wells with elevation data used in this study. Data for other wells (#76, 77, 78) from the late period are not shown.	22
Figure 8.	Illustration of method used to measure shortest distance from a well to a canal.	23
Figure 9.	Representative well hydrographs and their response to irrigation. These wells are located along a west to east line just north of Aberdeen (see Figure 6).....	24
Figure 10.	Example of how an average annual response hydrograph was constructed for well #2).....	25
Figure 11.	Average annual response amplitude of well water elevation and their spatial relation to canals and canal width. Canal flow is from north-east to south-west.	27
Figure 12.	Histogram of average annual amplitude responses in well water elevation over an irrigation season.	28
Figure 13.	Response hydrographs of double cased well #10.	29
Figure 14.	Spatial relation of wells with seasonal water elevation responses in the vicinity of well #10.	30
Figure 15.	Well response amplitude versus well depth.....	31
Figure 16.	Well response versus well distance from canal. The dark blue point is the deep well.	32
Figure 17.	Comparison of well responses over distance.....	35
Figure 18.	May contours of ground water interpolated from historical well water elevation data and the AARHs of each well. Ground water flow is from north-east to south-west.....	38
Figure 19.	Diagram illustrating how kriged map rasters were used to calculate means and standard deviations of interpolated water level at each grid cell. Each layer represents the interpolated water level with one data point withheld. Each layer simulates an alternate interpolation for each well. Cell statistics were calculated at each grid location for the multiple layers combined, for both May and August.	40

Figure 20.	Ground Water Elevations. August (A.) and May (B.) Raster of Means. ...	41
Figure 21.	Ground Water Elevations Difference map: August minus May raster of means.	43
Figure 22.	Identifying statistically meaningful positive differences in kriging estimates at a single location.....	44
Figure 23.	Identifying statistically meaningful negative differences in kriging estimates at a single location.....	44
Figure 24.	Tail offsets used for calculating positive significant differences in August (A) and May (B).....	45
Figure 25.	Tail offsets used for calculating negative significant differences in August (A) and May (B).....	46
Figure 26.	Tail offset elevations used for calculating positive significant differences in August (A) and May (B).....	47
Figure 27.	Areas of positive significant differences in red and statistically insignificant differences (yellow) at a 90% confidence level.	48
Figure 28.	Tail offset elevations used for calculating negative significant differences in August (A) and May (B).....	49
Figure 29.	Areas of negative significant differences in red and statistically insignificant differences (yellow) at a 90% confidence level.	50
Figure 30.	Areas of significant water elevation differences at 90% confidence level. A. Positive differences. B. Negative differences. Yellow areas are statistically insignificant at the 90% confidence level.	51
Figure 31.	Composite map of positive and negative changes in ground water levels over the irrigation season that are statistically significant at 90% confidence.	52
Figure 32.	Map showing relation of randomly selected wells to other wells.....	56
Figure 33.	Frequency distribution of estimated horizontal hydraulic gradients for May.	58
Figure 34.	Canal reaches associated with the highest and lowest estimated horizontal hydraulic gradients during May. Color coding corresponds to Figure 33: main canal line in blue, and lowline canal in red. Reaches associated with insignificant differences in ground water levels over the irrigation season were excluded from subsequent consideration.	59
Figure 35.	Spatial distribution of estimated horizontal hydraulic gradients beneath the canal system during May. Color coding corresponds to Figure 33: lower main line, dark blue, upper main line and laterals, light blue, lower lowline and laterals, dark red, upper lowline, light red.	60
Figure 36.	Frequency distribution of horizontal hydraulic gradients for August. Color coding corresponds to Figure 33.....	61
Figure 37.	Spatial distribution of horizontal hydraulic gradients estimated along the canal reaches in the study area during August. Color coding corresponds to Figure 36: main line, blue; lowline, red.....	62
Figure 38.	Spatial distribution of horizontal hydraulic gradients estimated along the canal reaches in the study area during August. Color coding corresponds to Figure 36: lower main line, dark blue; upper main line and laterals, light blue; lowline, dark red.	63

Figure 39.	Frequency distribution of rate of change of gradient, May to August.....	64
Figure 40.	Rate of change of gradient.....	66
Figure 41.	Frequency distribution of change in ground water elevation, May to August.....	67
Figure 42.	Canal reaches associated with the highest rates of change of ground water elevation.....	68
Figure 43.	Canal reaches associated with the largest values of the inverse of May gradient.....	69
Figure 44.	Spatial distribution of relative seepage in the canal system by area (A) and length (B) of the canal reaches. Details in the inset rectangles are shown in Figure 45 and 46.....	71
Figure 45.	Upper lowline canal showing relative seepage ranking by area (A) and length (B) of canal reaches.....	72
Figure 46.	Middle lowline canal relative seepage ranking by area (A) and length (B) of canal reaches.....	73
Figure 47.	Maps of significant changes in water table elevation between May and August. (A) with all fifty eight wells; and (B) without ten randomly selected wells. Yellow areas are not significantly different at the 90% confidence level.....	74
Figure 48.	Geographic relationship of canal seepage ranking to soil permeability... ..	76
Figure 49.	Rank correlation of relative seepage index versus soil permeability. The null hypothesis of no correlation can not be rejected.....	77

LIST OF TABLES

Table 1.	Summary of data analysis steps used in this study and outlined in this chapter.....	17
Table 2.	Test of significant difference in mean responses of "Shallow" and "Deep" wells. Calculated t exceeds t-critical, so there is a significant difference in the means at >99% confidence level.....	33
Table 3.	Test of significant difference in mean distances of low and high response wells. Calculated t does not exceed critical t, so there is no significant difference in the means at 95% confidence level.....	34

Abstract

CHARACTERIZATION, MODELING AND MAPPING OF CANAL SEEPAGE FROM GROUND WATER ELEVATION RESPONSES

Thesis Abstract—Idaho State University (2009)

Historic seasonal well water elevation responses were used with recent GPS-determined canal water elevations to estimate horizontal hydraulic gradients beneath a local canal system. These gradients, their rates of change and the well water elevation responses over the irrigation season were combined in a relative seepage index for the purpose of mapping and ultimately managing canal seepage. This was done using Darcy's law. The well responses over the irrigation season ranged from 1.8 to 16.7 feet (0.6 – 5.1 m) in individual wells. An average annual response hydrograph was constructed for each well location from which monthly water levels were extracted for kriging interpolation of the ground water levels. Distances measured between nearest wells and canals ranged from 9 feet to 5468 feet (2.7 – 1666.6 m). A lateral distance of 50 feet (15.24 m) was used to estimate the horizontal hydraulic gradients between the canal surfaces and the water table interpolated from the well water elevations.

The combined relative seepage index consisted of three components: (a) the inverse of the local horizontal hydraulic gradient, (b) the rate of change of the gradient, and (c) the seasonal change in ground water elevation. This combined index identified more and different canal reaches having higher seepage than did indices that relied only on individual gradient or water level factors.

Dedication

To all those who helped and to those who may find this useful.

Chapter 1 INTRODUCTION

This chapter presents a background to the overall problem of monitoring and management of canal water losses due to seepage, identifies aspects of the problem at the local level and defines the problem, study objectives, underlying principle, rationale, and scope.

1.1. Background

A lack of sufficient fresh water is one of the major crises facing the present generation. According to Pearce (2006), there are serious potential political ramifications of decreasing flow in the rivers on which two countries depend (e.g., Colorado River, Badlands Journal Administrator's blog, 2005). For example, there have been extensive negotiations between the U.S. and Mexico concerning the distribution of Colorado River water. In the recent past, interested parties along the Colorado River wanted to use all the water, including that lost to aquifer and wetlands via canal leakage. The Mexican border region of Calexico is competing against these few water interests, and is suing on behalf of Mexican farmers. The vastly wealthier city of Mexicali will subsidize the suit to stop a project to line 23 miles (37 km) of canal on the American side. This would reduce seepage and the amount of ground water available to farmers on the downstream Mexican side. Pearce (2003) raises the issue of what a canal really is, considering the rights of an affected economic community to defend their local irrigation system against massive, speculative California growth. He contrasts the Mexicans' great farming accomplishments (which depend on canal seepage) as far more significant than the practice of unrestricted development and building golf courses on the American side.

On the Eastern Snake River Plain Aquifer (ESPA), the use of canal water to

recharge the aquifer is being questioned by power companies as a potential loss of power generating capacity. However, this issue may not be pertinent to the local aquifer that underlies the study area near Aberdeen, Idaho. Water from this aquifer discharges into the American Falls Reservoir as ground water level rises and falls annually, coinciding with the irrigation season. This implies that recharge water (including canal leakage) returns to the reservoir in a relatively short time period that may or may not adversely affect power generation. A better understanding of what happens to the water in the local canal-ground water system is needed.

In addition to power generation, there is increasing water demand for agricultural, domestic and industrial purposes (Kumar, 2003). According to Hotchkiss et al. (2001), 70% of the world's freshwater use is for irrigation, or more than three times industrial usage and more than ten times domestic usage. Approximately 78% conveyance efficiency (the ratio of water that reaches a location and water diverted from a source) is obtained off-farm (not related to agriculture) in the United States (Interagency Task Force, 1979), where conveyance losses account for 27.5 billion gal/day (125 billion L/day) or more than ten times total domestic water usage in the U.S. (Herschy and Fairbridge 1998). Estimated seepage losses from unlined canals could range from 15 to 45% of total diversions (van der Leen et al. 1990). Losses from the Aberdeen-Springfield canal system are typically as much as 60% of annual diversions (Barnett and Barnett, 2000).

In many parts of the world, agricultural canal systems are uncovered and are subject to many potential problems (e.g., contamination from natural species, livestock and animal waste, agricultural chemicals and other surface runoff). However, these impacts

are manageable with appropriate monitoring and improved practices. More difficult to monitor and manage are losses due to seepage and leakage.

Irrigation systems are prone to several types of losses – evaporation, lateral leakage due to cracks and holes from various burrowing animals, and infiltration and seepage (Kumar, 2003; Swamee et al., 2000). In uncovered canal systems, the surface area and prevailing weather conditions largely control evaporation. Lateral leakage is usually visible, and therefore easily detectable and controllable. Subgrade seepage, however, is less easily detectable and usually accounts for larger seasonal losses (Contor, 2004). Apart from the physical loss of water from the canal, there are other important ramifications for the overall water balance of the local ground water system (Kumar, 2003). The water balance is essentially an accounting of inputs, outputs and storage changes in an aquifer, whether it is confined or unconfined. In an unconfined aquifer, changes in storage (water table level) can be sensitive indicators of canal leakage. Canal seepage affects the level of ground water, which in turn affects soil conditions, plant roots, pumping depth of wells, and the recharge potential of aquifers and ground water flow to streams or rivers.

For real world management situations, the overall complexity of the interacting surface and ground water hydrologic system needs to be recast in terms of the major factors and problems that define the local situation.

1.2. Problem Identification

The ground water level in the vicinity of canals is affected by the hydraulic conductivity of the soil, the presence of pumping wells and their distance from the canal, the general geology of the area in question (Smith, 2004) and canal construction. For

example, the water distributed by the Aberdeen-Springfield Canal Company in SE Idaho (Figure 1, 2, 3) is mainly via a system of uncovered canals with a small number of piped canals; only a few sections are lined. The canals traverse many soil types of varying thickness on fractured basaltic lava with the result that seepage losses during conveyance are non-uniform.

In the Aberdeen-Springfield area the canal system is one of three that are represented as “leaky” in the Eastern Snake Plain Aquifer Model Enhancement Project (Contor, 2004), with significant leakage assumed along reaches that do not correspond with the intended places of irrigation use. This study seeks to better characterize this leakage to improve the calibration of this aquifer model, which in turn will lead to better maintenance and management of the canal-ground water system.

To do so, it is necessary to assess the coupled canal-ground water system and develop a method to estimate the relative magnitude and locations of seepage losses along the canal system.

1.3. Study Area

The study area comprises an area of irrigated farmland northwest of American Falls Reservoir that is underlain by the Snake Plain Aquifer (Figure 1).

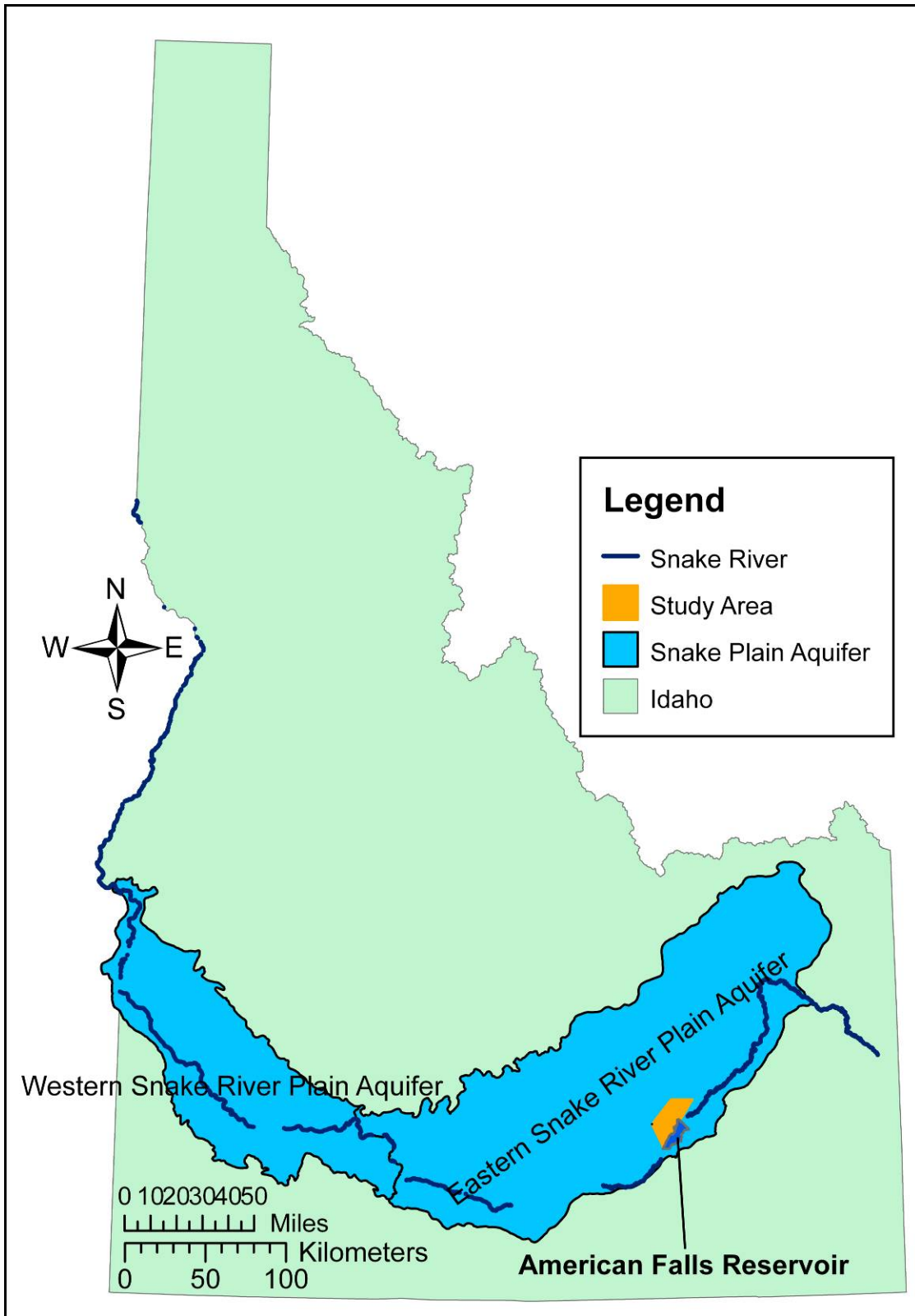


Figure 1. Index map showing extent of Snake Plain Aquifer that underlies the study area.

1.3.1. Geohydrology.

R.P. Smith (2004) provides a comprehensive review of the geology of the Snake River Plain Aquifer and its vadose zone. The tectonic and volcanic processes that formed the Plain strongly influenced the properties of both, resulting in abrupt spatial variations of their hydrologic properties. The vadose zone is comprised of very porous and permeable basalt lava flows that allow rapid infiltration of water and contaminants and deep penetration of air into the vadose zone through rubble zones and sub-vertical cooling fractures. These factors play a major role in controlling seepage losses in the local canal system. Generally fine-grained aeolian, alluvial, and lacustrine sediments interbedded within the basalt sequence commonly serve as aquitards below the water table and also affect infiltration and contaminant transport in the vadose zone (Smith, 2004).

1.3.2. Soils of the Area.

The complex geohydrology gives rise to many different soil types in the area, a number that is further increased by the great variation in terrain slopes. The soil factor of greatest interest in this study was soil permeability. This is because the amount of water flowing through a soil is directly proportional to its permeability and this might be expected to be related to canal seepage.

Figure 2 shows the general relationship of the study area's canal system to local soil permeability types in Bingham county.

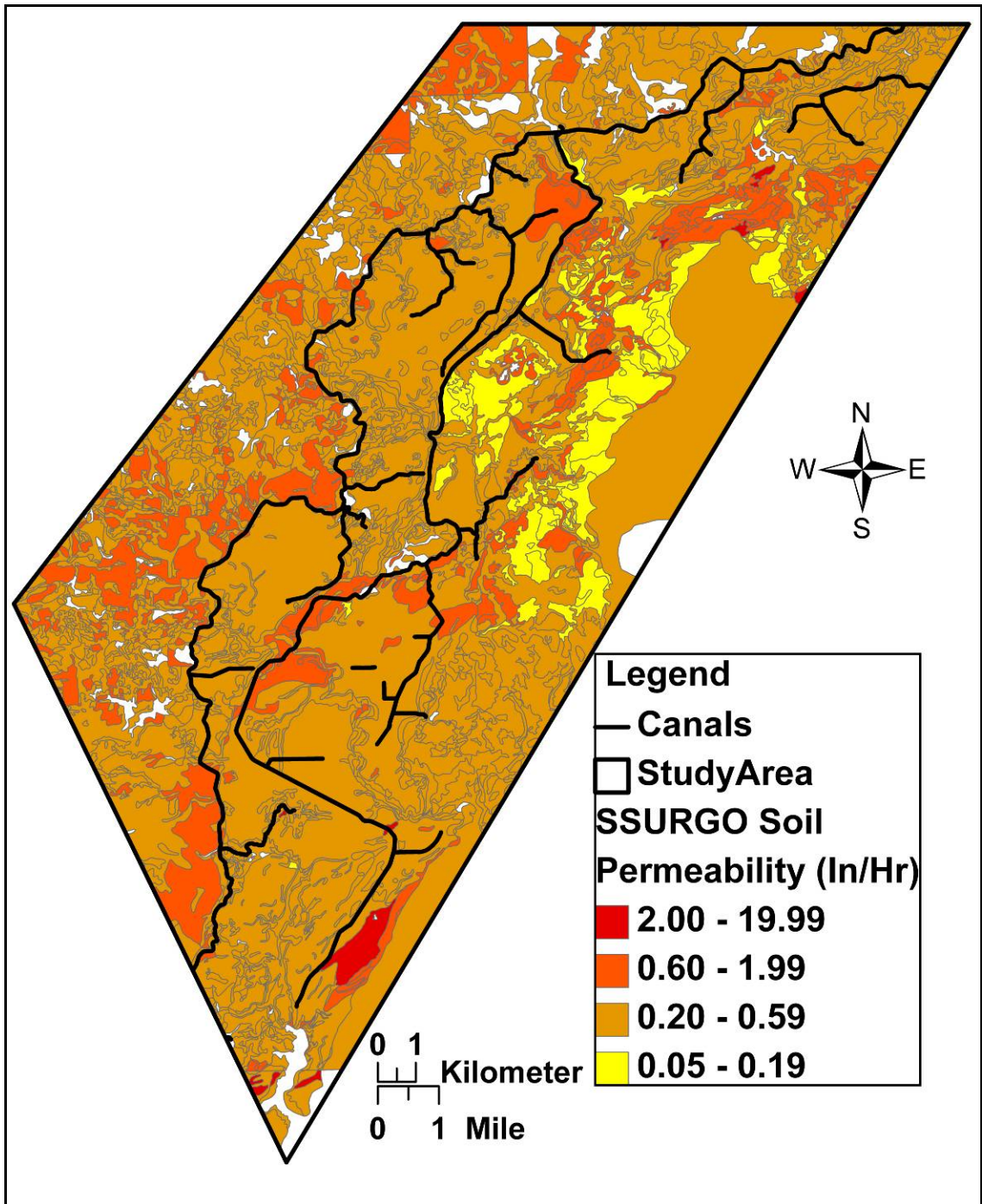


Figure 2. Soil permeability types of Bingham County soils in the study area derived from Soil Survey Geographic (SSURGO) Data Base.

1.3.3. Canal System and Wells.

The pertinent factors here are the spatial locations and data availability. The location of the study area is in Bingham County, Idaho, west of American Falls

Reservoir, including the system of canals, wells and check structures (adjustable water level controls) between the cities of Aberdeen and Springfield and south of Aberdeen (Figure 3). Data availability will be discussed in Chapter 3.

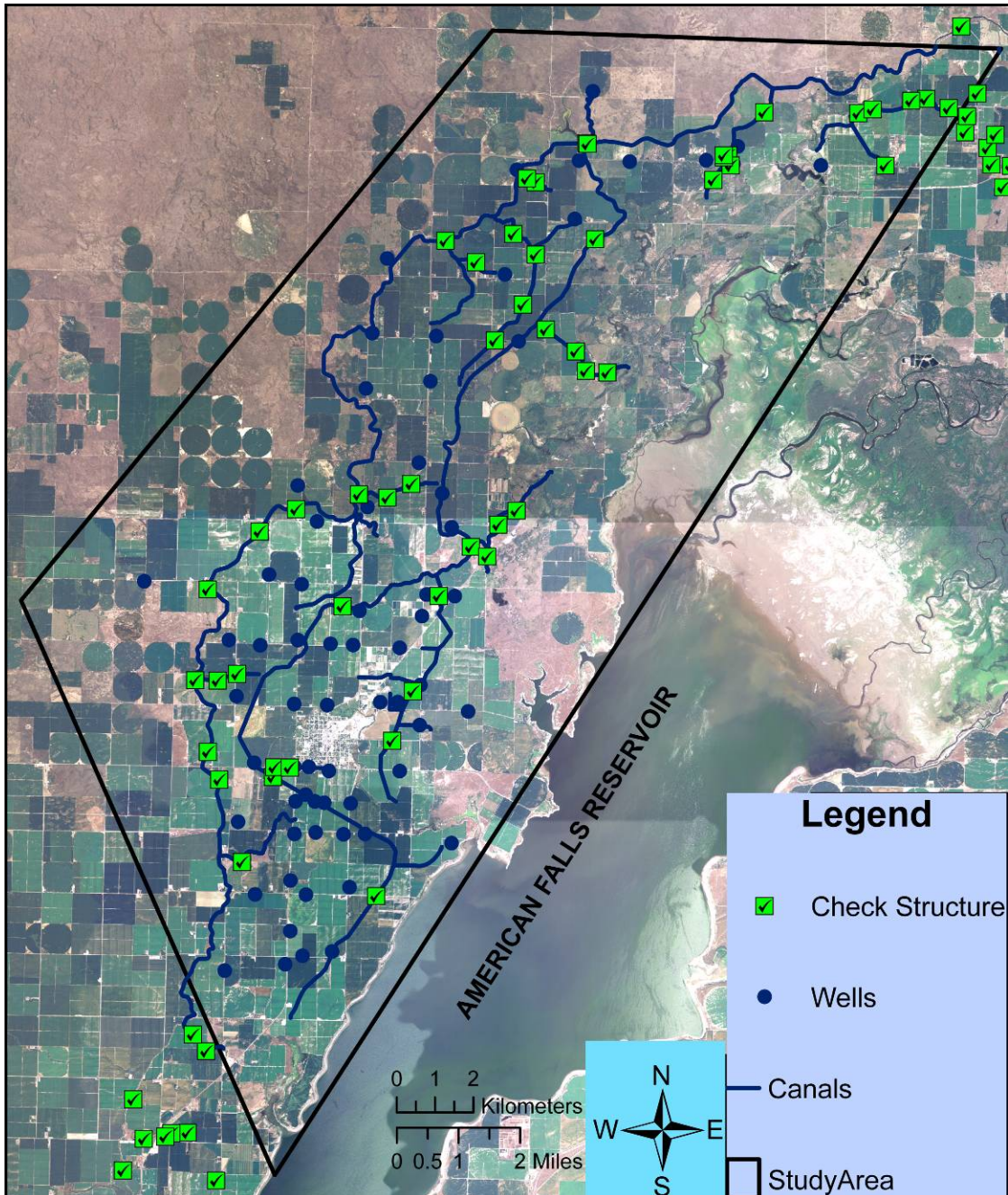


Figure 3. Seepage study area in relation to canal system, wells, check structures (adjustable water level control points) and American Falls Reservoir. Background is Bingham County Digital Ortho Image Compressed County Mosaic.

1.4. Objectives and Scope

The objectives of the study are to:

1. Characterize the temporal and spatial nature of well responses to seepage from the Aberdeen-Springfield canal system.
2. Develop a method to identify the leakier parts of the canal system.
3. Map areas of greatest leakage to better manage the canal system.

The Aberdeen-Springfield Canal Company provided funding for this study and provided historic data on seasonal water levels in observation wells along the canal distribution system. The well data were supplemented and integrated with Geographic Information Science (GIS) technology and Global Positioning System (GPS) measurements of canal locations and water levels. Historic well water level data span approximately 48 years of record in 60 wells located in an area of 342 square kilometers (132 sq. miles), containing about 27 kilometers (17 miles) of canal length. Availability of well data restricted the study to the central-most part of the canal system.

Chapter 2 THEORY AND APPROACH

This chapter presents the theoretical and conceptual as well as applied considerations pertinent to the Aberdeen-Springfield area. These are surface and ground water dynamics, Darcy's law, rationale for the study and seepage losses in the study area. There is a large body of literature pertaining to water conveyance by canals and water loss. For a more detailed review see the Appendix A (1-5). The theory and concepts (1), evapotranspiration (2), seepage losses (3), methods of quantifying and modeling seepage (4), and management of seepage (5) are reviewed.

Many theoretical models exist to describe a variety of real world and managerial situations. Many of these models utilize numerous parameters that would be too expensive to implement in most practical field situations. In small-scale experiments, variables such as infiltration rate, soil conductivity and evapotranspiration can be monitored and parameterized. On larger scales, involving miles (kilometers) of canals with different soil types and crop conditions it would be cost-prohibitive to adequately sample and monitor all the necessary variables to parameterize and validate such complex models.

As a prerequisite to understanding the system behavior, there must be some foundational objectives to instruct further direction and developments. In the large-scale field situation of the current study area, a simplifying assumption is made: it will be assumed that the system is self integrating and that an appropriate response model can be represented by a relatively small number of relevant variables or factors. It is hypothesized that during the course of an irrigation season saturated soil conditions are

attained and differences in water elevations, distances between canals and wells and the local soil characteristics are the main factors affecting changes in the level of the water table. It is expected that the model can be used to monitor changes in system behavior due to lining sections of canal, new leaks or occurrences of sink holes.

2.1. Theory and Concepts

The storage and movement of water is determined by the general hydrological cycle. This is an accounting of the inputs to, outputs from, and storage changes in, a system (see Appendix A.1 for review of system water balance). In practical applications, one or more of these inputs and outputs may be negligible or may predominate over others at different times. This is the situation in the Aberdeen-Springfield canal-aquifer system.

2.1.1. Surface and Ground Water Dynamics

For canals, the relevant water balance is between river diversion rate (input), evapotranspiration and seepage losses during conveyance, and deliveries (outputs). Changes in storage are assumed to be negligible. For studies not focused on the evapotranspiration component of the water balance, it may not be necessary to measure it, or it could be estimated through modeling (See Appendix A.2). For this study, evapotranspiration losses were neglected, which is equivalent to assuming that evapotranspiration per mile of canal is uniform over the study area, and the predominant factor was assumed to be the interaction between surface water in the conveyance system and ground water in the aquifer (Welhan, 2008).

The dissipation of canal seepage losses to the local groundwater system tends to be dominated by horizontal groundwater flow because hydraulic conductivity in

sedimentary materials is typically so much greater in the horizontal than the vertical direction. This is because of anisotropy of layered media. A principal focus of this study will be the use of Darcy's Law, the relationship that explains fluid flow in porous media.

2.1.2. Darcy's Law

The generalized relationship governing flow in porous media is Darcy's Law (Brown 1995). This states that the flow is a function of the hydraulic head, the flow area, the flow path length and the hydraulic conductivity (a proportionality constant) of the medium. For one-dimensional laminar (i.e., non-turbulent) flow, it may be stated as

$$Q = AK\Delta h/L \quad \text{(Equation 1)}$$

where,

Q = volumetric flow rate (m^3/s or ft^3/s),

K = hydraulic conductivity (m/s or ft/s),

L = flow path length (m or ft),

h = hydraulic head (m or ft),

A = flow area perpendicular to L (m^2 or ft^2), and

Δ = denotes the change in h over the path L .

The Darcy flux is defined as, $q = Q/A$ (m/s or ft/s). The Darcy flux is the volumetric flow per unit area, so that $q = K\Delta h/L$. The hydraulic gradient, $\Delta h/L$, is often represented as I .

Figure 4 conceptualizes Darcy's Law in a canal seepage situation. Here Δh is the difference in water levels between the canal and well (or between wells), and L is the distance between them.

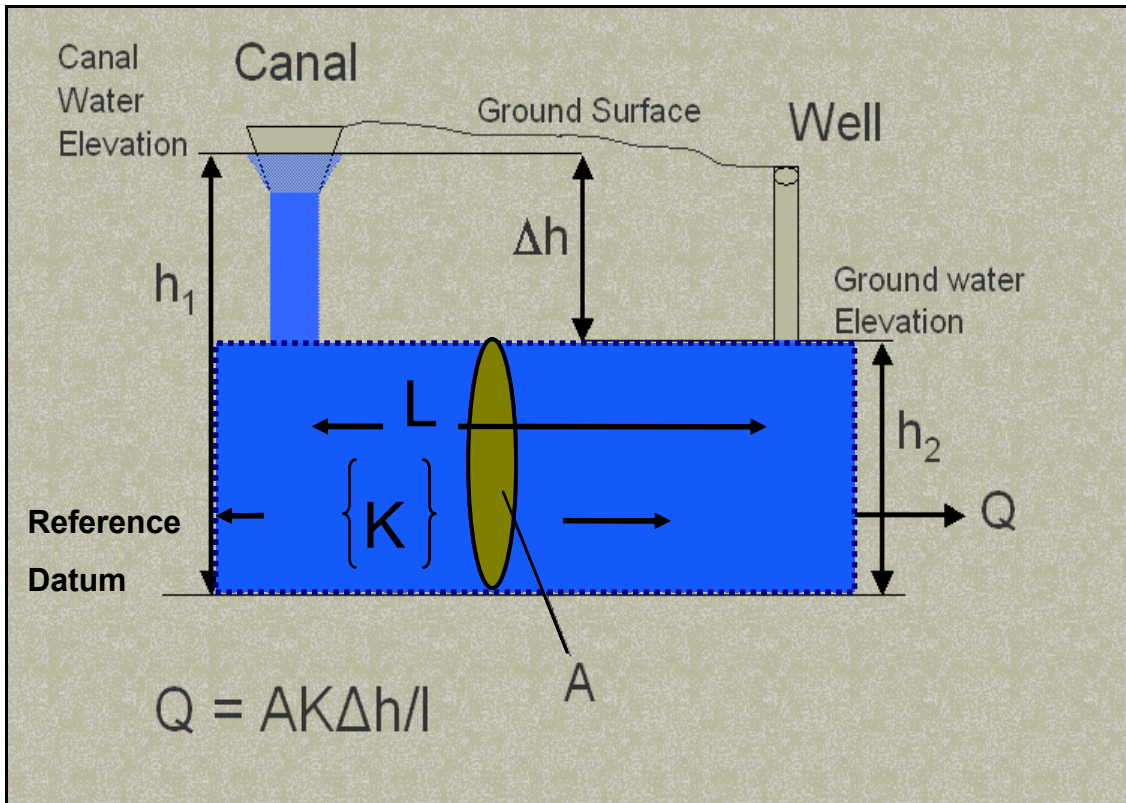


Figure 4. Cross-sectional diagram of how Darcy's Law was applied to the canal system. See text for definition of symbols.

This provides the basis of the computational method developed in this study.

2.1.3. Rationale for the Study

On this basis, mapping of hydraulic gradients and water levels can help discriminate between areas of different relative hydraulic conductivity. By mapping the changes in I and h during canal filling (and/or draining) periods and combining these with maps of I and h at different times, regions of greatest infiltration loss could be identified.

Furthermore, under static conditions, Darcy's Law predicts that the hydraulic gradient I , ($\Delta h/L$), varies as the inverse of hydraulic conductivity (K) for a given groundwater flux ($q = KI$). That is, for a given rate of horizontally dissipated canal seepage, horizontal hydraulic gradients in the vicinity of the canal would tend to be greatest in low- K porous media and vice versa. Under transient conditions, the local horizontal hydraulic

gradients, the rates of change of local horizontal hydraulic gradients, hydraulic heads, and response times to changes in canal water levels all should provide information on the spatial variability of horizontal hydraulic conductivity. For example, after a canal has filled, the horizontal hydraulic gradient will be greatest where the conductivity is lowest and vice versa, i.e., I varies as $1/K$. Similarly, the rate of change of I ($\Delta I/\Delta t$) between the canal and nearby wells (and among nearby wells), and the rate of change of water level ($\Delta h/\Delta t$) in individual wells would tend to be greatest in areas where infiltration loss (hence, K) is greatest. Also, the lag time between canal filling and nearby well water level rise would be the shortest. Similar relationships could be expected following draining of the canal, although the recessional responses would be slower and possibly more sensitive to local boundary conditions such as the falling ground water levels.

Data needed to apply the Darcy method are: the locations of the wells and canals; the time intervals and water levels in the canals and wells to calculate the hydraulic head differences (Δh) and rates of change of gradient ($\Delta I/\Delta t$); and well depth information and aquifer lithology, because the presence of aquitards (section 1.3.1) could cause deep wells to respond differently than shallow wells.

The locations of wells in this study were mapped with a GPS unit. To facilitate application of the Darcy method across the whole study area, ground water contours were interpolated and tabulated. The limited available well depth information was extracted from the drilling log archives and incorporated into the attribute tables for the wells. The elevations of the high water marks of the check structures along the canals were measured assuming that the water level in each reach of canal is determined by the downstream check structure. The data were analyzed and combined in ArcGIS to

develop a relative seepage index.

2.2. Practical Applications

The approach used by Contor (2004, see Appendix 5.1 for more details) for estimating canal seepage losses in the Snake River Basin Adjudication (SRBA) aquifer model, used a constant seasonal leakage rate for portions of the canals. For the Aberdeen-Springfield Canal portion, leakage was represented as a percentage of diversions. Contor discussed the temporal distribution of leakage but did not use this in the calibration of the model due to inadequate data. However, the model allows for this in future scenarios. In Idaho, seepage losses can exceed 40% of diversion rate, primarily as leakage to the aquifer.

This study would provide an approach for better calibration of the Aberdeen-Springfield portion of the SRBA model. The study may also be applicable to other leaky canal systems in the SRB and would provide an alternative to other techniques for quantifying seepage that require large numbers of parameters and are cost-prohibitive to implement. This practical field application would provide more economically feasible decision support for improving the maintenance and management of leaky canal systems.

Chapter 3 MATERIALS, METHODS AND RESULTS

The computers, GPS units and accompanying software of the Aberdeen-Springfield Canal Company (mainly ArcGIS – Environmental Systems Research Institute, Inc., Trimble GeoXT with TerraSync and ProXR with TSC1 Asset Surveyor) and Idaho State University GIS Center (mainly ArcGIS) were used in this study.

The equipment and types of data and calculations needed to apply the Darcy's flux approach are outlined in this chapter. These include the locations of wells, canals and check structures; distances, time, and elevations of the water levels in the canals and wells; and calculation of water levels, gradients and their rates of change. Well water elevations were interpolated by kriging to estimate ground water elevations and gradients at any canal location. Average widths of canal reaches were measured from Bingham County Digital Ortho Image Compressed County Mosaic (BCDOICCM) using the Data Toolbar measuring tool in ArcMap. Soil information for the study area was obtained from the Natural Resources Conservation Service's (NRCS) online Soil Survey Geographic Database (SSURGO).

Some of the wells in the study area no longer exist and for those that do, the location information consisted of little more than a Public Land Survey System location (to the nearest quarter-quarter section) and, in most cases, a brief phrase or note in the Aberdeen-Springfield Canal Company's records. Most of the wells were located in the field by following the note, and/or interviewing residents and previous owners/managers of the land who are knowledgeable of the area. Because of the difficulty of finding the correct well locations from the notes and the paucity of accurate well elevation and depth

data, the study was conducted in a number of phases, outlined in the following sections. The flow chart outlined in Table 1, based on Arc Toolbox Model Builder's flow chart format, provides an overview of the numerous steps taken to analyze and synthesize the data (Table 1).

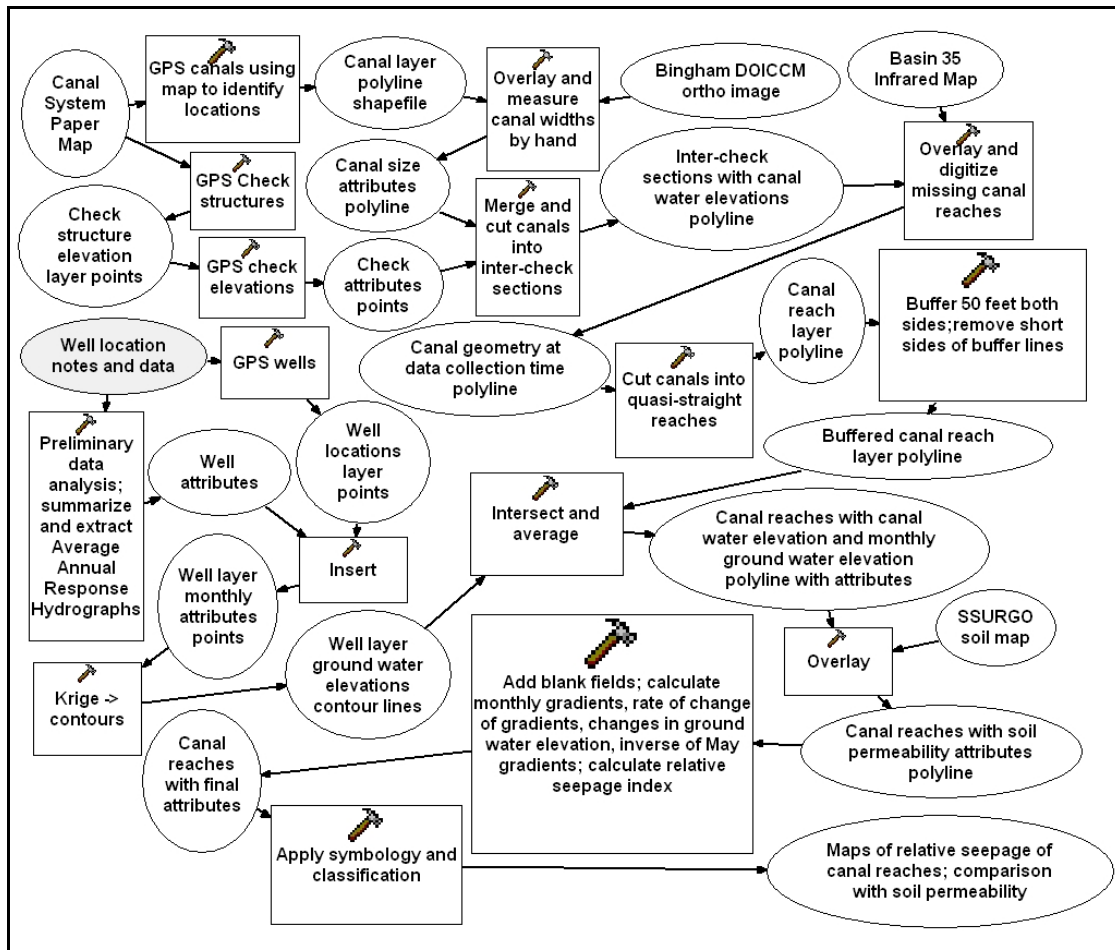


Table 1. Summary of data analysis steps used in this study and outlined in this chapter.

The initial mapping of the canal system was done with different software before the project was developed. Because of uncertainty of finding the wells and of the adequacy of the available data the study was not done in as logically flowing a manner as might be desired. The canal system paper map and well location notes and data are included as two starting points though they were largely separated in time. The canal data layer

obtained from mapping the system with the GPS unit was overlaid with the Bingham DOIICCM so as to measure the widths of the canals. The check structure data layer was obtained by more than one sequence of GPS data collection while determining the necessary number of data points for the required accuracy for the canal water to move downstream. These check elevation data were then merged with the canal width data to produce inter-check canal reaches with water elevation attributes. This output was then overlaid with Basin 35 infrared map and digitized to obtain the canal geometry at the data collection time. After this the output of the process of cutting the canals into quasi-straight reaches was buffered by fifty feet to produce a buffered canal reach layer.

From the other “starting” point, a well location layer was mapped by GPS and well attribute data derived from preliminary data analysis and extraction of AARH, was inserted. The output from this was a well layer with monthly attributes. This was kriged and contoured to produce a well layer with ground water elevations.

The prior buffered canal reach layer was then intersected with the ground water elevation layer and the points of intersection averaged. The output from this was then overlaid with the SSURGO soil map data layer to add soil permeability attributes. Fields were then added to this output and the needed calculations for the study were done. This produced the final attribute table to which classification and symbology were applied so as to produce the maps for the study.

3.1. Historic Well Data and GPS Measurements

In the first phase of the study, wells that had historic water level data from the period (1944 – 1949) were analyzed because there was a large gap (1949 -1957) with no data, and much less data was available in later years.

Canal and well locations were mapped with a Trimble GeoXt GPS unit and historic wellhead elevations, and water elevation data were used to characterize the average spatial and temporal changes in elevation of the water table during the irrigation season (April to October). GPS corrections were carried out in Pathfinder Office using Standard Carrier Processing and the CORS base station in Pocatello, Idaho ($43^{\circ}14'38.73365''\text{N}$, $113^{\circ}14'28.35993''\text{W}$). Occasionally, a local base station (Trimble Pro-XR with TSC1 Asset Surveyor at $42^{\circ}56'30.66406''\text{N}$, $112^{\circ}50'23.01138''\text{W}$) was used.

3.1.1 Locations of Canals and Wells

Canal locations for the study area were obtained as part of the mapping of the entire canal system. Small reaches, which are no longer in existence but which were present at the time of the original well water level data collection (1944 – 1949), were digitized from previous infrared photography and /or the BCDOICCM. Canal reaches which did not exist at the time of original water level data collection were excluded. Figure 5 shows the location of the wells and their relation to the canal system, indicating that the spatial density of wells and branching canals is greater near the town of Aberdeen than elsewhere in the study area.

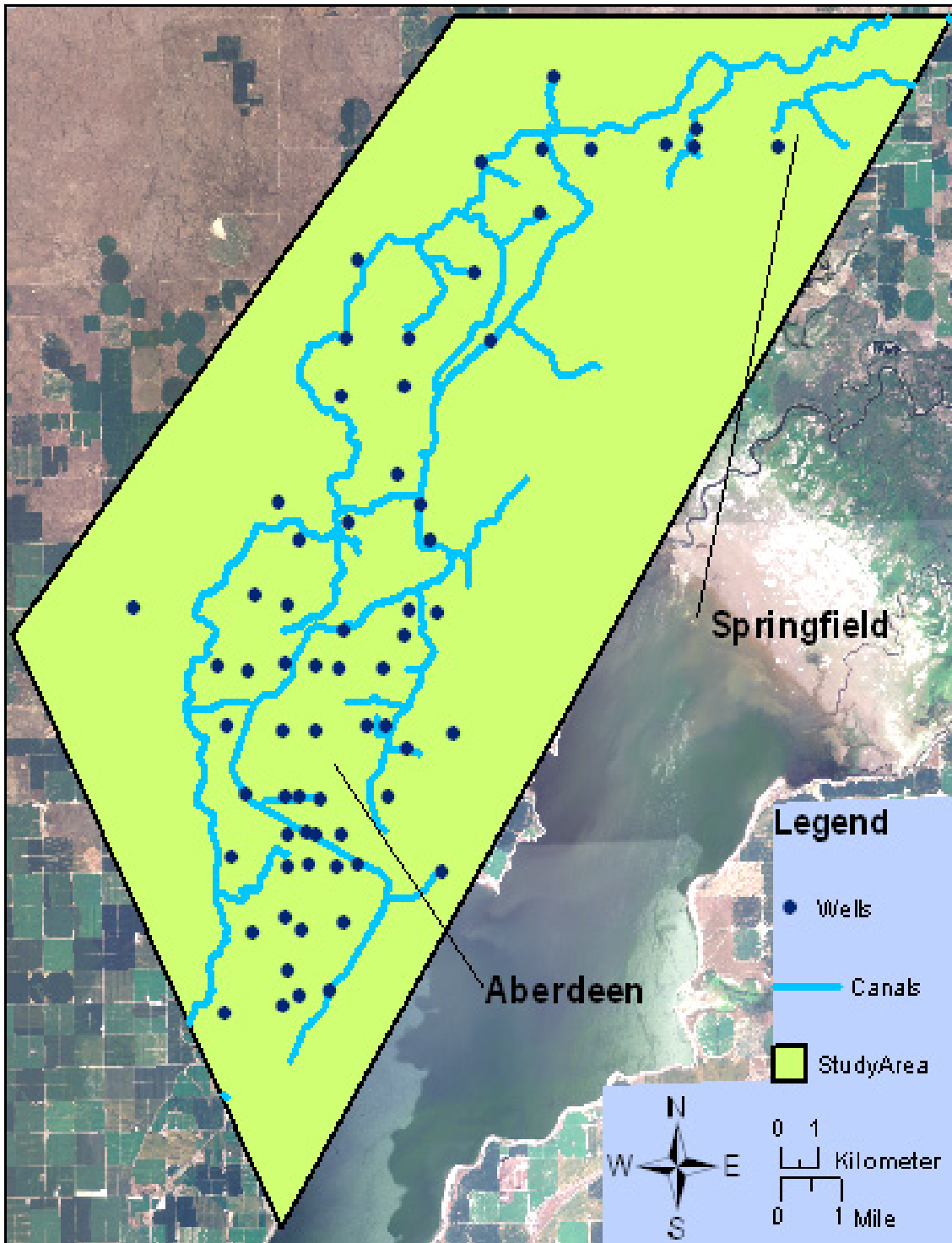


Figure 5. Relative location of wells and canal system in the study area.

The available historic well data consisted of an early period when many wells were sampled and a late period when only a few wells were sampled (Figure 6). Only three

wells have data in both periods.

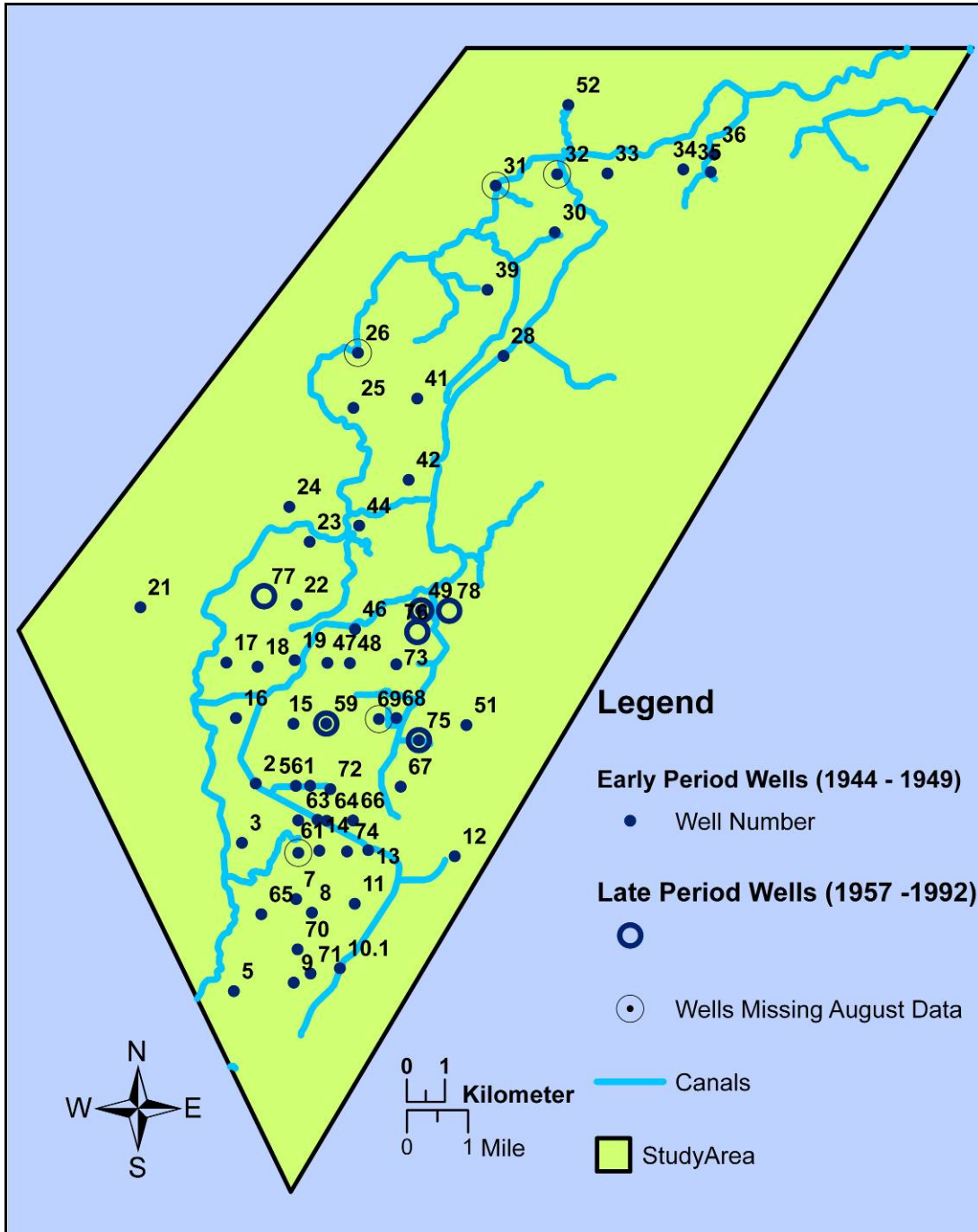


Figure 6. Wells with historic water level data in early period 1944-49 (58 locations) and late period 1957-92 (6 locations).

Figure 7 summarizes these two periods showing the gap of seven years when there were no data available.

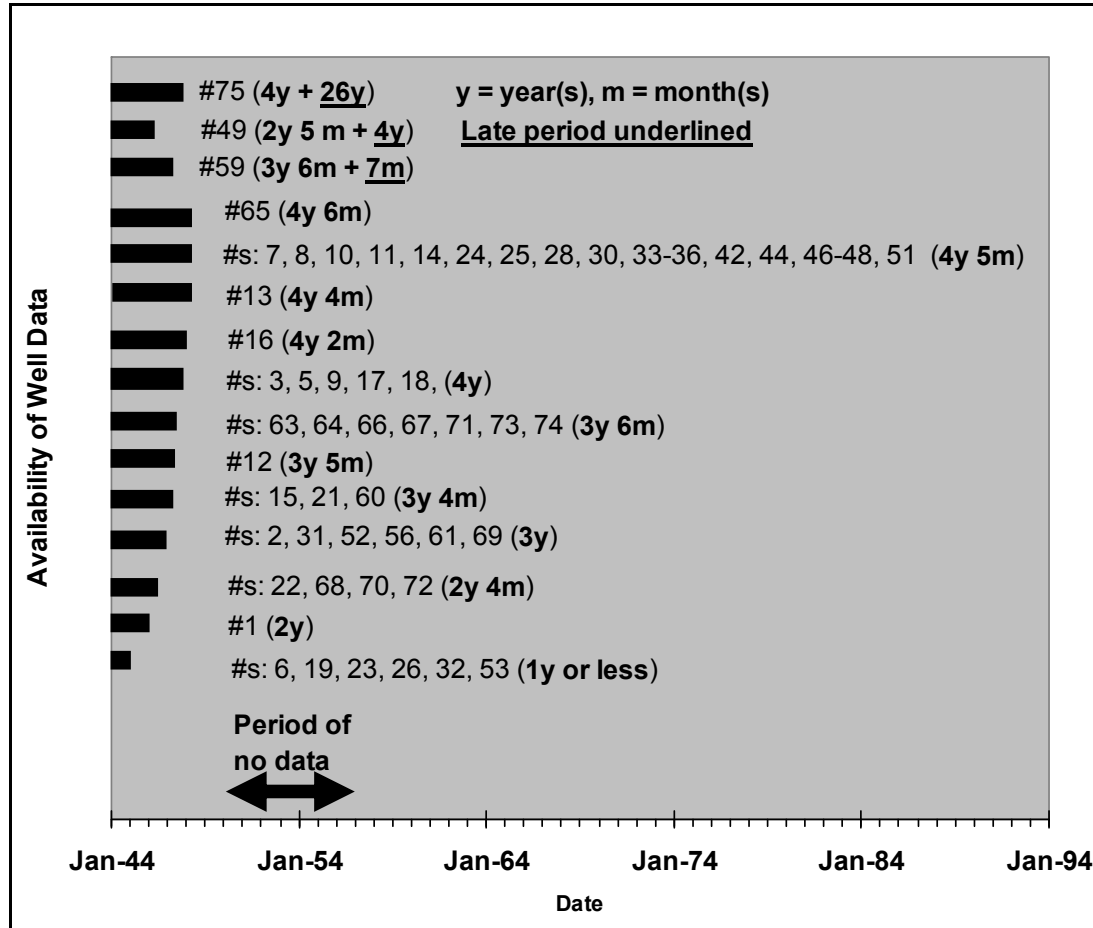


Figure 7. Summary of temporal coverage in the 58 historic wells with elevation data used in this study. Data for other wells (#76, 77, 78) from the late period are not shown.

The wellhead elevations and water level depths are accurate to the nearest 0.1 foot (3 centimeters). The water level depths were subtracted from the wellhead elevations to obtain water level elevations.

3.1.2 Distances between Wells and Canals

Canal and interpolated ground water elevations together with canal buffer distance were used to rank the relative seepage of the canals using Darcy's Law. Shortest distances between the wells and the canals were obtained using the distance-distance tool on the Editor toolbar to find the canal's point of tangency on a circle centered on a well;

the distance-measuring button in ArcMap was used to measure the radius (Figure 8).

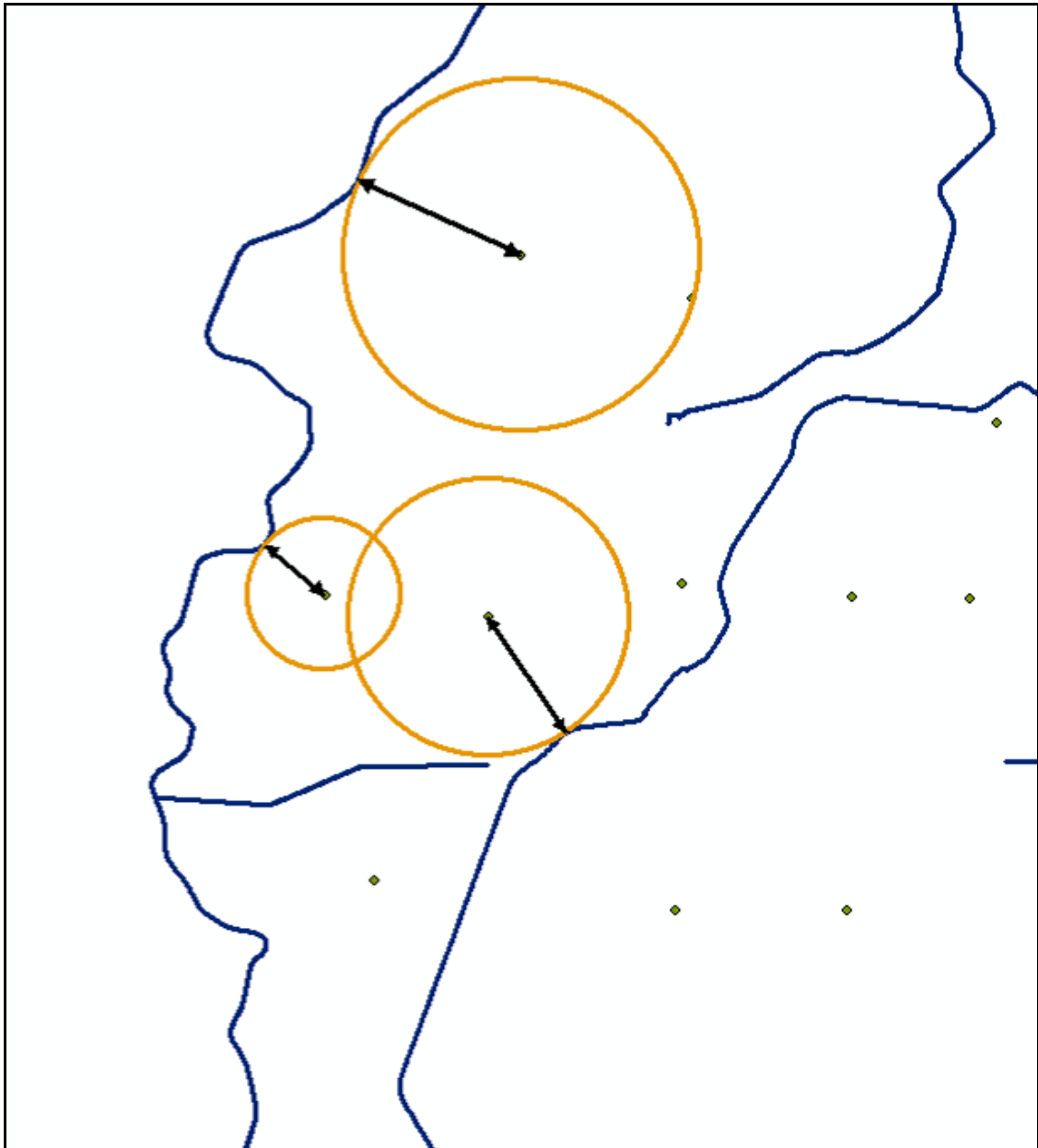


Figure 8. Illustration of method used to measure shortest distance from a well to a canal.

Although it is understood that the water does not always travel the shortest distance, these measurements were taken to characterize the spatial layout of the system.

Distances measured between nearest wells and canals ranged from 16 feet to 5450 feet (4.8 – 1661 m). A uniform distance of 50 feet (15.24 m) was used to estimate the

horizontal hydraulic gradients between the water surfaces of canal reaches and the water table interpolated from the well water elevations. The buffer distance was chosen so as to avoid possible complications from sharp canal turns, canal branches and situations where canal reaches were parallel and relatively close to each other.

3.1.3 Well Water Levels

In the second phase of the study, exploratory data analysis characterized the water table elevations over time and space and eliminated wells having insufficient data and data outliers. Data adequacy restricted subsequent analysis to wells having adequate water level records.

The preliminary data analysis showed an annual cyclical rise and fall of well water elevations in response to the irrigation season when plotted versus time (Figure 9).

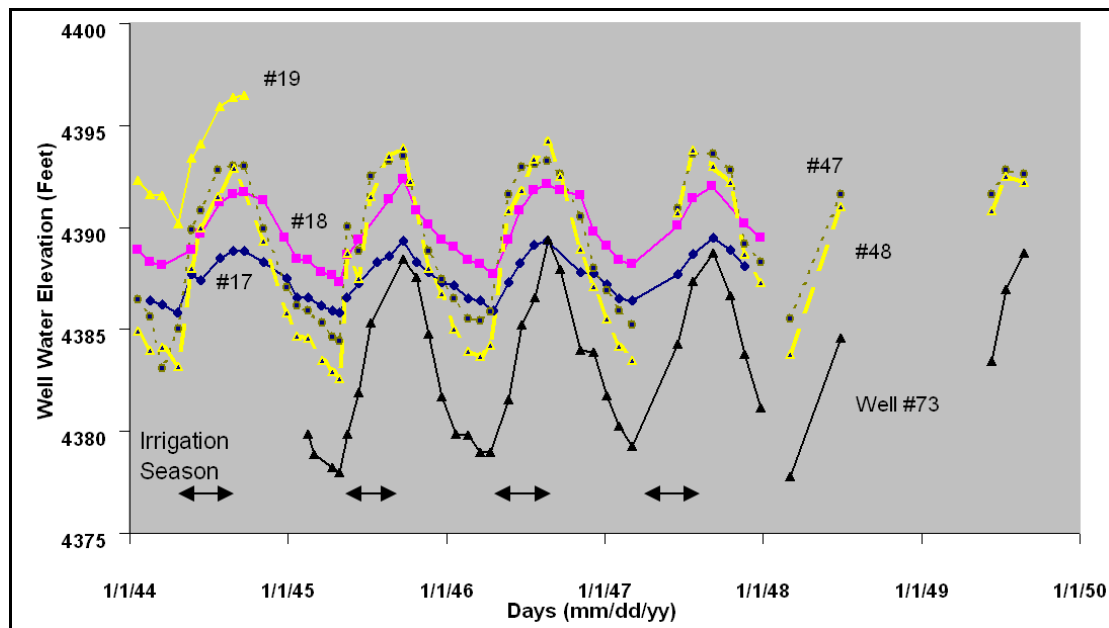


Figure 9. Representative well hydrographs and their response to irrigation. These wells are located along a west to east line just north of Aberdeen (see Figure 6).

3.1.4 Average Annual Response Hydrograph Analysis

The raw water level data had to be further manipulated prior to modeling. Since

there were variations in the dates of data collection as well as missing data, an average annual response hydrograph (AARH) for each well was created for the subsequent analysis of the data. This was accomplished by averaging the monthly water elevations for each well across years (Figure 10). The maximum and minimum between January and December were used in calculations to avoid the continued draining in the early part of the year from distorting the calculated rise of the previous season. This was important in some situations where the post season elevations were not as uniform as shown in Figure 10.

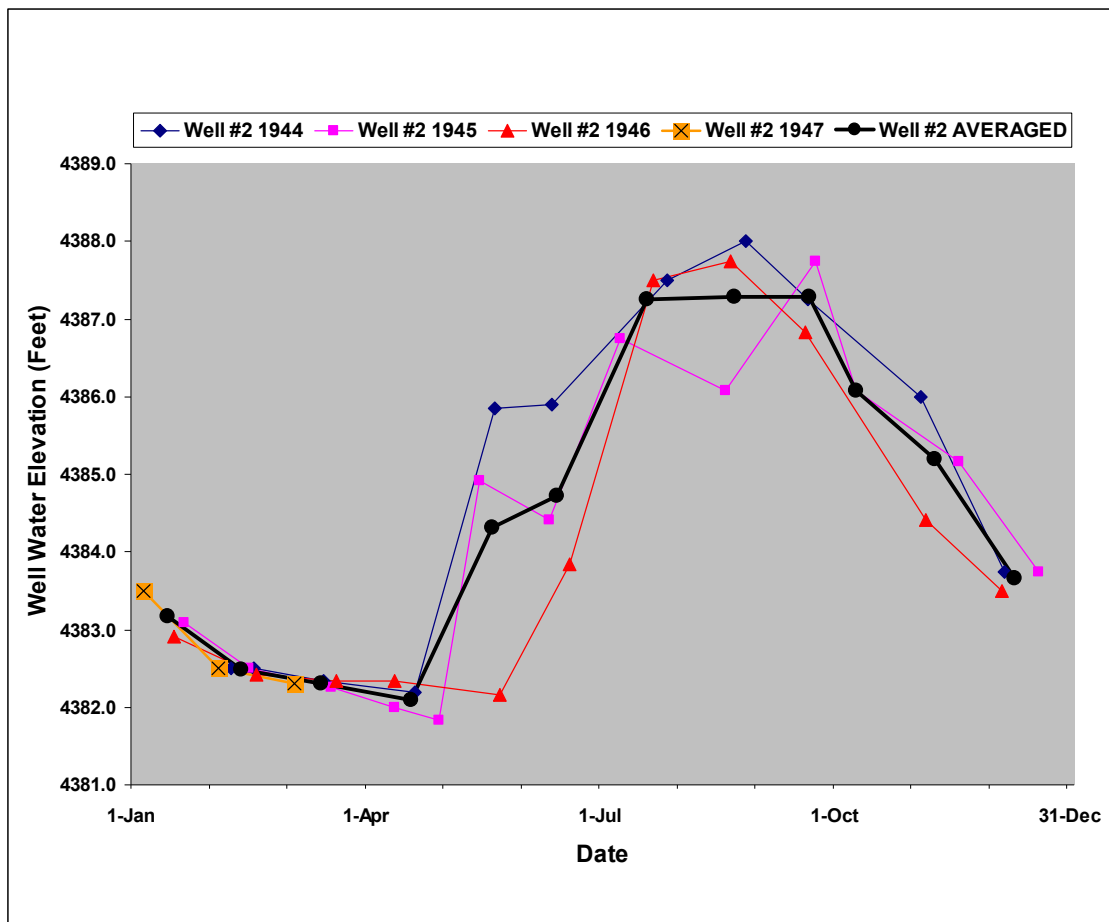


Figure 10. Example of how an average annual response hydrograph was constructed for well #2).

The original field notes were used to justify exclusion of some extreme spikes and dips

in the otherwise regular data, e.g. when a well had been pumping close to the time of data collection or if a well had been flooded by surface water (possibly during spring runoff, flood irrigation, etc.).

3.1.5 Analysis of Shallow versus Deep Well Responses

Figure 11 shows the average annual response amplitude of wells, distances to nearest canals and canal width. Largest response amplitudes are in the middle and slightly lower portion of the study area (around Aberdeen). Intermediate and smaller responses are spread along the system with a tendency to smaller responses along the main canal.

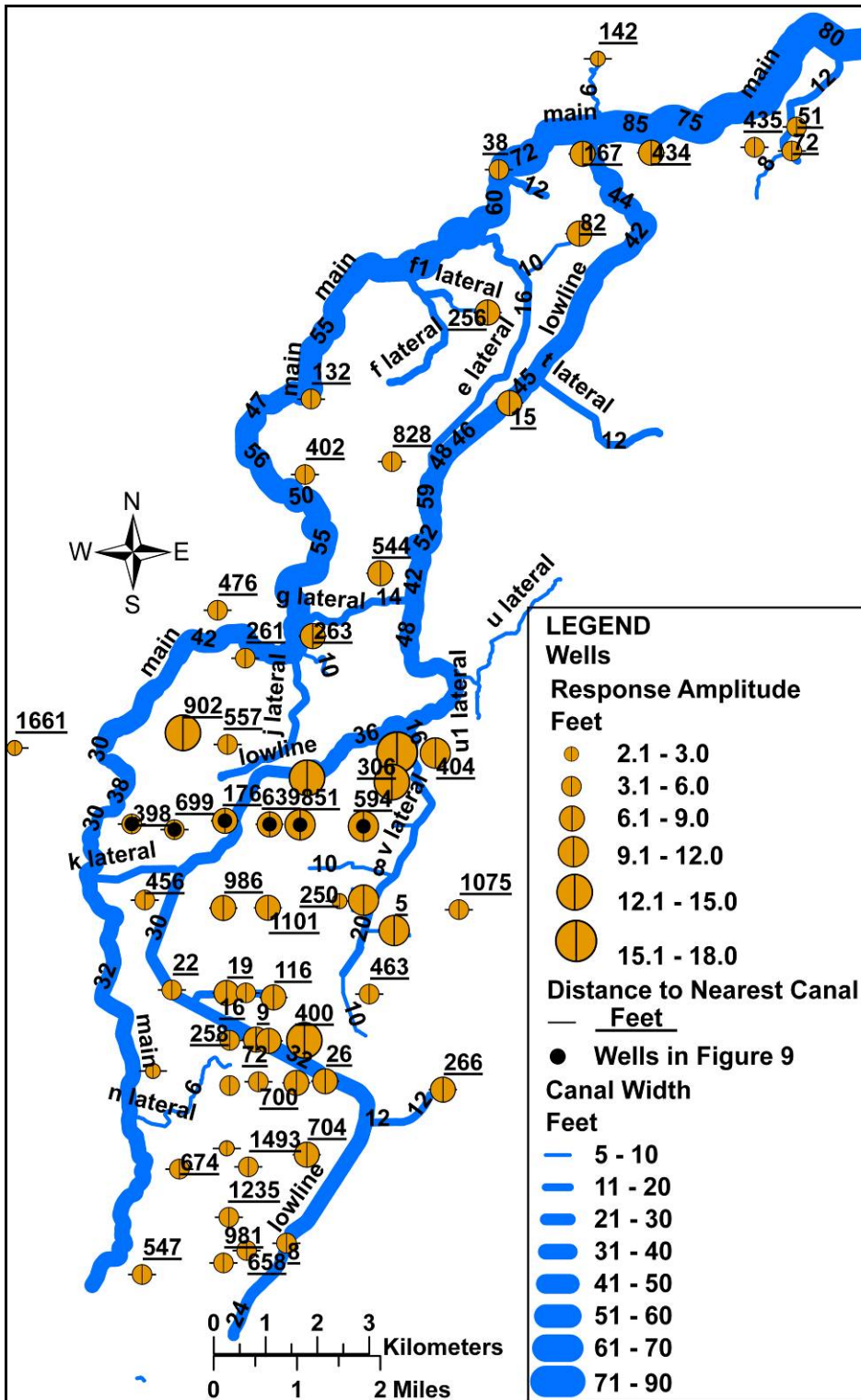


Figure 11. Average annual response amplitude of well water elevation and their spatial relation to canals and canal width. Canal flow is from north-east to south-west.

Attempts were made to identify and discriminate between shallow and deep wells,

as their water levels would likely respond differently to canal leakage. Well depth information was extracted from the drilling log archives and incorporated into the attribute tables for the wells. Idaho Department of Water Resources microfiche archives were searched but depth information was only available for eight wells in the study area. A frequency distribution of the changes in well water elevations was examined and the amplitude of each AARH and its spatial location relative to the canals were compared in an attempt to restrict subsequent analysis only to shallow wells. It was expected that shallow wells tapping the shallow aquifer respond with a greater amplitude compared to deep wells completed below the shallow aquifer. A histogram of well water response amplitudes did not show a distinct bimodal distribution and so could not be used directly to distinguish between shallow and deep wells (Figure 12).

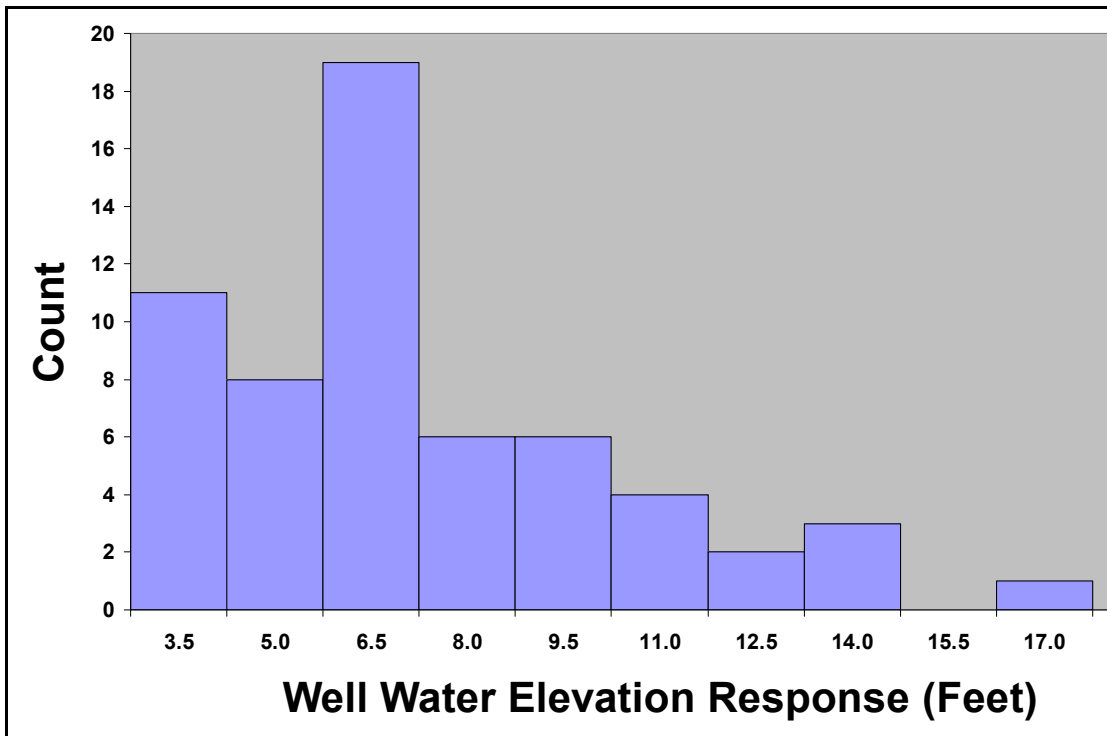


Figure 12. Histogram of average annual amplitude responses in well water elevation over an irrigation season.

The range of well response amplitudes over the irrigation season was from 1.8 to 16.7

feet (0.6 –5.1 m), based on the AARHs. The only example of a difference in AARH amplitude attributable to well depth was seen in a double cased well, where the deeper cased part (well #10.2 at 140 feet total depth) showed relatively small responses compared to the shallow portion at 40 feet TD (well #10.1; Figure 13).

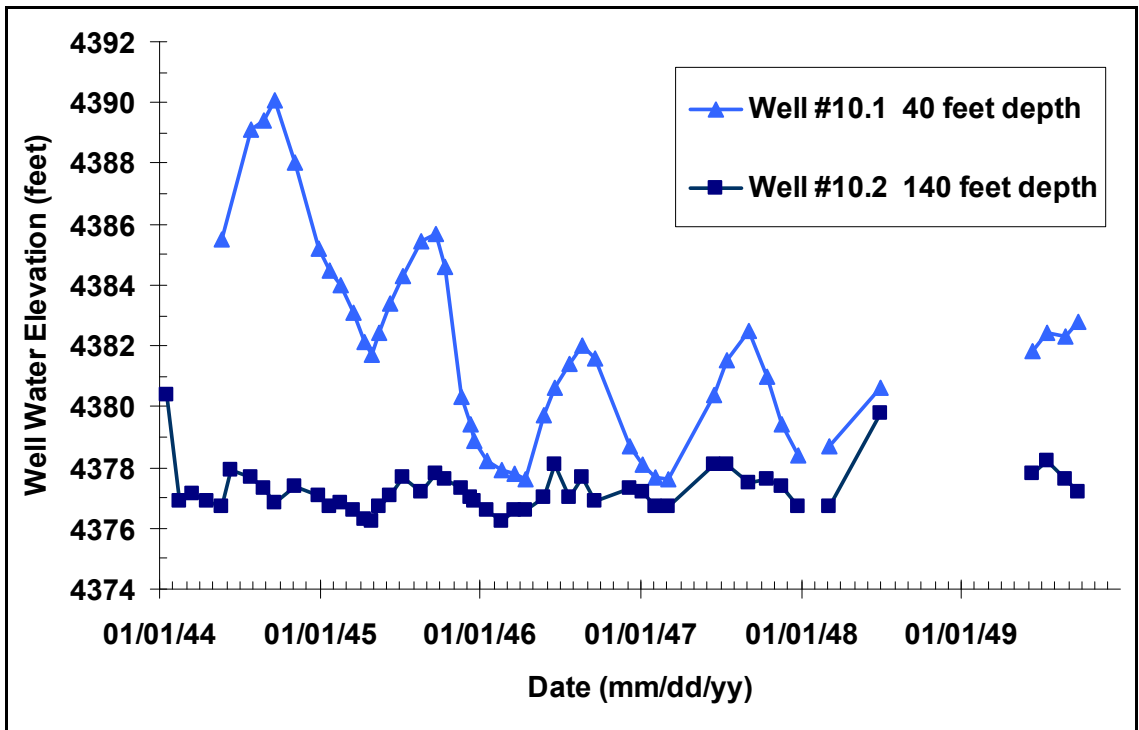


Figure 13. Response hydrographs of double cased well #10.

Other wells in the vicinity (Figure 14) show a gradation in responses relative to well #10. It is likely that the large response amplitude of well #10.1 reflects, in part, the well's proximity to a canal.

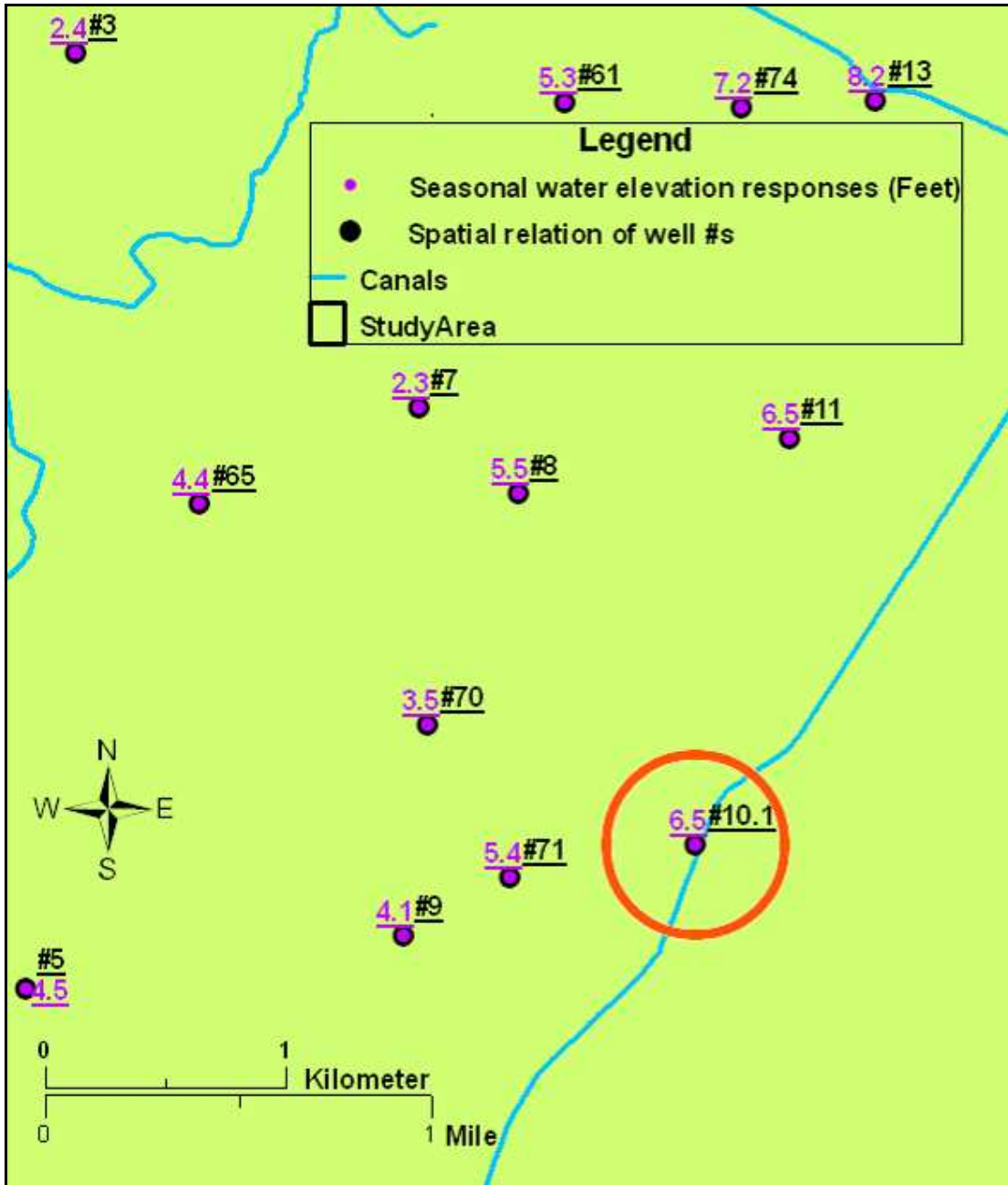


Figure 14. Spatial relation of wells with seasonal water elevation responses in the vicinity of well #10.

Archived well depth data were available for only eight wells including well #10.1.

These wells, having AARH amplitude larger than well #10.2, ranged in depth from 7 feet to 134 feet (2.1 – 40.8 m).

Figure 15 indicates a slight but not statistically significant relationship (95% confidence level) between response amplitude and well depth in wells of known depths.

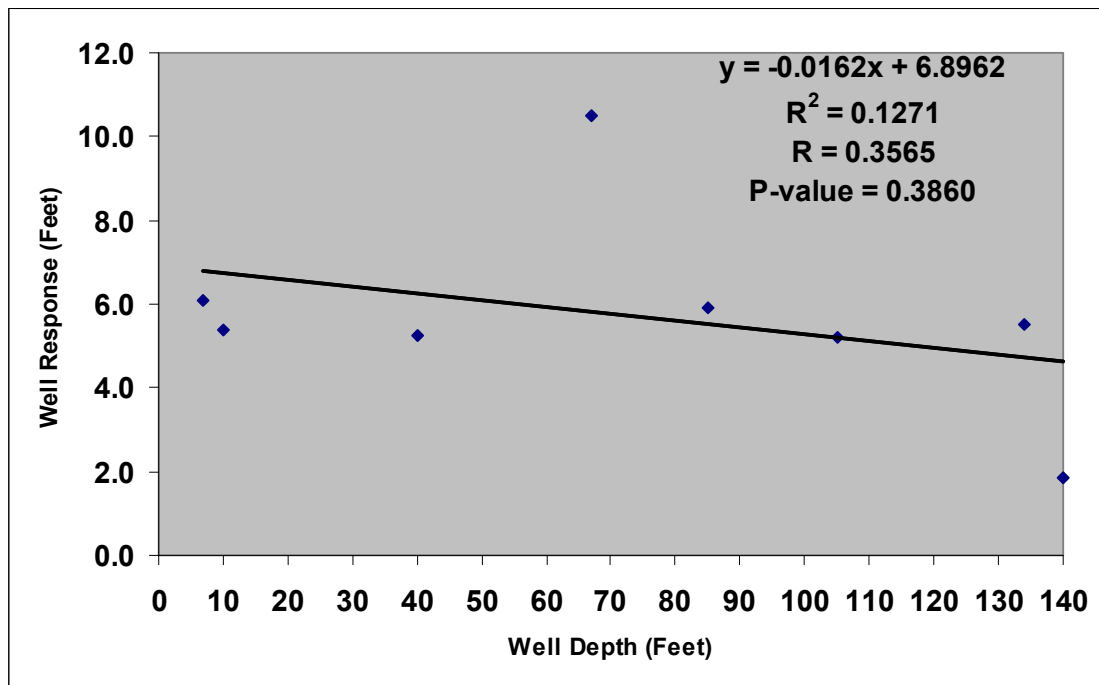


Figure 15. Well response amplitude versus well depth.

Figure 16 indicates there is not a statistically significant relationship at the 95% confidence level between well response and distance from a canal as might be expected if the wells were responding similarly. However, the data set is too small.

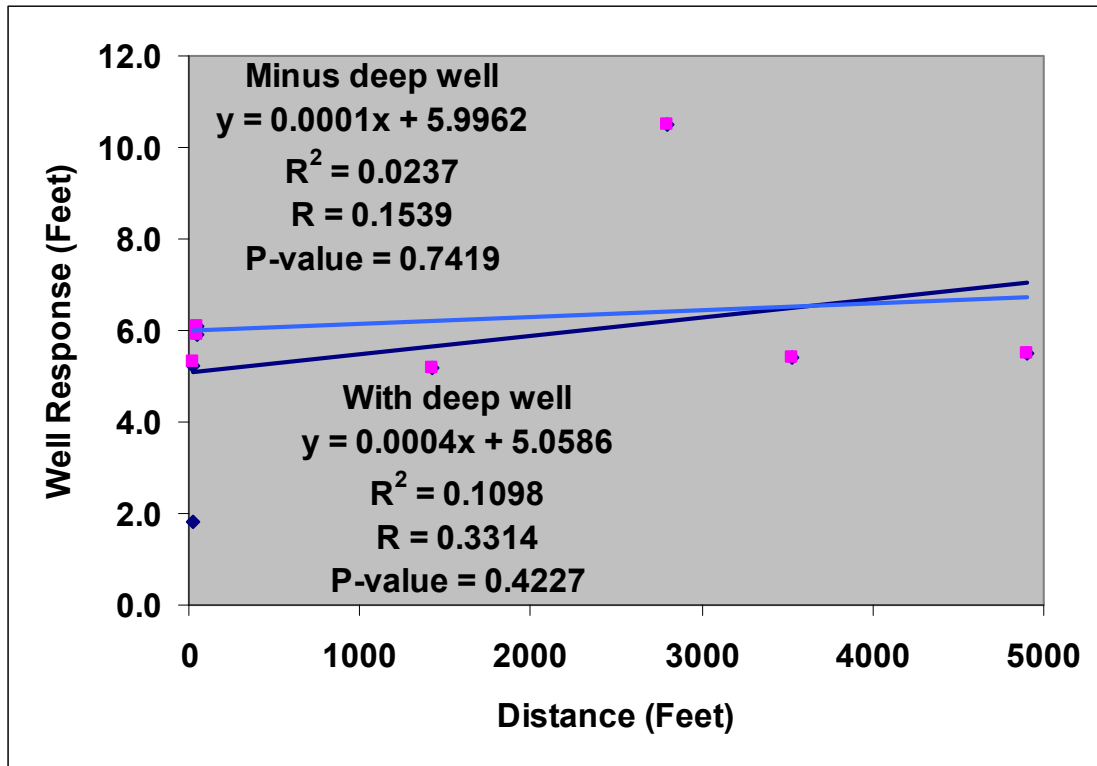


Figure 16. Well response versus well distance from canal. The dark blue point is the deep well.

To further attempt to segregate shallow and deep wells, the responses of well #10 (Figure 13) were used as a guide to simulate the two groups. Assuming the distribution of amplitudes in deep wells is lognormal (as for all wells in Figure 12) the amplitude responses of Figure 12 were first transformed logarithmically. These transformed values were then used to estimate average amplitudes (A_1 , A_2) and standard deviations (s_1 , s_2) of all shallow and deep wells respectively. Maximum amplitude expected in deep wells was defined as $(A_2 + N*s_2)$, where N is the one-tailed standard normal critical value for a confidence level of 99.99%. Conversely, minimum amplitude expected in shallow

wells was defined as $(A1 - N*s1)$. Next, amplitudes below the shallow minimum were allocated to the “Deep” group. Additional amplitudes up to the maximum expected were randomly allocated to the “Deep” group to approximate a normal distribution. The remaining amplitudes were allocated to the “Shallow” group. A t-test with the null hypothesis of no difference was used to compare these two groups of log-transformed values. Table 1 shows that the calculated t-value exceeded the critical t-value and hence the null hypothesis is rejected. This means that the wells were responding differently.

t-Test: Two-Sample Assuming Unequal Variances		
Well Response	"Deep"	"Shallow"
Mean	0.881078	1.864739
Variance	0.018839	0.153996
Observations	6	55
Hypothesized Mean Difference	0	
df	17	
t Stat	-12.7633	
P(T<=t) one-tail	1.95E-10	
t Critical one-tail	1.739607	
P(T<=t) two-tail	3.9E-10	
t Critical two-tail	2.109816	

Table 2. Test of significant difference in mean responses of "Shallow" and "Deep" wells. Calculated t exceeds t-critical, so there is a significant difference in the means at >99% confidence level.

Table 2 shows that the mean distance of these "Deep" wells from the nearest canal were not significantly different (larger) from that of the "Shallow" wells (under the null hypothesis of no difference). Therefore, either response amplitudes are not a simple reflection of Darcy's Law, or these wells represent a mixture of shallow and deep well responses.

t-Test: Two-Sample Assuming Unequal Variances		
Well Distance	<i>"Deep"</i>	<i>"Shallow"</i>
Mean	2146.6667	1387.1273
Variance	3618372.7	1387847.9
Observations	6	55
Hypothesized Mean Difference	0	
df	5	
t Stat	0.9582267	
P(T<=t) one-tail	0.190978	
t Critical one-tail	2.0150484	
P(T<=t) two-tail	0.381956	
t Critical two-tail	2.5705818	

Table 3. Test of significant difference in mean distances of low and high response wells. Calculated t does not exceed critical t, so there is no significant difference in the means at 95% confidence level.

Figure 17 shows that there is not a statistically significant relationship between the well responses and well distances for either the “Shallow” or “Deep” wells (as segregated on page 33). Because the only known deep well is very close to a canal and the limited amount of depth data (Figure 15, 16); and the uncertainty of wells segregated as “Deep”, it was assumed that all response amplitudes reflected shallow wells; and only well #10.2 was excluded from subsequent spatial analysis.

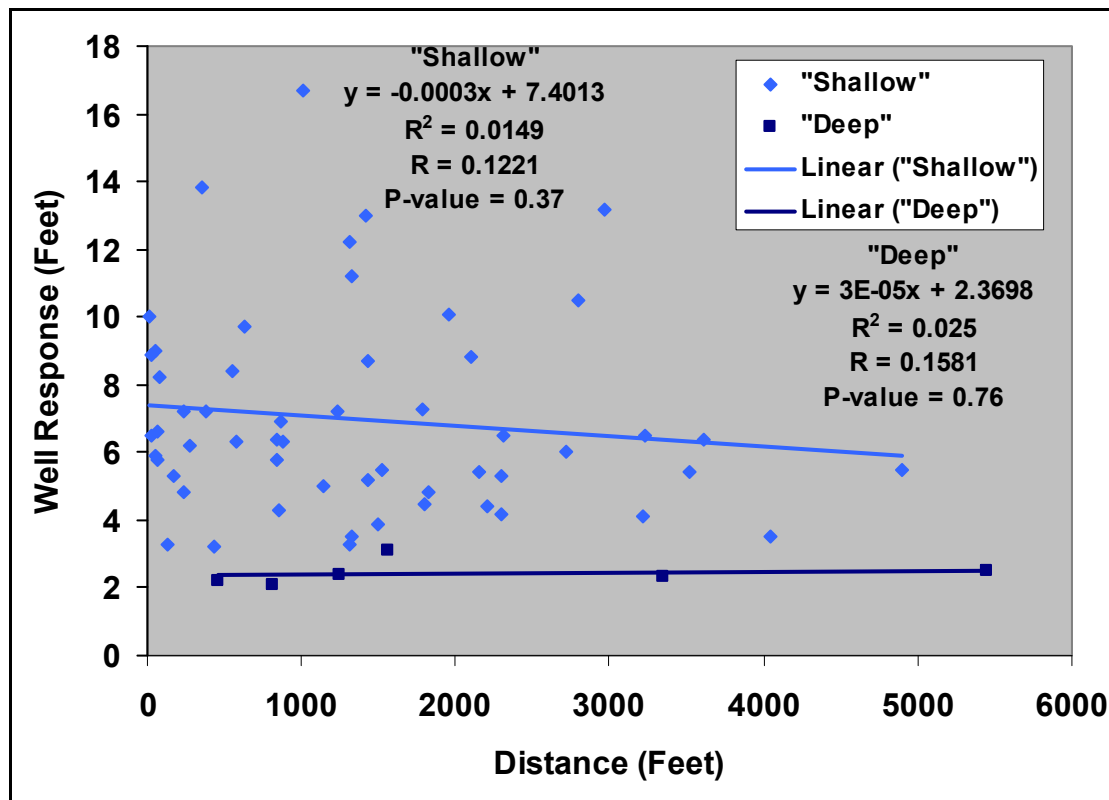


Figure 17. Comparison of well responses over distance.

3.1.6 Canal Water Levels

In the second phase of the study, GPS elevation measurements were made at the high water mark of the canals at the check structure locations. It was assumed that the water level in each reach of canal was determined by the downstream check structure, and canal water levels at canal check structures remained constant during the irrigation

season. The elevations of the canal water levels were measured with the GPS unit at 1-2 decimeter precisions (99% precisions setting) with the Trimble GeoXt equipped with Terrasync software. This required a combination of factors. The minimum number of satellites was set at six. In most instances more than six satellites were obtained. The Dilution Of Precision (DOP) value is a measure of satellite configuration on GPS accuracy (Trimble, 2000). The satellite geometry is strong and the DOP value is low when visible satellites are far apart. Such a configuration provides better positional accuracy because of the wider angular separation between the satellites used to calculate the position of a GPS unit.

DOP is expressed in several forms: horizontal (HDOP), vertical (VDOP), positional (PDOP, 3-Dimensional) and time (TDOP). The maximum PDOP (PDOP mask) was set at six, which is recommended as the highest allowable setting to obtain reliable measurements for most applications and mapping receivers (Trimble, 2000). This usually controlled the VDOP as well as the HDOP (the GeoXT did not have an independent control for VDOP). In most instances the VDOP was less than 2.5. The elevation mask was set higher than the base station to ensure that signals for post processing corrections were received from the same satellites. Thirty points were considered adequate if the VDOP was two or less and the overall final precision was 1-2 decimeters. Sometimes data collection was a trade-off between rapidly changing weather conditions and numbers and orientation of satellites, while trying to determine an adequate number of readings. If clouds were forming rapidly (with the likelihood of increased multipath errors) or if the time period of adequate satellites was nearly ended, a smaller number of points were collected so as not to lose the collection opportunity

entirely. Number of points tested varied from 10 to over 900. The final consideration of adequacy was whether the combined data within the precision limits was consistent with water flowing downstream. In other words, no reach of canal could have a higher elevation than one upstream. If the data implied this, the number of data points, VDOP, etc. were examined to determine which elevations should be rechecked.

3.2. Data Modeling and Calculations

In the third phase, several data transformations and calculations were performed. This included (1) estimating ground water elevations for gradient calculations via kriging, (2) evaluating the uncertainty of kriged ground water level estimates, and (3) developing a seepage index. Kriging was chosen because it is the best linear unbiased estimator (BLUE), i.e. minimizing the variance of the predicted values.

3.2.1 Estimating Ground Water Elevations for Gradient Calculations.

To facilitate application of the model across the whole study area, ground water contour data were calculated, extracted and tabulated for the model inputs. Interpolated monthly ground water levels were estimated from the well data by kriging, a geostatistical interpolation technique for estimating values from nearby measured values. Kriging is a smoothing interpolator that minimizes prediction error variance at all measurement locations. It is a best linear unbiased estimator using a search strategy that assigns greater weights to closer neighbors than farther neighbors while constraining the sum of weights to 1.0. The same search strategy is applied over the full extent of the data. Elevations read from the kriged water table surface were subsequently used to conduct the Darcy flux analysis at any given location. Sample results of the contours obtained from interpolation of the monthly well elevation data are shown below (Figure

18).

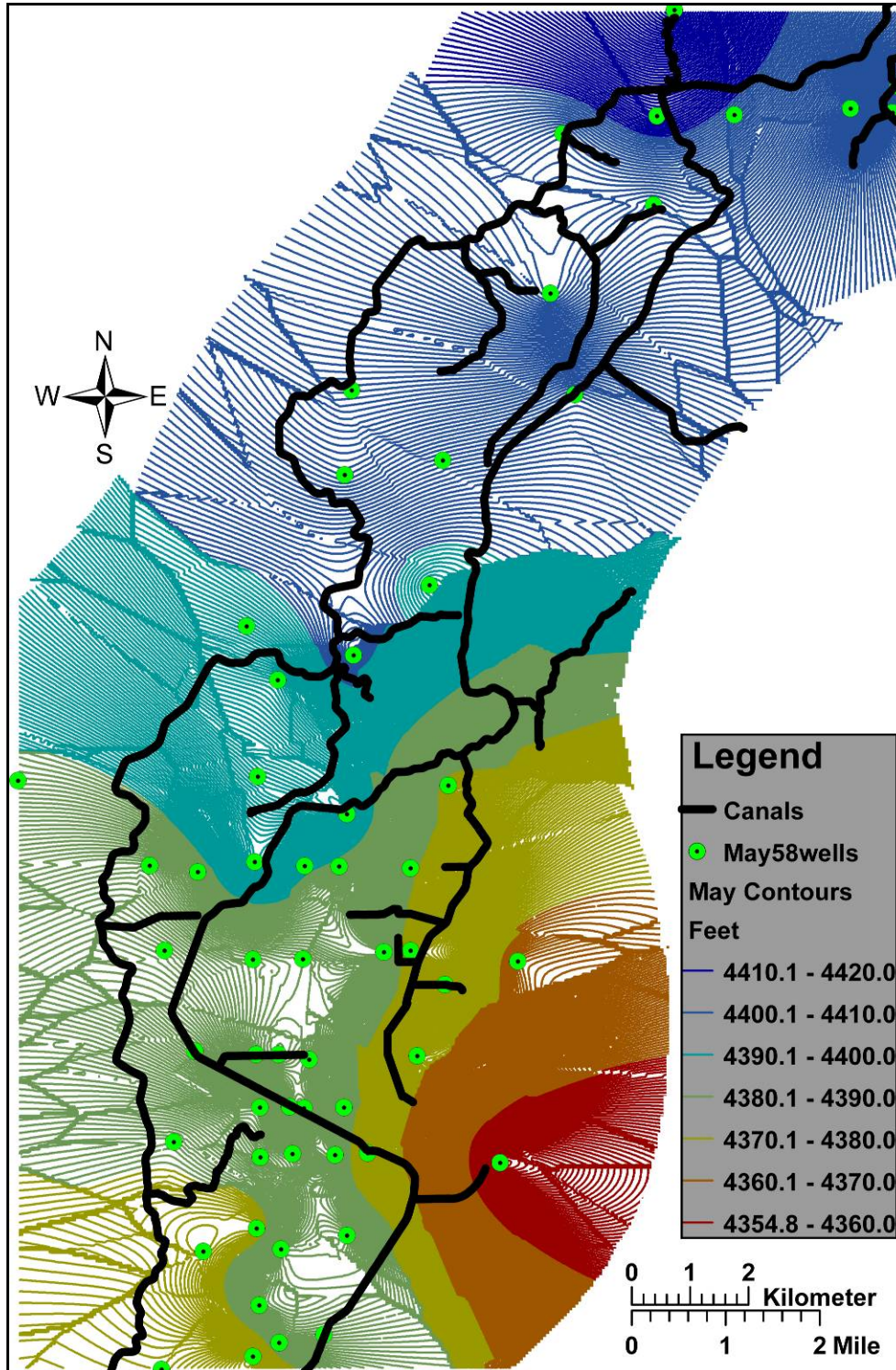


Figure 18. May contours of ground water interpolated from historical well water elevation data and the AARHs of each well. Ground water flow is from north-east to south-west.

3.2.2 Evaluating Uncertainty of Kriged Ground Water Level Estimates

The spatial and temporal differences in water elevation responses predicted by kriging were evaluated in two stages. In the first, the uncertainty of the kriged water table elevations were evaluated for each season (May versus August) to simulate uncertainty due to sample location. For May, kriging was repeated with sequential removal and replacement of each of the 57 wells, thereby generating 58 slightly different water level maps. The kriged surfaces were saved as rasters (Figure 19) and the process repeated for August (only 53 wells). The resulting Gaussian distribution of ground water elevations at each well location was used to test for significant differences between May and August's interpolated ground water levels. Since all of the ground water elevations near the canals are derived from interpolation, and well density was low in some areas, it was decided to use all available well location data (May, $n = 57$; August, $n = 53$) rather than only locations that had data for both May and August.

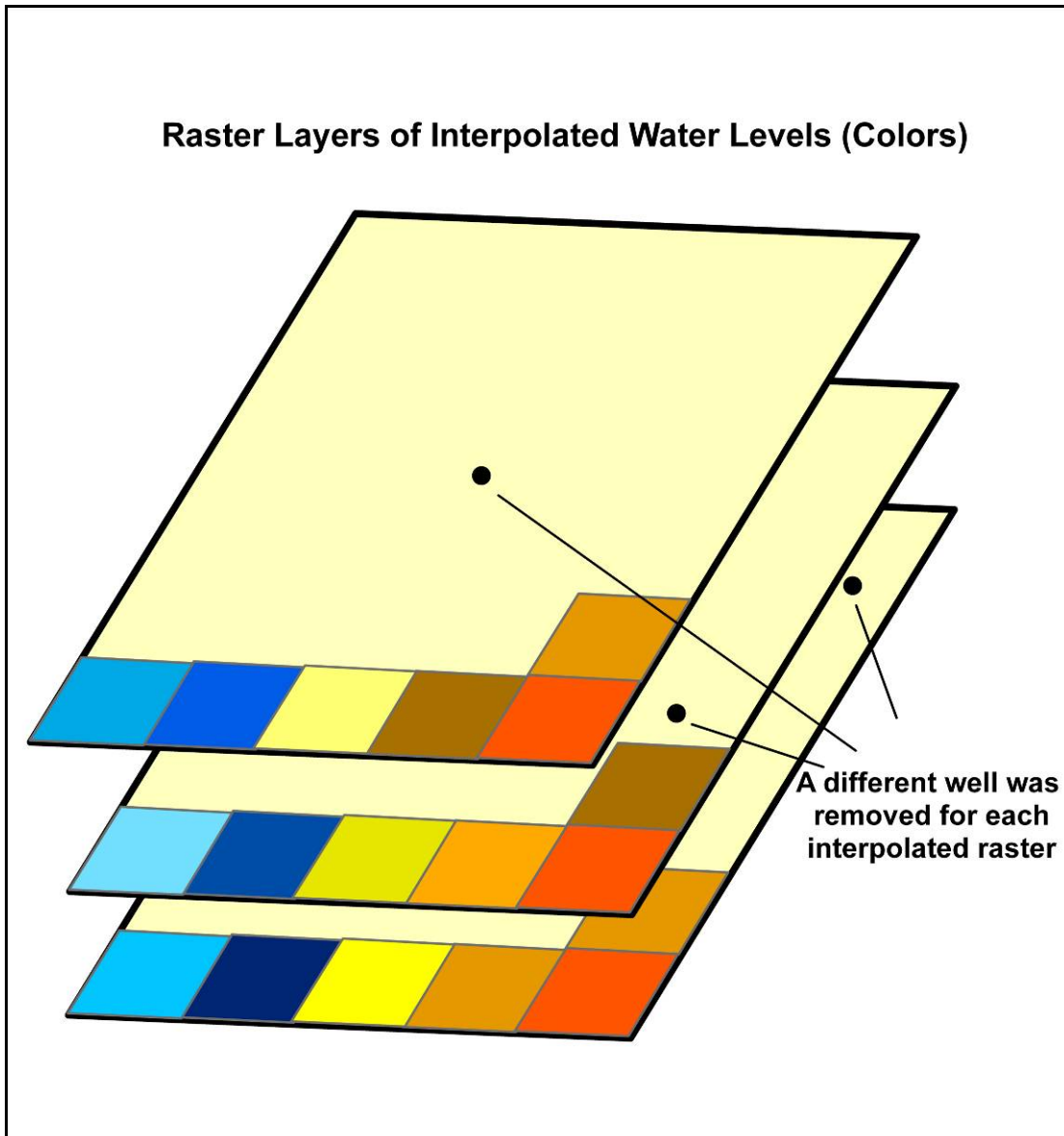


Figure 19. Diagram illustrating how kriged map rasters were used to calculate means and standard deviations of interpolated water level at each grid cell. Each layer represents the interpolated water level with one data point withheld. Each layer simulates an alternate interpolation for each well. Cell statistics were calculated at each grid location for the multiple layers combined, for both May and August.

Figure 20 shows the resulting raster maps of the mean interpolated water elevation contours for August and May. The mean and standard deviation among the multiple maps at each grid location were calculated with Spatial Analyst's cell statistics tool. The means were examined to determine whether August's interpolated water levels were

significantly greater than May's, especially in the area where five well locations have missing data for August (Figure 6). Results will be discussed in subsequent sections.

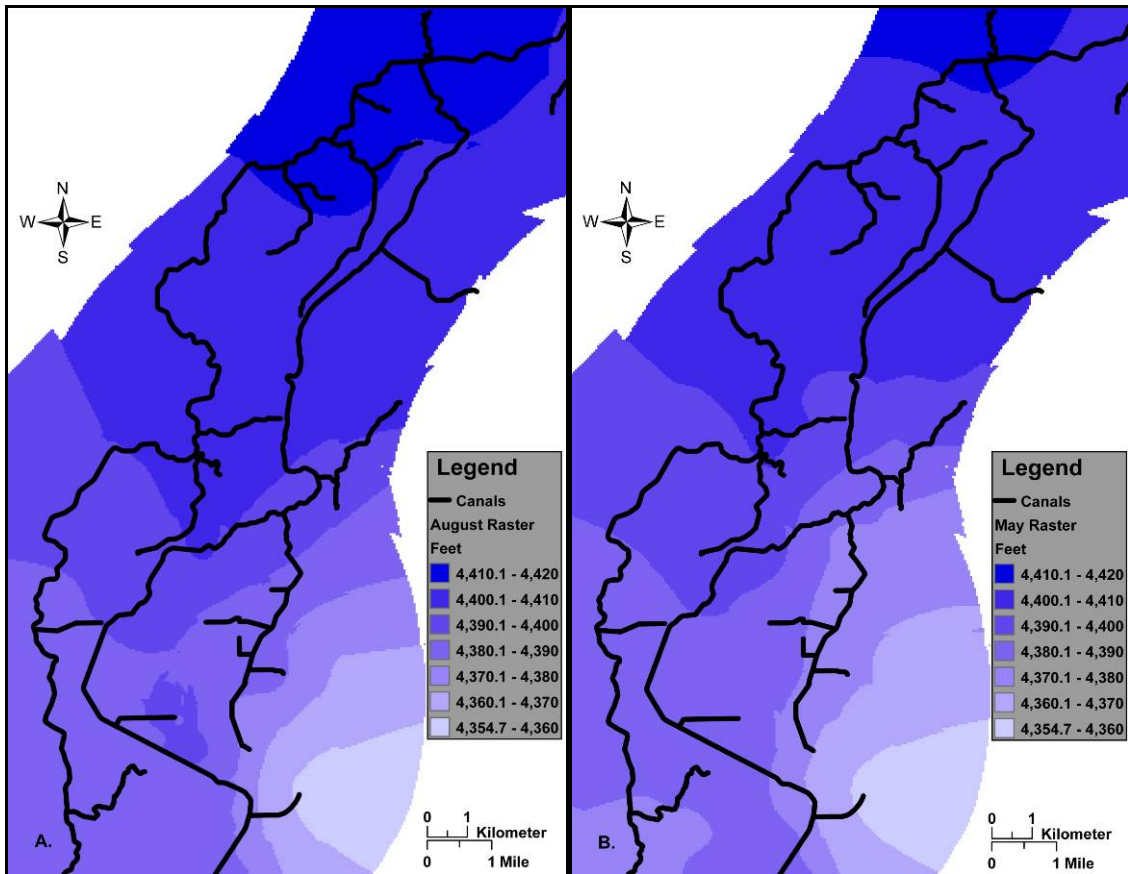


Figure 20. Ground Water Elevations. August (A.) and May (B.) Raster of Means.

The second stage of the evaluation consisted of identifying statistically meaningful differences between the months. The null hypothesis is that August and May water elevations are statistically indistinguishable at each grid cell. The alternate hypothesis is that they are different. This is accomplished in the following eight steps (modified after Welhan, 2005):

1. Choice of confidence levels. In testing for temporal differences, too low a level of significance increases the false negative error rate. That is, if the risk (α) of rejecting a true null hypothesis is set too small, the risk (β) of accepting a false null hypothesis is

increased. This would decrease the power of the test ($1-\beta$). Here, the 90% confidence level ($1-\alpha$) is chosen to provide more power for the test.

2. Calculation of a Difference Map between the May and August water level rasters (Difference = August raster minus May raster). Figure 21 shows the calculated differences.

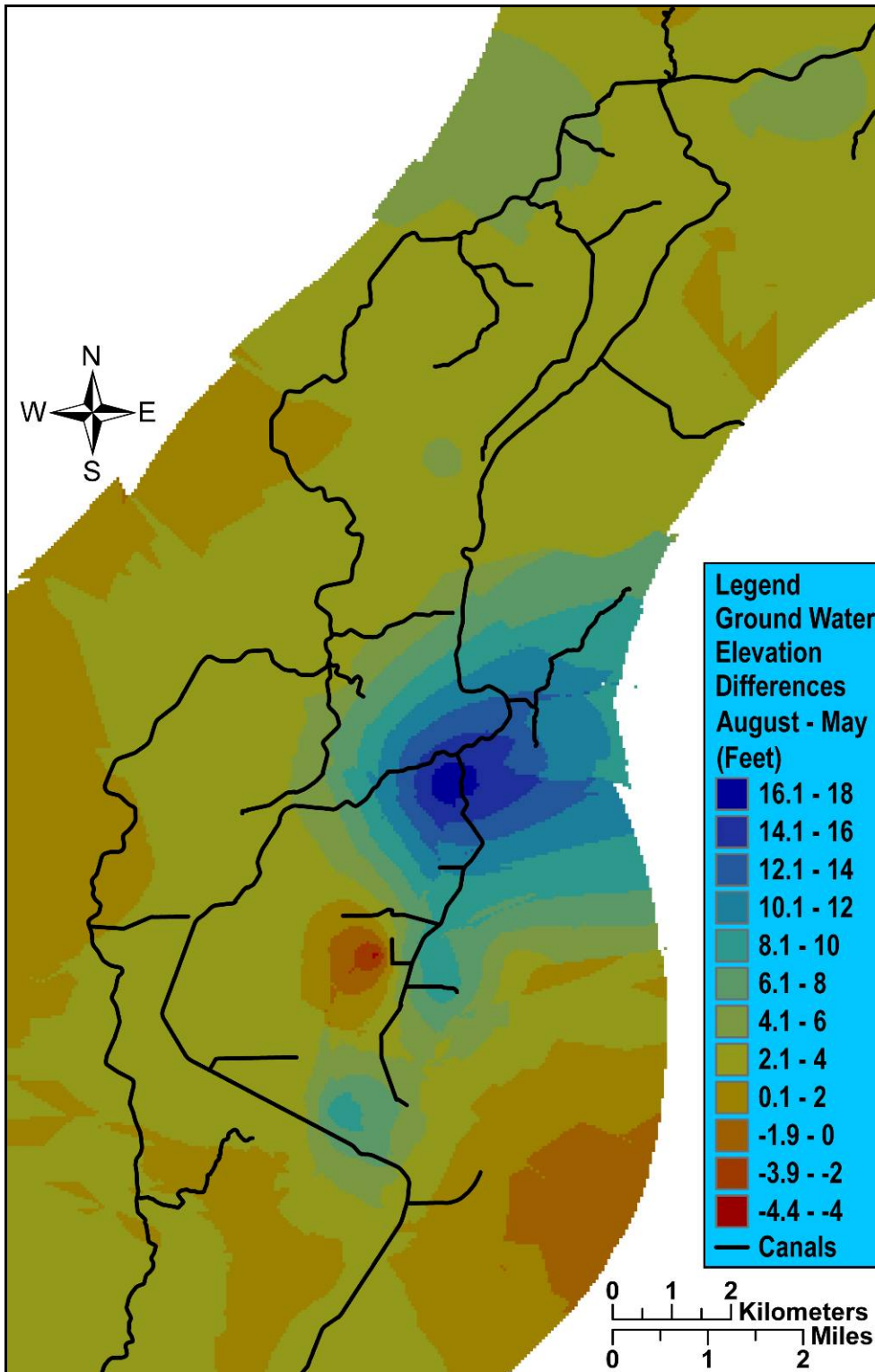


Figure 21. Ground Water Elevations Difference map: August minus May raster of means.

3. Calculation of the tail offsets (O_i) above and below the mean at each grid cell

location, for each month. Differences in the estimates of the mean ($\mu_{\text{Aug}} - \mu_{\text{May}}$ or $\mu_{\text{May}} - \mu_{\text{Aug}}$) that fall between the tail areas are significantly different at the chosen level of significance (Figure 22 and 23).

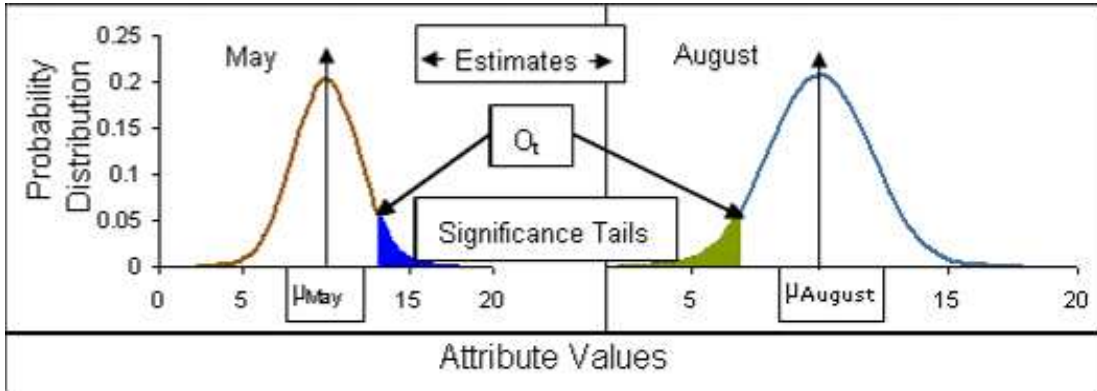


Figure 22. Identifying statistically meaningful positive differences in kriging estimates at a single location.

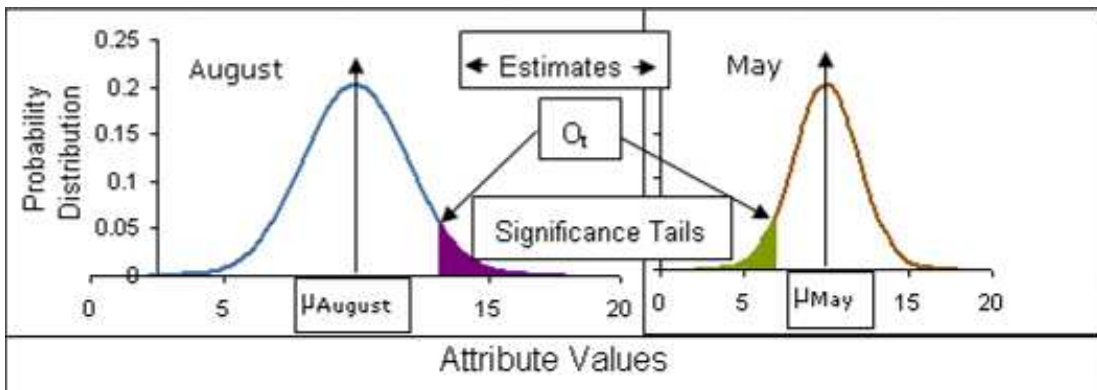
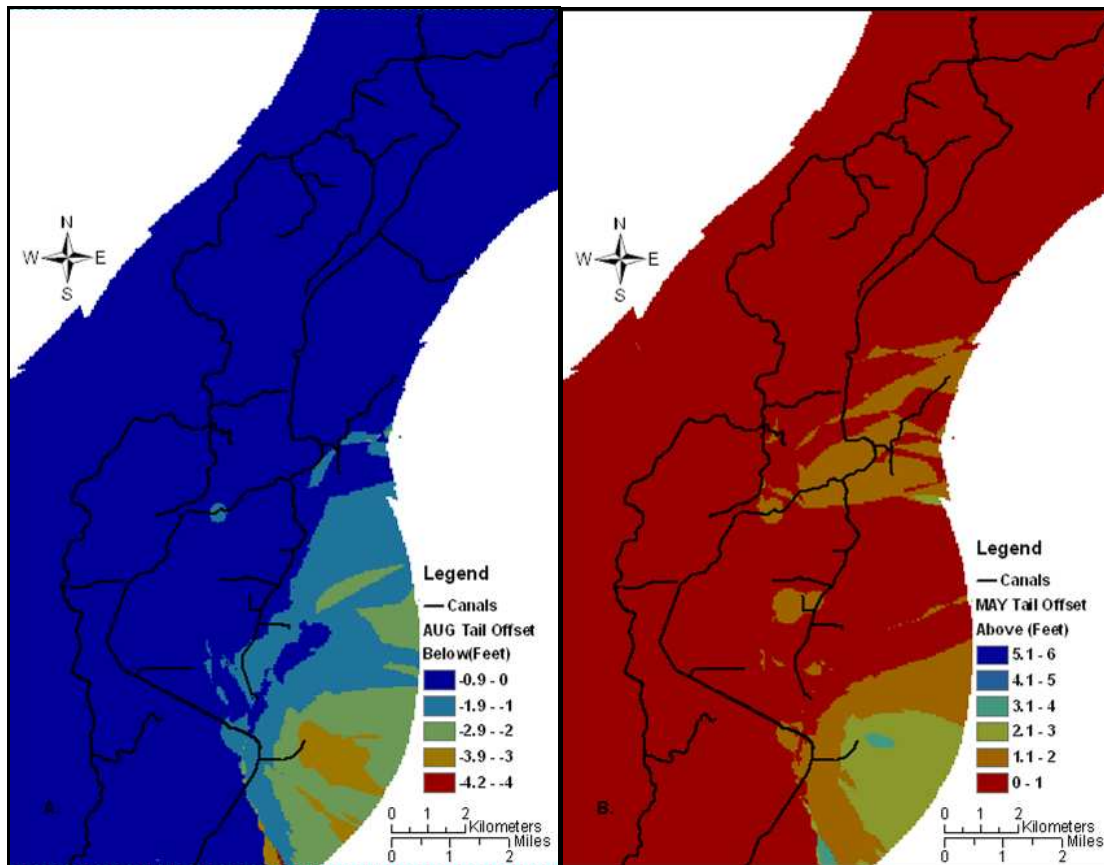
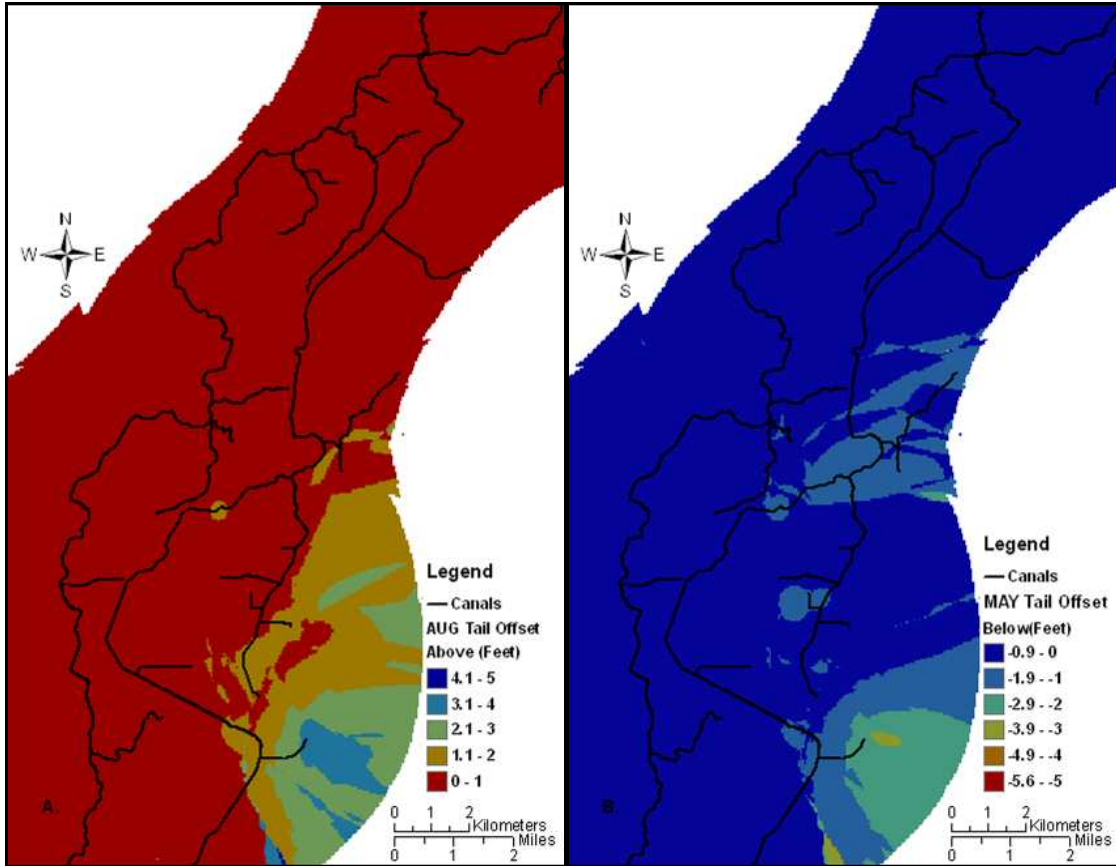


Figure 23. Identifying statistically meaningful negative differences in kriging estimates at a single location.

Calculation of the values outside of the confidence limits is accomplished in the following manner: The value of the product of the standard normal deviate (O_i), for a particular confidence level, and the standard deviation (σ) must be added to or subtracted from the kriging estimated mean (μ_{May}, μ_{Aug}) to calculate tail offsets, beyond which the values are significantly different from the estimated mean. Figures 24 and 25 show the distribution of the tail offset values for May and August.



A. Tail Offset Below Mean –AUGUST B. Tail Offset Above Mean - MAY
 Figure 24. Tail offsets used for calculating positive significant differences in August (A) and May (B).



A. Tail Offset Above Mean - AUGUST B. Tail Offset Below Mean -MAY
 Figure 25. Tail offsets used for calculating negative significant differences in August (A) and May (B).

The tail offsets above (O_{tMay}^{above} , O_{tAug}^{above}) and below (O_{tMay}^{below} , O_{tAug}^{below}) the mean at a 90% confidence level, are all 1.28 standard deviation units (this is a one-tailed test since the interest is in whether one mean exceeds the other). Estimates of the means were set equal to the kriging means (μ_{May} , μ_{Aug}), and KSD_{May} , KSD_{Aug} are the kriging standard deviations at each grid cell. The subsequent calculations are:

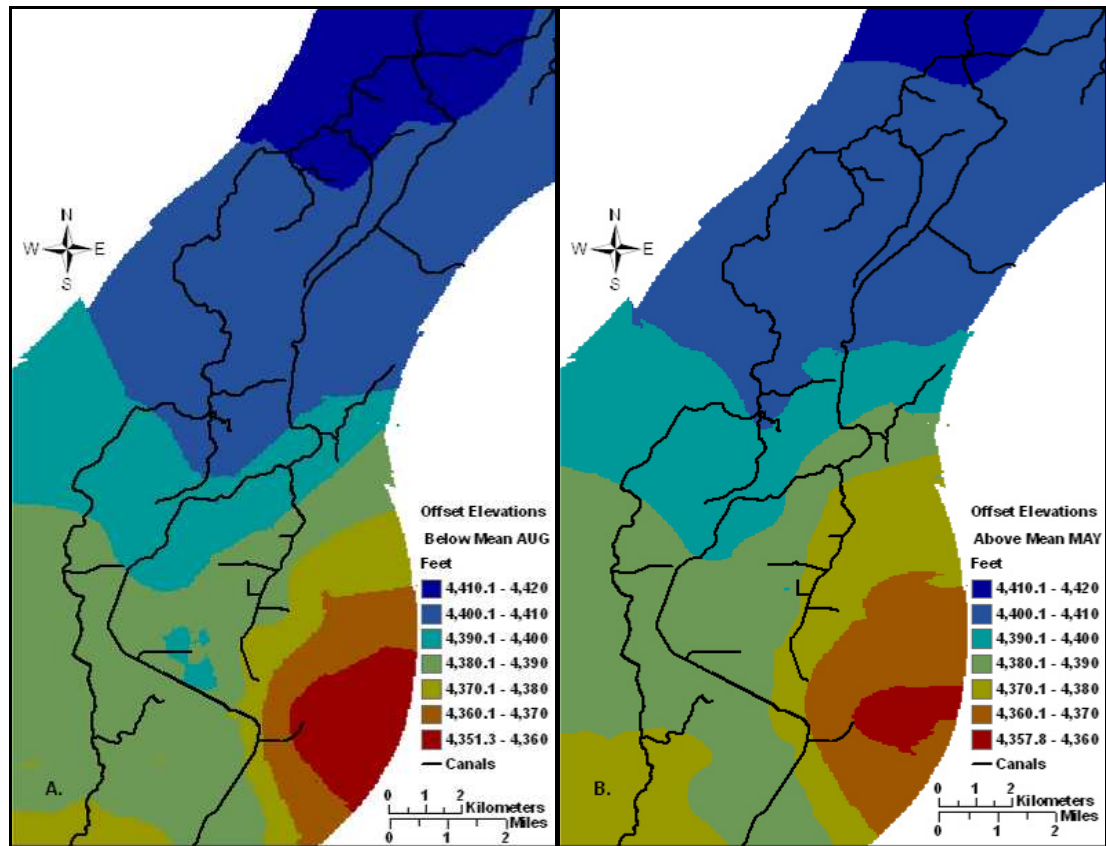
$$O_{tMay}^{above} = [\mu_{May} + O_t * KSD_{May}] \text{ and } O_{tAug}^{above} = [\mu_{Aug} + O_t * KSD_{Aug}]$$

$$O_{tMay}^{below} = [\mu_{May} - O_t * KSD_{May}] \text{ and } O_{tAug}^{below} = [\mu_{Aug} - O_t * KSD_{Aug}].$$

4. Significant positive differences were identified as follows: If the lower tail offset in August O_{tAug}^{below} , is greater than the upper May tail offset, O_{tMay}^{above} then the difference is significant at 90% confidence (= 1). If the difference is less than zero, the

distributions overlap to such an extent that the values in the first distribution are not significantly different outside the confidence limits of the other distribution ($= 0$).

Figure 26 shows the offset elevations used to calculate the significant positive differences between August and May.



A. Tail Offset Elevation – AUGUST ($\mu - O_t$ KSD) B. Tail Offset Elevation – MAY ($\mu + O_t$ KSD).

Figure 26. Tail offset elevations used for calculating positive significant differences in August (A) and May (B).

Figure 27 shows the resulting areas of significant positive differences in ground water elevations between August and May. The largest area of insignificant change is in the south eastern corner of the study area where well control was lacking.

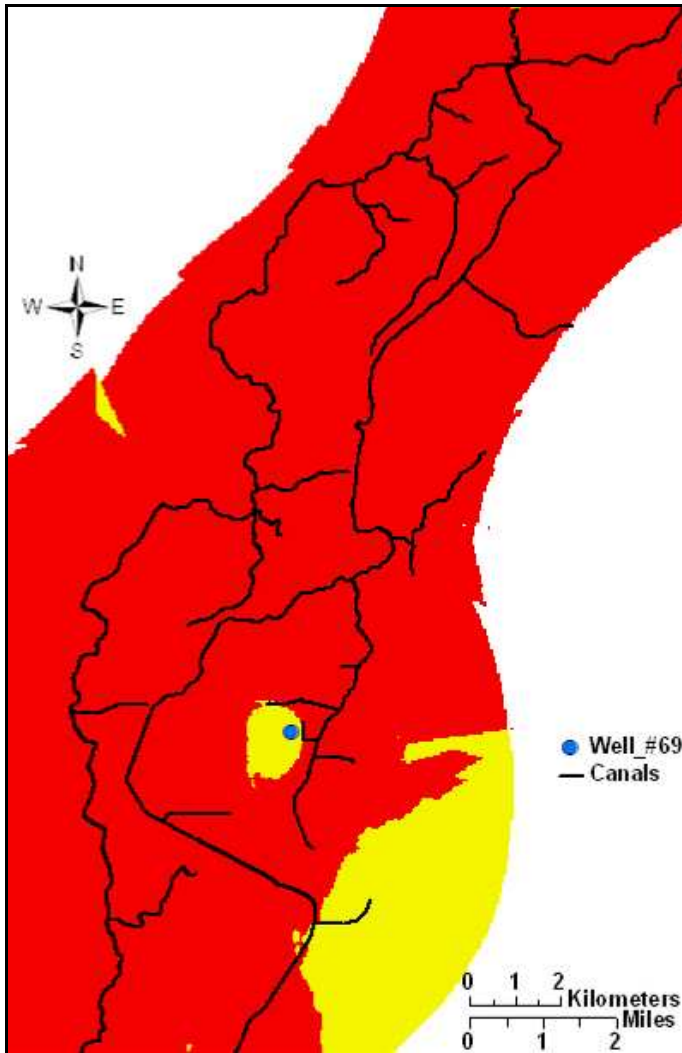
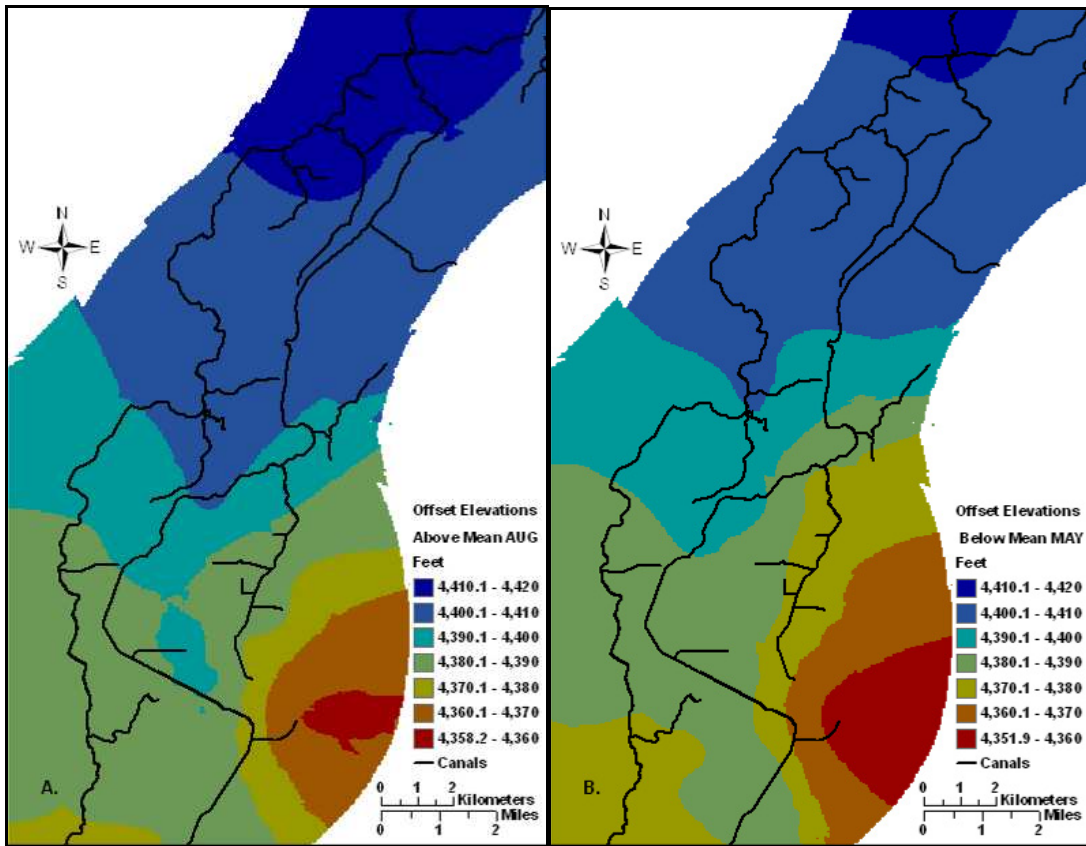


Figure 27. Areas of positive significant differences in red and statistically insignificant differences (yellow) at a 90% confidence level.

The kriging estimates for locations near well #69 (Figure 27), with missing data for August, were lower in August than in May, in contrast to other locations (#26, 31, 32) missing data for August, so that the estimates around this location produced negative differences.

5. Significant negative differences were identified in a similar manner. The

reasoning is analogous to step 4 but in the opposite sense. Figure 28 shows the resulting offsets used to identify the significant negative differences between August and May.



A. Tail Offset Elevation – AUGUST ($\mu + O_t$ KSD) B. Tail Offset Elevation – MAY ($\mu - O_t$ KSD).

Figure 28. Tail offset elevations used for calculating negative significant differences in August (A) and May (B).

Figure 29 shows the resulting areas of significant negative differences in ground water elevations between August and May. Except for the vicinity of well #69, there are no significant decreases in ground water elevation between May and August.

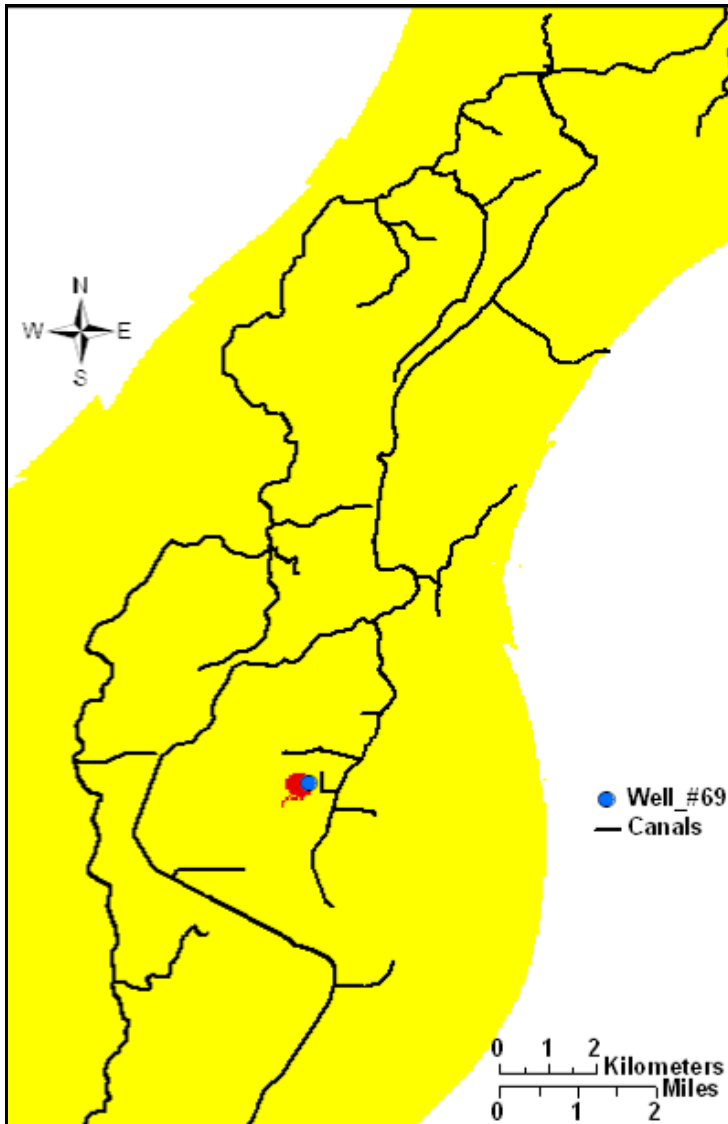


Figure 29. Areas of negative significant differences in red and statistically insignificant differences (yellow) at a 90% confidence level.

6. Maps of significant positive differences were then obtained by multiplying the difference map from step 2 by the results of step 4 (Figure 30A).

7. Maps of significant negative differences were then obtained by multiplying the

difference map from step 2 by the results of step 5 (Figure 30B).

8. These two maps were added to give a final composite map of differences that are significant at the 90% confidence level (Figure 31).

Figure 30 shows that except for the immediate vicinity of well #69, significant positive differences in ground water elevation between the beginning and end of the irrigation season occur throughout the canal system, with the greatest increase in the central study area, beneath a portion of the lower canal system.

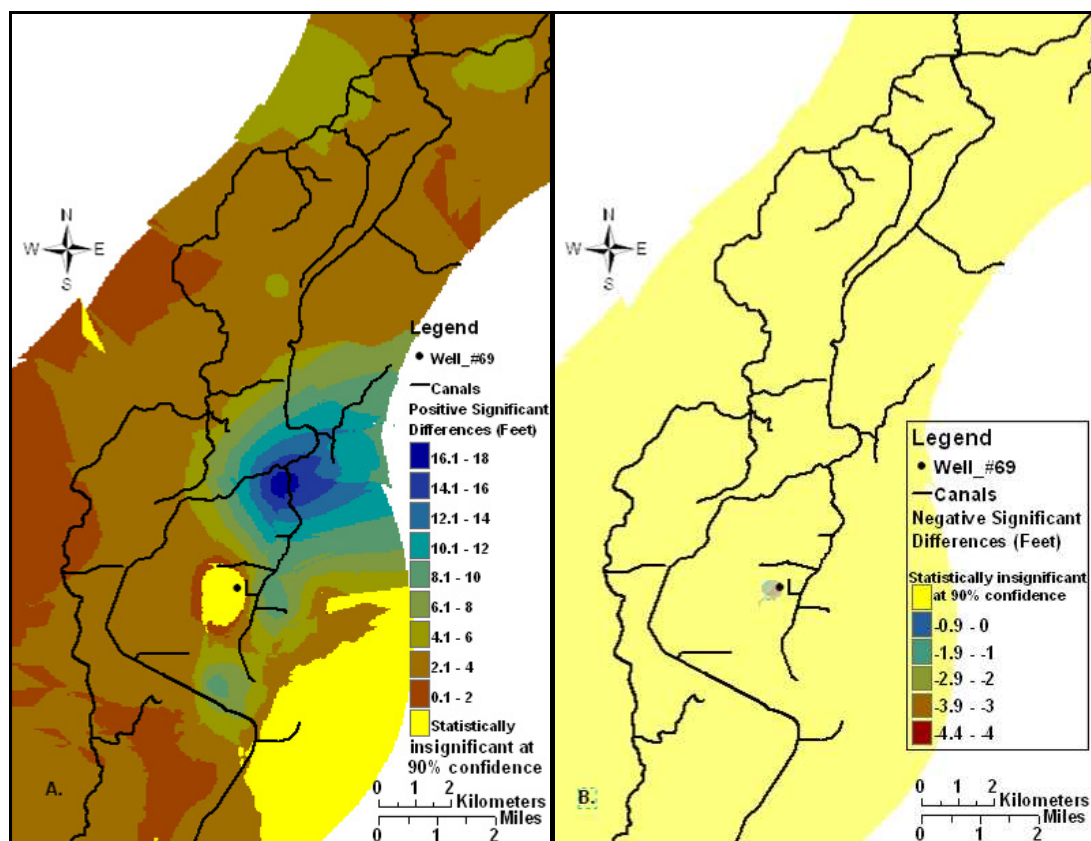


Figure 30. Areas of significant water elevation differences at 90% confidence level. A. Positive differences. B. Negative differences. Yellow areas are statistically insignificant at the 90% confidence level.

Since regional ground water elevations decrease in all areas of the ESRP during the irrigation season due to pumping withdrawals (IDWR, hydro.online-gwl, 2009), it is concluded that canal leakage and/or surface over-irrigation must have a substantial

impact on local, shallow ground water levels in this area.

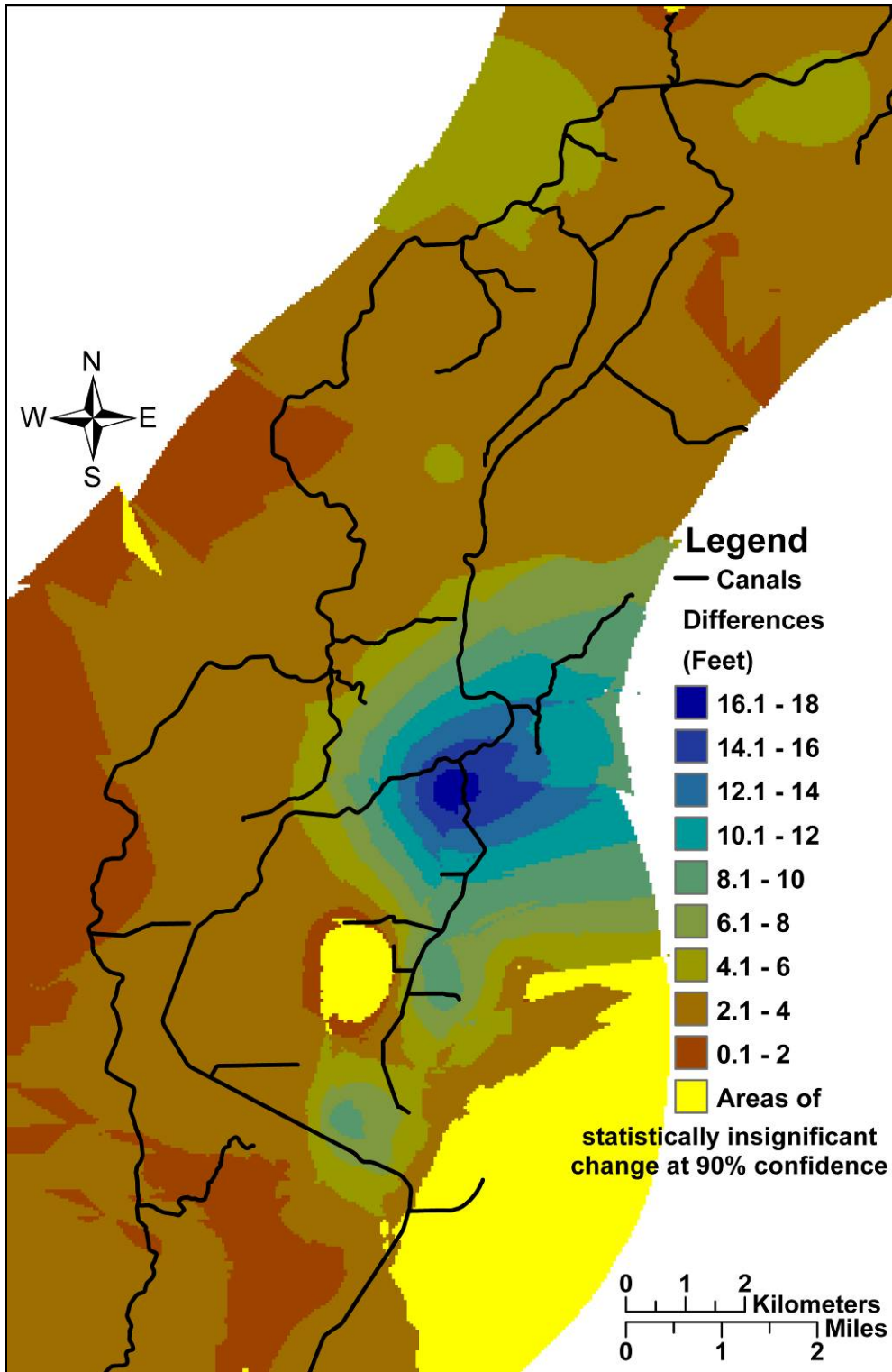


Figure 31. Composite map of positive and negative changes in ground water levels over the irrigation season that are statistically significant at 90% confidence.

3.2.3 Horizontal Hydraulic Gradient Calculations at Any Canal Location

The canal reaches where ground water elevation differences were statistically significant were used to estimate hydraulic gradients and changes in gradient. To facilitate the analysis, the canal reaches between check structures were split into sub-reaches thereby dividing canals with substantial bends or turns into quasi-linear reaches. The interpolated ground water elevations for each canal reach were obtained by intersecting the contour lines in Figure 18 with a 50 foot (15.24 m) buffer zone boundary on either side of the canals. The upstream and downstream values of the ground water contours at the intersections with the buffer were averaged for each canal reach, providing a single value for calculating local hydraulic gradients. The average horizontal hydraulic gradient perpendicular to each canal reach was calculated by subtracting the average ground water contour intersection value from the elevation of its canal reach and dividing by a distance of 50 feet.

The rates of change of gradients between May and August were also computed for each canal reach. The following equations were used in these calculations:

I_{May} , I_{Aug} = the horizontal hydraulic gradient between the canal water elevation (h_{canal}) and the estimated ground water elevation (h_{gw}) at the 50-foot buffer distance from the canal, for May and August, respectively;

$$\text{where } I_{May} = (h_{canal} - h_{gwMay}) / 50 \quad \text{ft/ft} \\ \text{(m/m)}$$

$$\text{and } I_{Aug} = (h_{canal} - h_{gwAug}) / 50 \quad \text{ft/ft (m/m),}$$

$$\Delta I / \Delta t_{MayAug} = \text{the monthly rate of change of gradient between May and August} = \\ (I_{May} - I_{Aug}) / 3 \quad \text{ft/ft/mth (m/m/mth);}$$

$\Delta h / \Delta t_{\text{AugMay}}$ = monthly rate of change in ground water elevation between May and August = $(h_{\text{gwAug}} - h_{\text{gwMay}}) / 3$ ft/mth.

3.2.4 Calculating a Seepage Index

In order to rank the canal reaches in terms of relative seepage loss, a relative seepage index, X was defined for the factors that might reflect hydraulic conductivity variations. Three factors were considered: the inverse of the gradient at the beginning of the season, $1/I_{\text{May}}$, the rate of change of gradient over the season, $\Delta I / \Delta t_{\text{MayAug}}$, and the rate of change in ground water elevation over the season, $\Delta h / \Delta t_{\text{AugMay}}$. These three factors were used to calculate the primary indicators although others could have been used. The inverse of the May gradient ($1 / I_{\text{May}}$) was used because, under static conditions, Darcy's Law ($q = KI$) predicts that the lateral hydraulic gradient (I) varies as the inverse of lateral hydraulic conductivity (K) for a given horizontal groundwater flux ($q = Q/A$). The inverse of August gradient was not used as it was considered that any variance introduced by background depletion of the area groundwater would be greater in August than in May. The form of the seepage index then is:

$X = a * 1 / I_{\text{May}} + b * \Delta I / \Delta t_{\text{MayAug}} + c * \Delta h / \Delta t_{\text{AugMay}}$ i.e. a weighted sum, weighted by each factor's relative contribution to seepage and the length and/or area of their contributing canal reaches. An average weight for each factor based on canal length was calculated from the sum of the products of the individual factor and reach length divided by the sum of the individual reach lengths ($= \sum(1 / I_{\text{May}} * L_n) / \sum L_n$, where L_n is the length of the individual canal reach). For weighting by area, the calculation uses individual reach top surface areas, A_n , (= canal length * canal width) in place of lengths. These weights are designated by the subscripts L and A for length and area, respectively.

The average weights by canal length are $a_L, b_L, c_L = \sum(X_i * L_n) / \sum L_n$ where X_i is $1 / I_{May}, \Delta I / \Delta t_{MayAug}, \Delta h / \Delta t_{AugMay}$, respectively.

Similarly, the average weights by canal area are: $a_A, b_A, c_A = \sum(X_i * A_n) / \sum A_n$.

Prior to summing the factors, each was normalized relative to its maximum value in order to equalize the magnitudes of the factors before combining into a final index:

$$X = a / I_{May} / \text{maximum} (1 / I_{May}) + b * \Delta I / \Delta t_{MayAug} / \text{maximum} (\Delta I / \Delta t_{MayAug}) + c * (\Delta h / \Delta t_{AugMay}) / \text{maximum} (\Delta h / \Delta t_{AugMay}).$$

3.2.5 Ranking Relative Seepage Loss

The relative seepage index, X , was then ranked and the results compared to rankings based on the individual factors. The relative seepage indices were mapped and overlaid on the canal reaches in the study area using a ten percent classification interval to highlight areas of the highest seepage loss.

3.2.6 Sensitivity Analysis of Kriged Water Levels

Because the relative seepage index is defined wholly in terms of hydraulic head terms estimated by kriging the available well water level data, the kriging process was subjected to a sensitivity analysis. Forty eight multiple alternative water level maps were generated with sequential removal and replacement of wells (as described in section 3.2.2), but this time withholding a subset of ten randomly selected well locations (Figure 32).

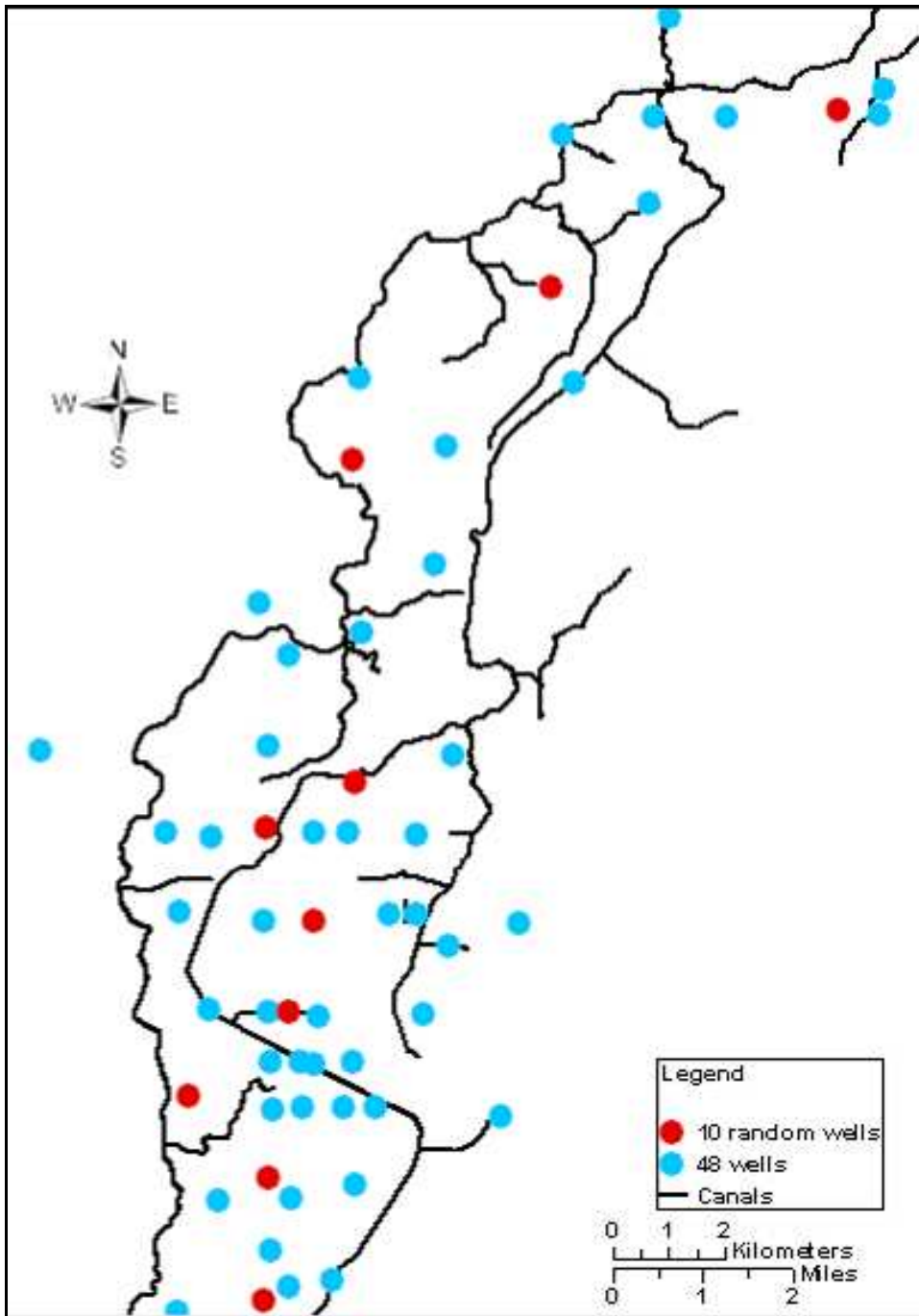


Figure 32. Map showing relation of randomly selected wells to other wells.

As before, the raster cell means and standard deviations were used to map significant water level differences between kriged water levels for the subset and for the entire data set (Sec. 3.2.2), at the ten well locations.

The purpose was to test the sensitivity of kriging predictions with more or fewer

well locations. That is, if similar significant differences were still observed using 48 versus 58 wells, the implication would be that a smaller well data set would be adequate for future seepage index calculations. Alternatively, the conclusion would be that the size and/or spatial arrangement of the existing well data set was inadequate for accurate kriging and seepage index estimation. Results are discussed in Chapter 4.

Chapter 4 RESULTS AND DISCUSSION

4.1. Horizontal Hydraulic Gradient Calculations at Canal Reaches

Some negative horizontal hydraulic gradients for May were excluded from the seepage analysis in a few short reaches of the canal system, because the interpolated ground water level was above the canal. This situation is likely to occur where well data are unavailable in areas of a large elevation change in the canal system, and kriging happens to overestimate the local ground water elevation.

Figure 33 and 34 show that the horizontal hydraulic gradients estimated from the kriged water levels for May are negatively skewed with some segmentation.

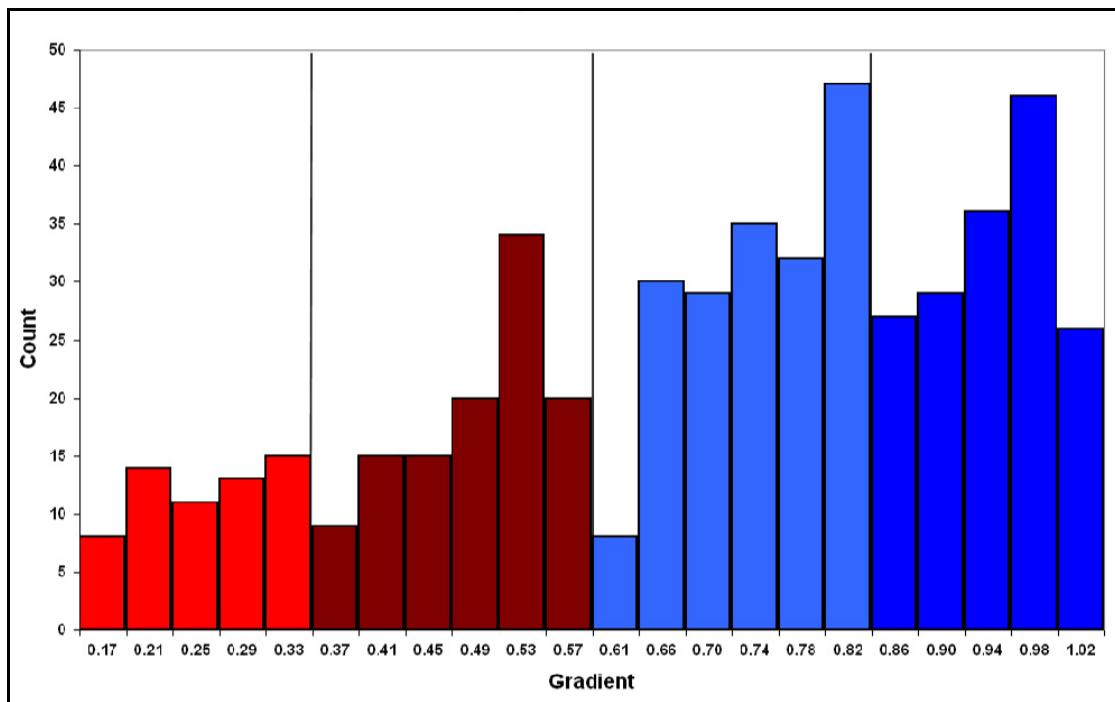


Figure 33. Frequency distribution of estimated horizontal hydraulic gradients for May.

The right and left halves of the gradient distribution in Figure 33 correspond to the reaches of the upper canal line (main) and the lower (lowline) portions of the canal system (Figure 34), with the main canal line having the higher gradient values.

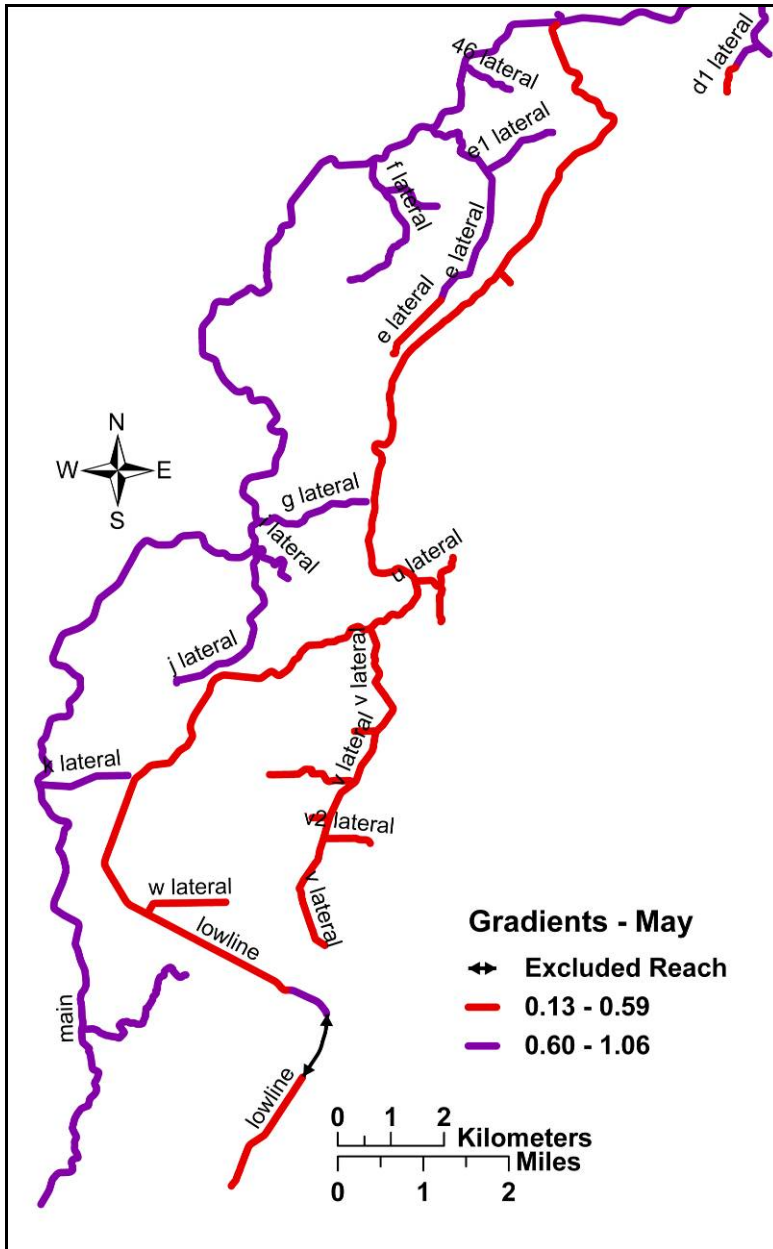


Figure 34. Canal reaches associated with the highest and lowest estimated horizontal hydraulic gradients during May. Color coding corresponds to Figure 33: main canal line in blue, and lowline canal in red. Reaches associated with insignificant differences in ground water levels over the irrigation season were excluded from subsequent consideration.

Further segmentation of the lowest and highest gradients in Figure 33 corresponds to differences between the main canal and its laterals, and between the upper and lower parts of the lowline and highline systems (Figure 35).

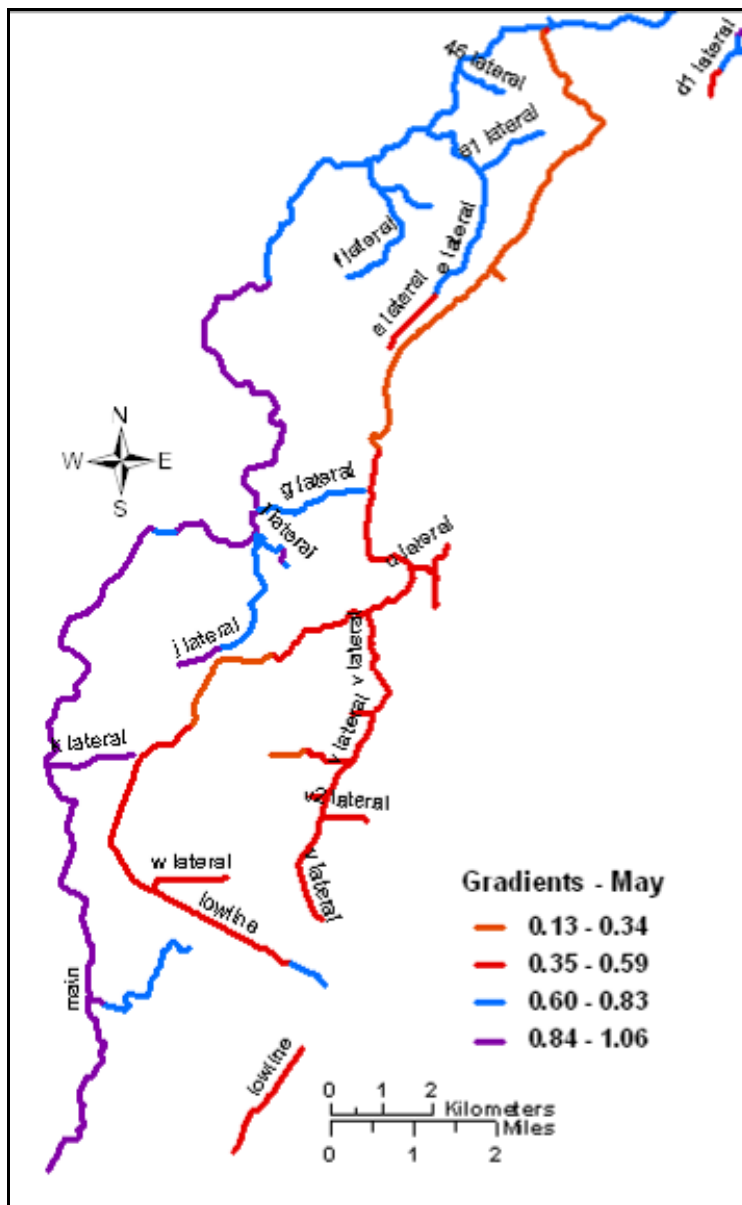


Figure 35. Spatial distribution of estimated horizontal hydraulic gradients beneath the canal system during May. Color coding corresponds to Figure 33: lower main line, dark blue, upper main line and laterals, light blue, lower lowline and laterals, dark red, upper lowline, light red.

The horizontal hydraulic gradients for August (Figure 36) also show a multi-modal

distribution that reflects segregation between the main and lowline parts of the system (Figure 37).

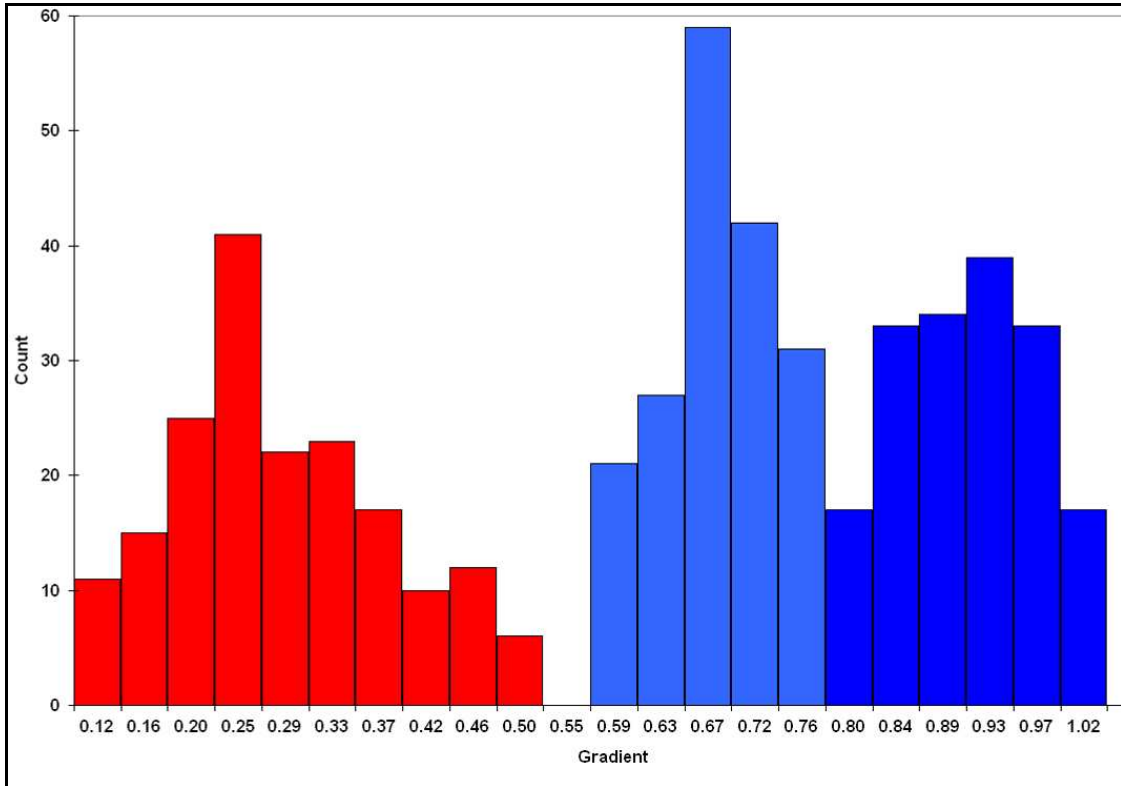


Figure 36. Frequency distribution of horizontal hydraulic gradients for August. Color coding corresponds to Figure 33.

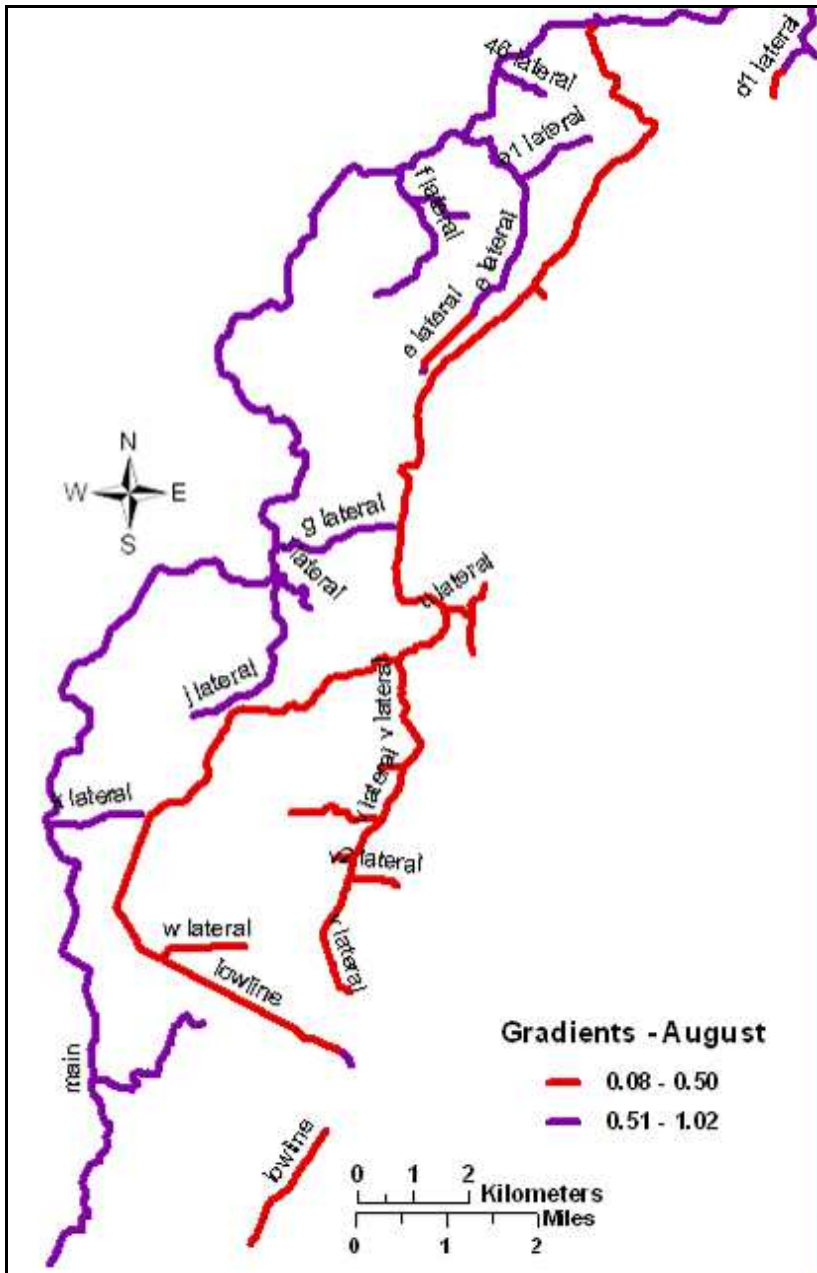


Figure 37. Spatial distribution of horizontal hydraulic gradients estimated along the canal reaches in the study area during August. Color coding corresponds to Figure 36: main line, blue; lowline, red.

The trimodal distribution (Figure 38) indicates less gradient segregation in August between the lowline and its laterals, compared with May (Figure 35).

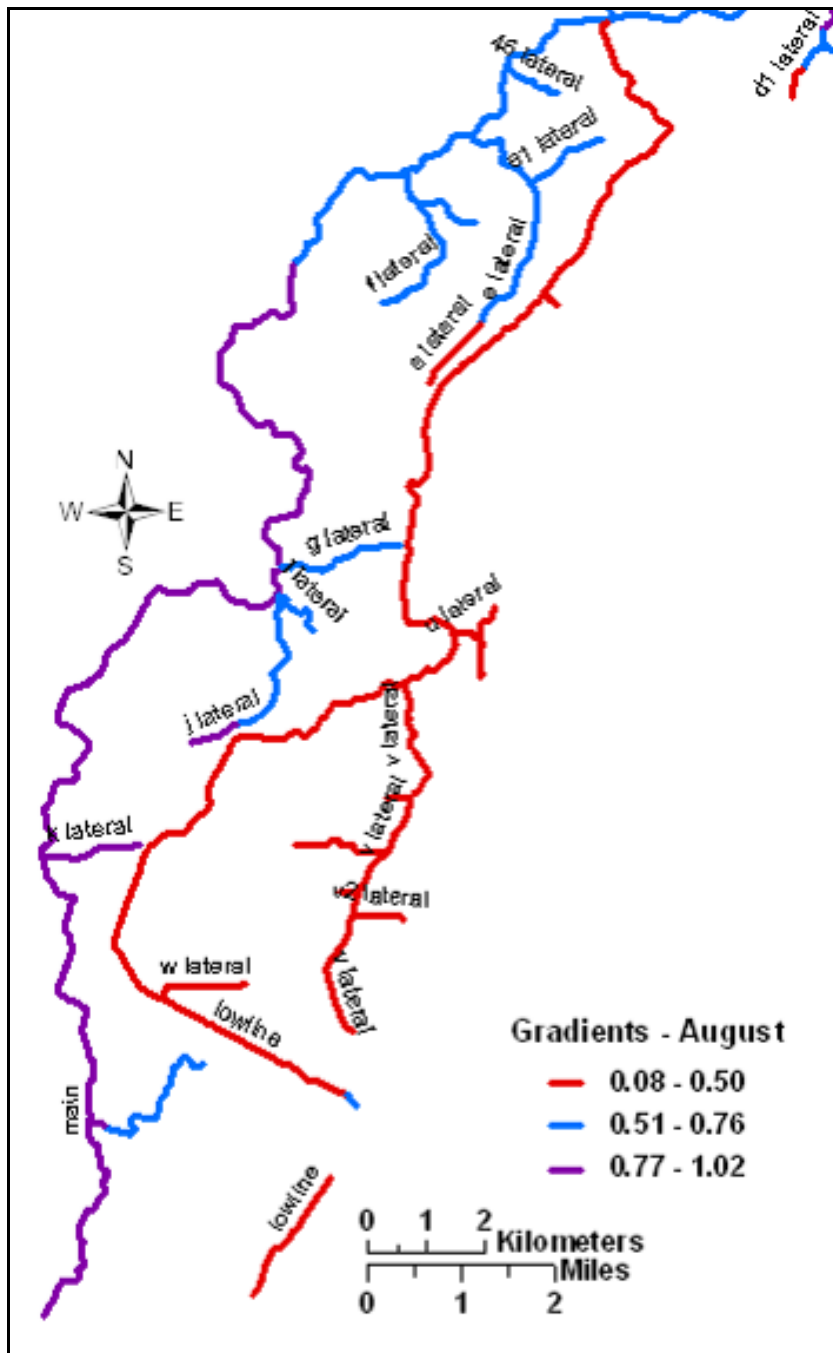


Figure 38. Spatial distribution of horizontal hydraulic gradients estimated along the canal reaches in the study area during August. Color coding corresponds to Figure 36: lower main line, dark blue; upper main line and laterals, light blue; lowline, dark red.

The rate of change of gradient from May to August shows a positively skewed,

possibly lognormal distribution (Figure 39).

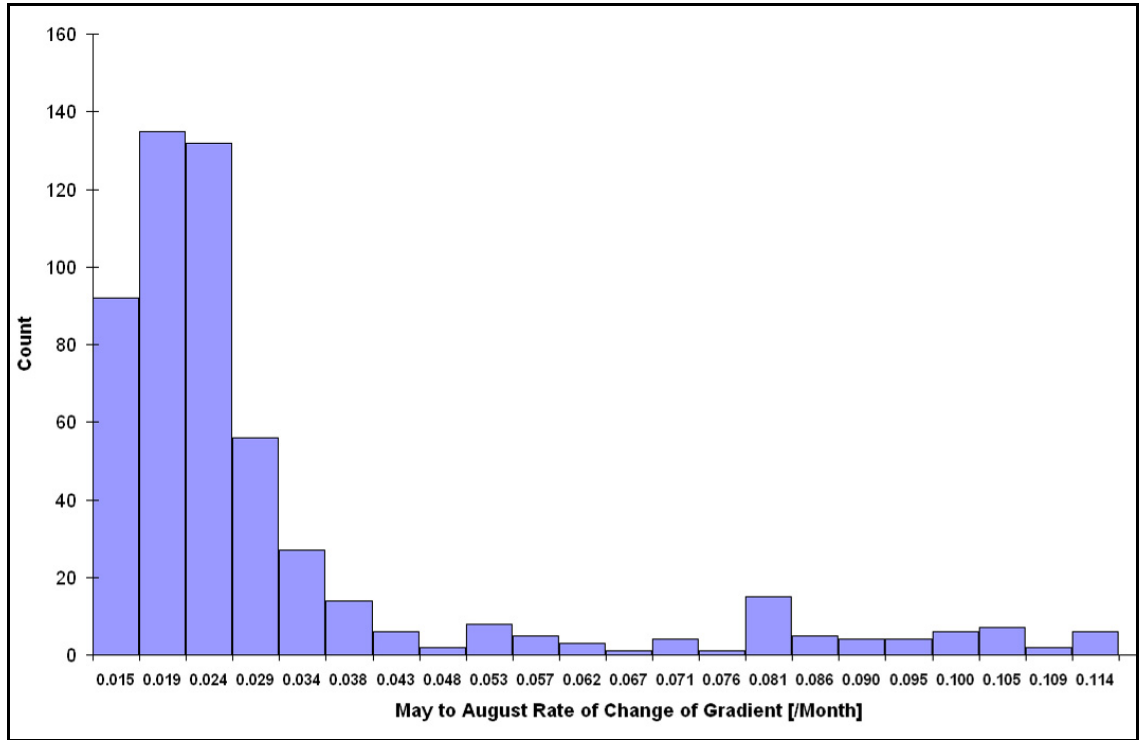


Figure 39. Frequency distribution of rate of change of gradient, May to August.

A lognormal distribution is commonly the result of a variable being the product of a large number of independent, identically-distributed variables (Limpert et al., 2001). Such distributions are generated by many small random effects that are additive for the normal distribution and multiplicative for the log-normal. For example, a lognormal distribution is typical of saturated hydraulic conductivity (Mesquita et al., 2002). As indicated by Darcy's law, the seepage rate is directly proportional to hydraulic conductivity. Since the rate of change of gradient has a similar lognormal distribution to saturated hydraulic conductivity, it seems that this factor, too, has the potential of being a good indicator of differences in seepage. Figure 40 shows the rate of change in ground water gradients from May to August.

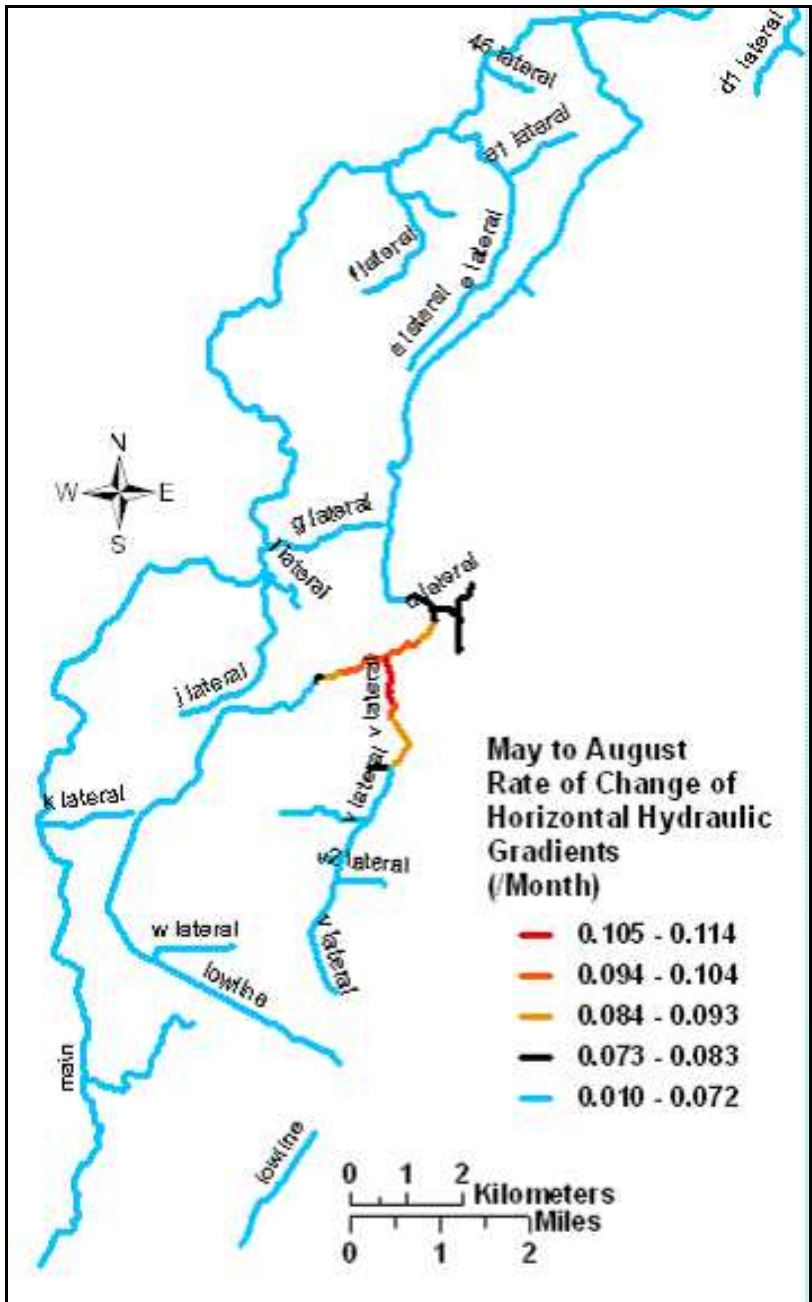


Figure 40. Rate of change of gradient.

Figure 41, which shows the frequency distribution of the change in ground water elevation from May to August, has the same shape as the rate of change of gradient.

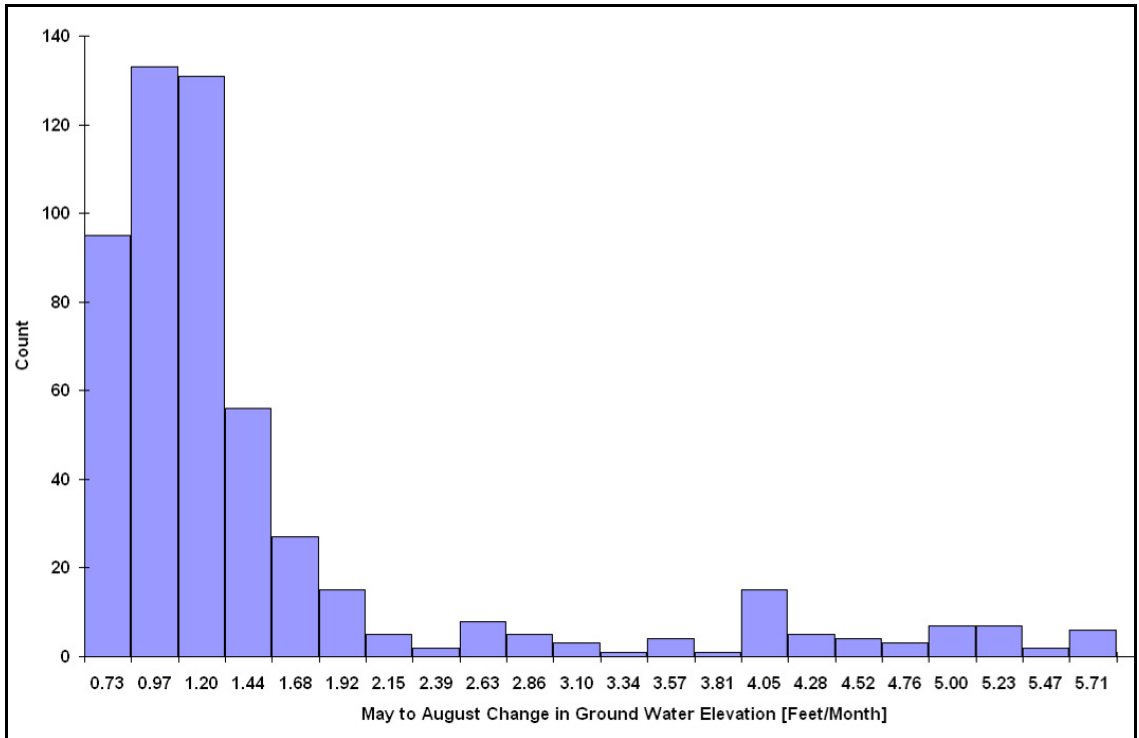


Figure 41. Frequency distribution of change in ground water elevation, May to August.

Since the change in ground water elevation seems to reflect canal seepage, and has a similar distribution to saturated hydraulic conductivity, it seems that this factor also has the potential of being a good indicator of differences in seepage. Figure 42 shows canal reaches associated with the largest changes in ground water elevations from May to August.

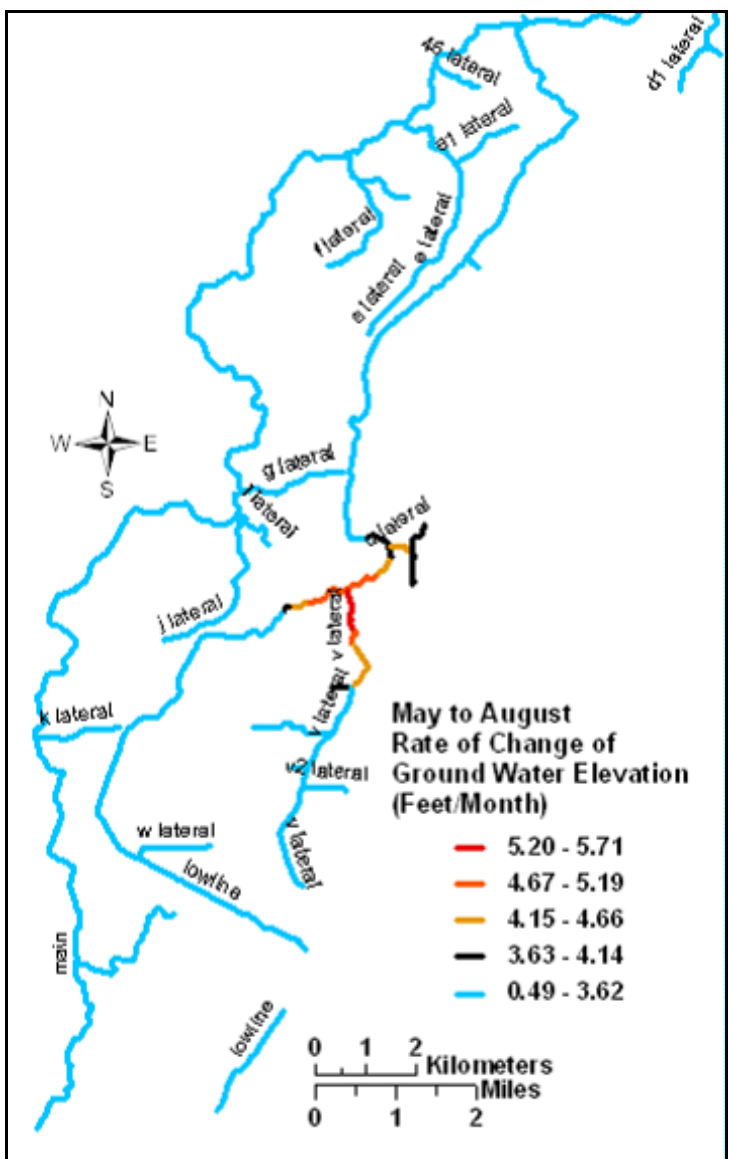


Figure 42. Canal reaches associated with the highest rates of change of ground water elevation.

In comparison, Figure 43 shows canal reaches associated with the largest values of the inverse of the May gradient (that is, areas of highest K) whose locations are considerably different than those indicated by either the rate of change of gradient or rate of change of ground water elevation, which show similar areas of high conductivity (seepage). These will be discussed in subsequent sections.

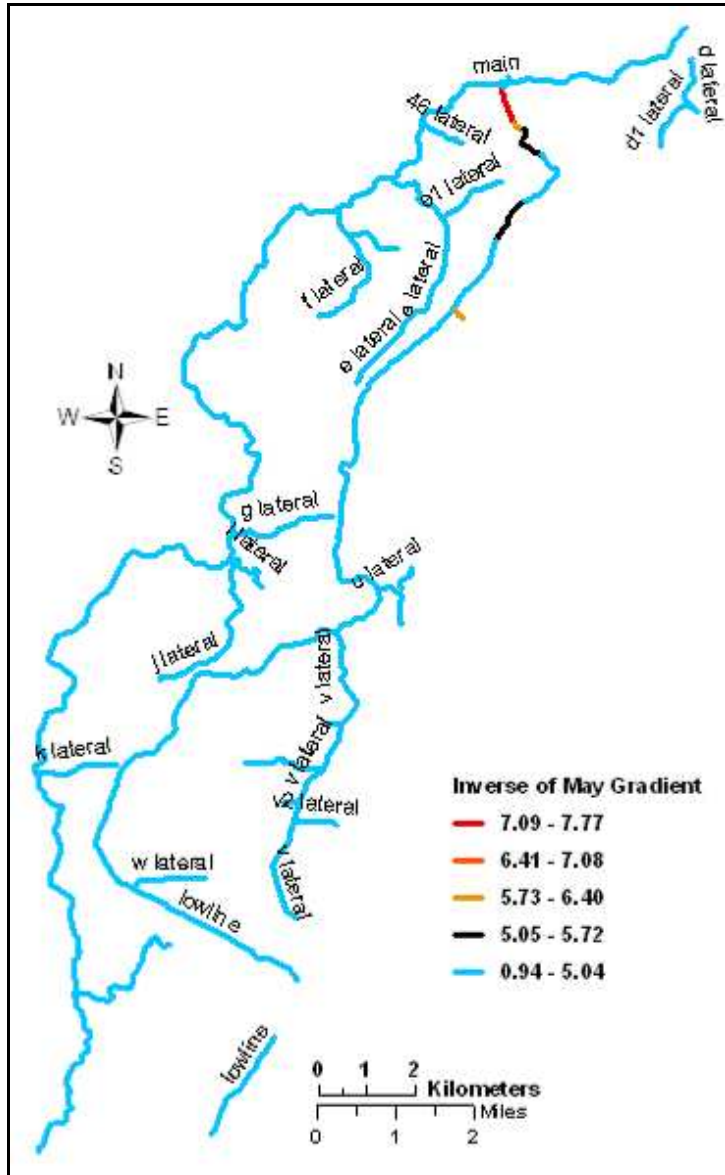


Figure 43. Canal reaches associated with the largest values of the inverse of May gradient.

4.2. Calculating a Relative Seepage Index

Recall from section 3.2.3 that a, b, c are the weights for the inverse of the May gradient, rate of change of gradient, and the change in ground water elevation, respectively.

The results of the relative seepage index calculations are:

By length of canal reach: $a_L = 1.8865$, $b_L = 0.0274$, $c_L = 1.3679$

By area of canal reach: $a_A = 1.9000$, $b_A = 0.0255$, $c_A = 1.2767$

And the final seepage index, weighted by length of canal segment, is:

$$X_{seep}^L = 1.8865 * 1/I_{Maytr} + 0.0274 * \Delta I/\Delta t_{MayAugtr} + 1.3679 * \Delta h/\Delta t_{AugMaytr}$$

And weighted by area:

$X_{seep}^A = 1.9000 * 1/I_{Maytr} + 0.0255 * \Delta I/\Delta t_{MayAugtr} + 1.2767 * \Delta h/\Delta t_{AugMaytr}$, where the suffix “tr” indicates the factors are normalized

Note that the weights for the gradient and change in ground water elevation (a, c) are substantially larger than that for the change in gradient (b). This indicates either that the change in gradient may not be as sensitive an indicator of relative seepage, or that changes in gradient should be calculated (Sec. 3.2.3) more frequently (e.g. weekly) or at a different time (e.g. two or three weeks after the start of canal flow).

4.3. Mapping Relative Seepage Loss

Figure 44 shows relative seepage index rankings based on area and length of canal reach, and Figures 45 and 46 show more detail in areas of highest seepage index.

For management purposes the size of defined interval of classification can be varied depending on the detail required for specific projects. The overall ranking shows that the greatest seepage occurs in the lowline portion of the canal system where it branches from

the main canal, and the next greatest seepage largely in the vicinity of the most statistically significant changes in seasonal water table elevations.

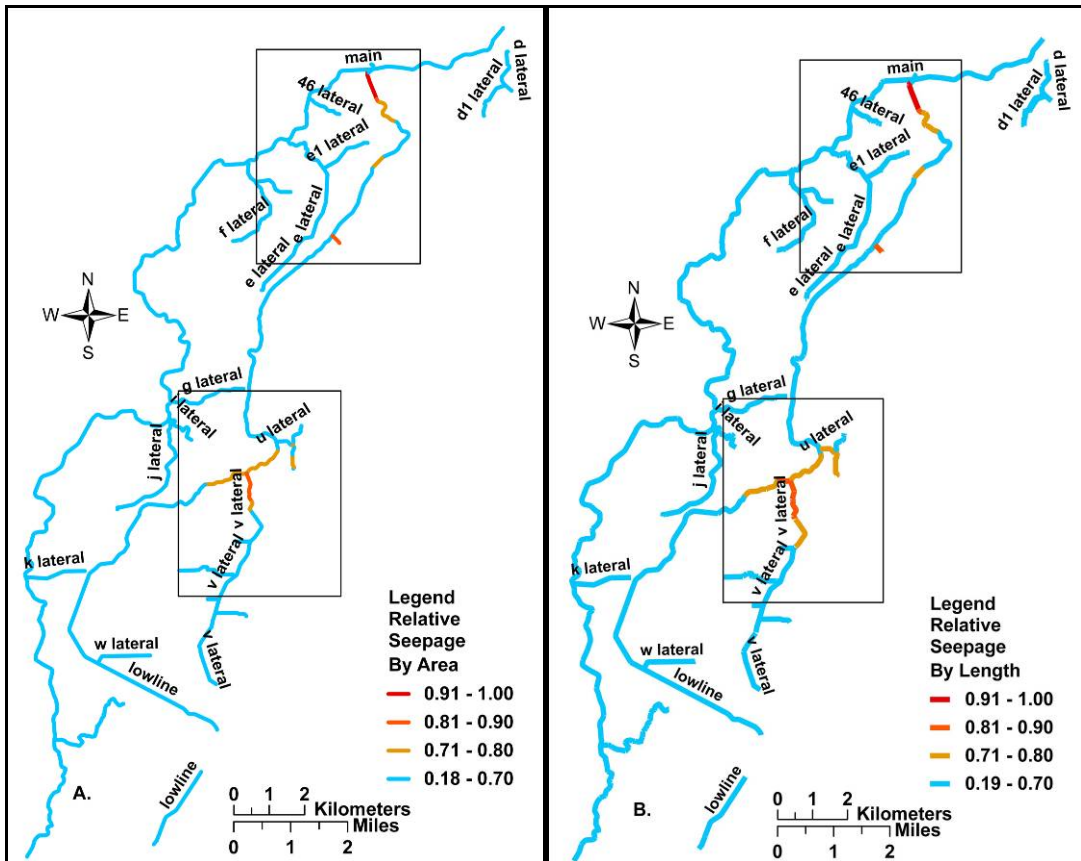


Figure 44. Spatial distribution of relative seepage in the canal system by area (A) and length (B) of the canal reaches. Details in the inset rectangles are shown in Figure 45 and 46.

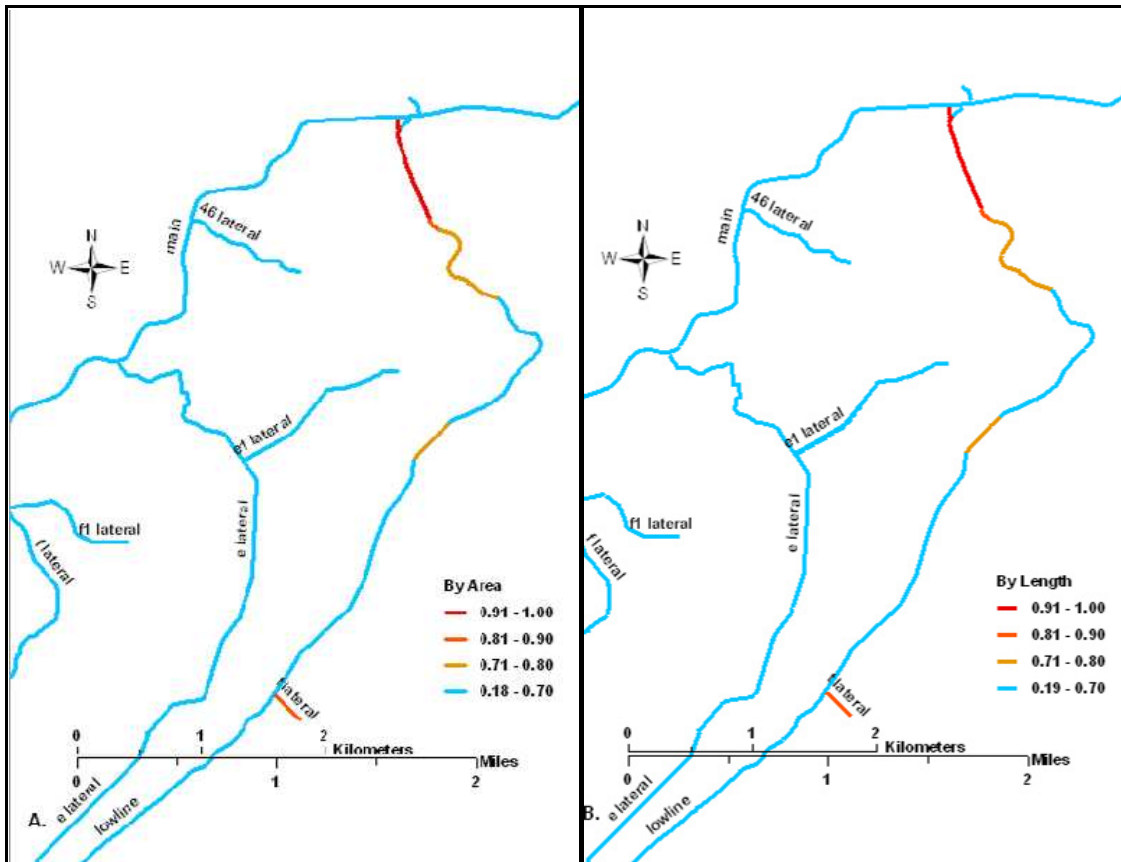


Figure 45. Upper lowline canal showing relative seepage ranking by area (A) and length (B) of canal reaches.

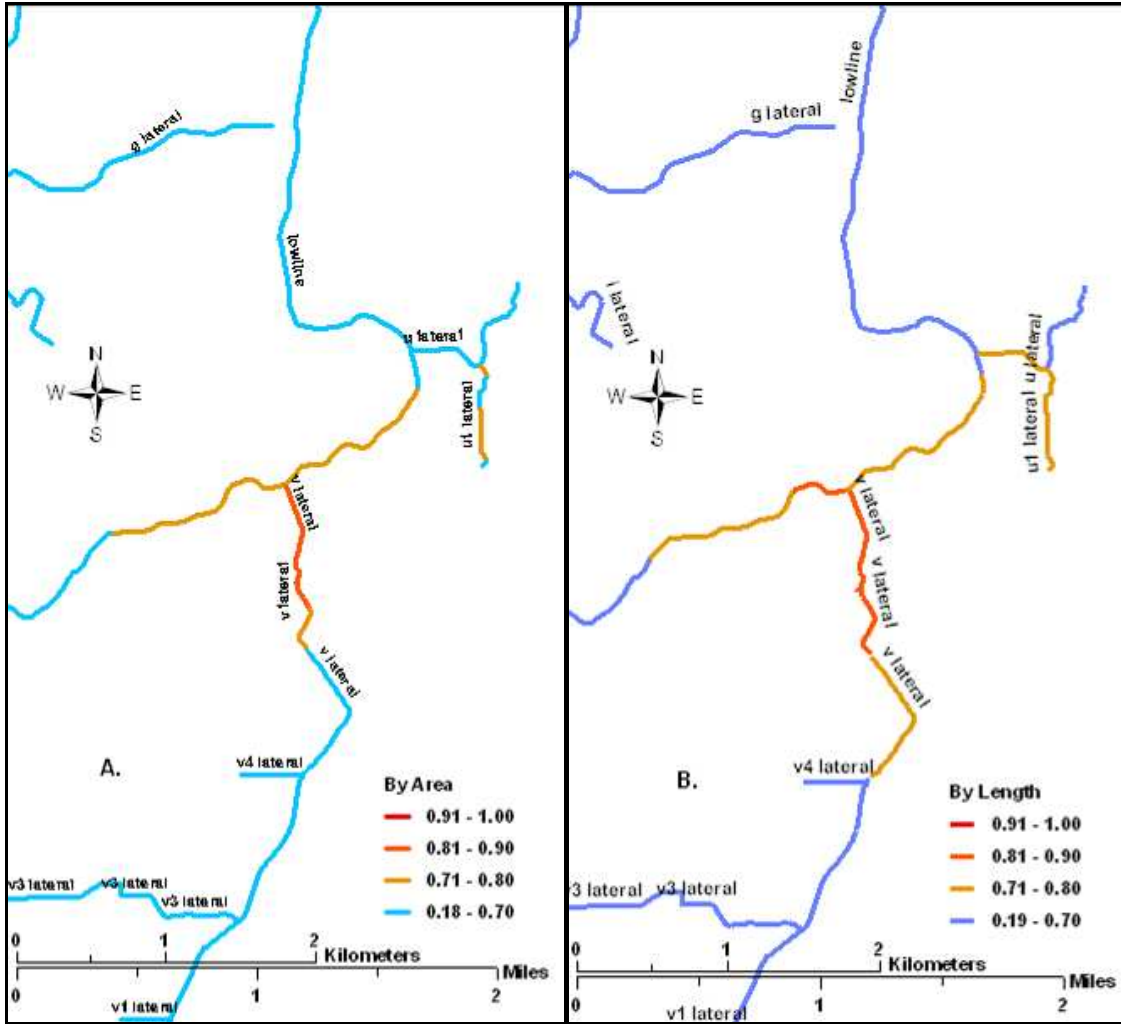


Figure 46. Middle lowline canal relative seepage ranking by area (A) and length (B) of canal reaches.

Since Darcy flow is proportional to area (Equation 1, Section 2.1.2), the ranking based on areas of canals of varying widths may be more representative of relative seepage, although the ranking based on length seems to provide a good approximation in this canal system. The reaches with the forty percent highest relative hydraulic conductivity as indicated by the inverse of May gradient (Figure 43) are quite different than the areas having the forty percent highest seepage as indicated by the rate of change of gradient (Figure 40), or rate of change of ground water elevation (Figure 42). It is note-worthy that the combined relative seepage index revealed within its top twenty

percent the canal reaches having the ten percent highest seepage based on the individual factors, (Figure 44, 45, 46).

4.4. Model Adaptability and Applicability

The results of the sensitivity analysis of kriged water levels described in Section 3.2.5 are summarized in Figure 47.

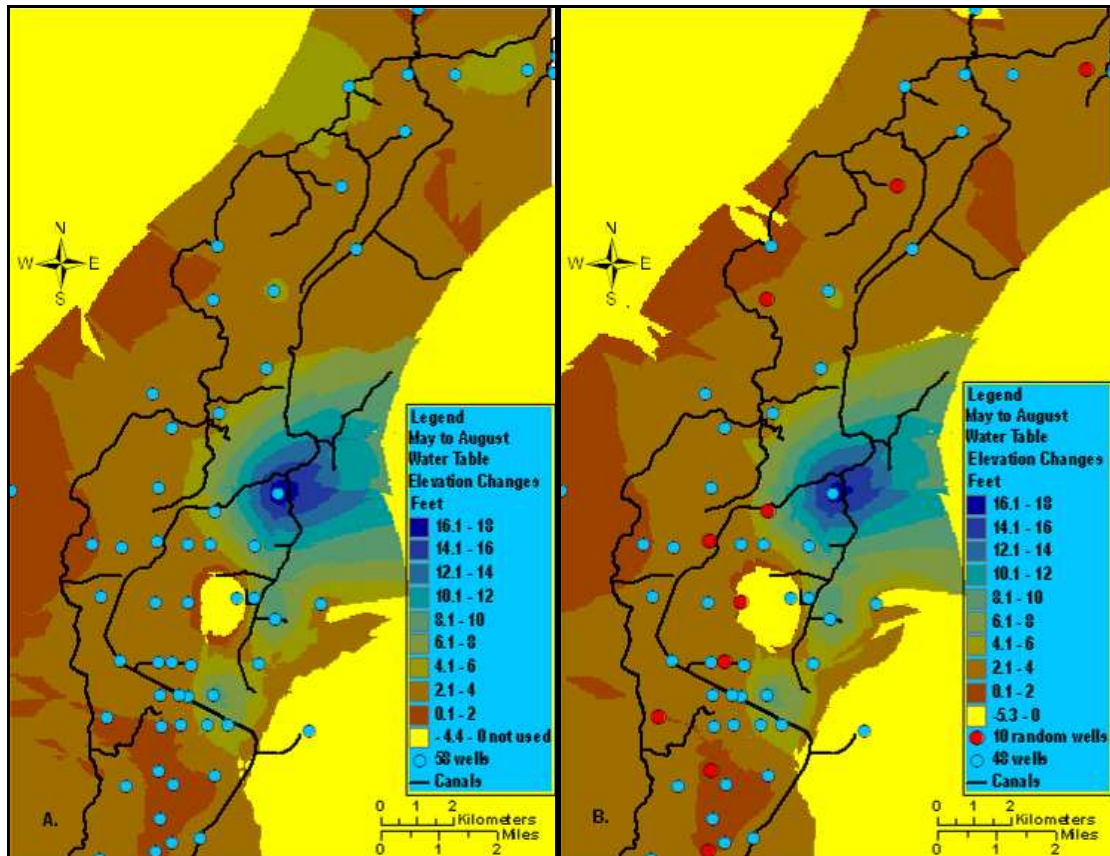


Figure 47. Maps of significant changes in water table elevation between May and August. (A) with all fifty eight wells; and (B) without ten randomly selected wells. Yellow areas are not significantly different at the 90% confidence level.

This analysis shows that the area of significant differences decreased slightly with fewer wells, but the changes in the vicinity of the excluded wells remained statistically significant. The basic behavior of the model was unchanged, implying that fewer wells could be used for future seepage modeling in this canal system.

4.5. Relationship of Relative Seepage Ranking and Soil Permeability

Yearly canal maintenance often involves the re-digging of portions of canal reaches, a process that inevitably disrupts the canal's soil lining. This layer is reformed to some extent by material deposited after the canal refills. If this layer remains as permeable as the underlying soil in which the canal was constructed, it might be expected that canal seepage would be higher under reaches that are underlain by higher permeability soils. The SSURGO soil data were used to map ordinal permeability variations under the canal system to examine the relationship between the estimated relative seepage index and soil permeability (Figure 48). The predominant permeability near the canals is 0.20 - 0.59 inches/hour (1.02 - 3.0 mm/min) with substantial areas of 0.6 - 1.99 inches/hour (3.05 - 10.11 mm/min). Whether there is a correlation or not, such a comparison can provide insights that may be useful in future management decisions.

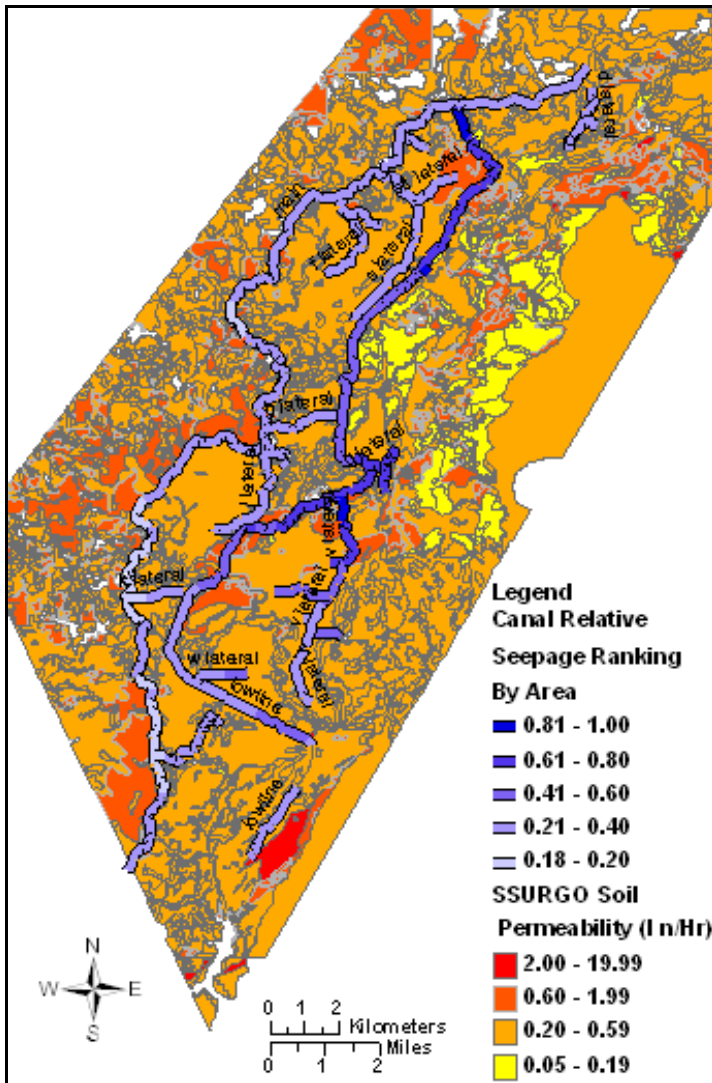


Figure 48. Geographic relationship of canal seepage ranking to soil permeability.

Figure 49 shows the correlation results of relative seepage index and SSURGO permeability of the soil underlying each canal segment. The non-parametric Spearman rank correlation coefficient (corrected for ties in the ranking) was used because the soil permeability data were not normally distributed. The correlation coefficient is much smaller than the critical value so the null hypothesis that there is no correlation cannot be rejected. So the calculated relative seepage index does increase along canal reaches where the soil permeability increases, as might be expected. This may be due to

SSURGO's coarse permeability classification or to the fact that in some situations the land level along the canal path had to be built up or lowered for continuous flow of canal water, and soil other than the local soil was used. Here, the soil permeability can not be used to predict the relative seepage of the canal reaches.

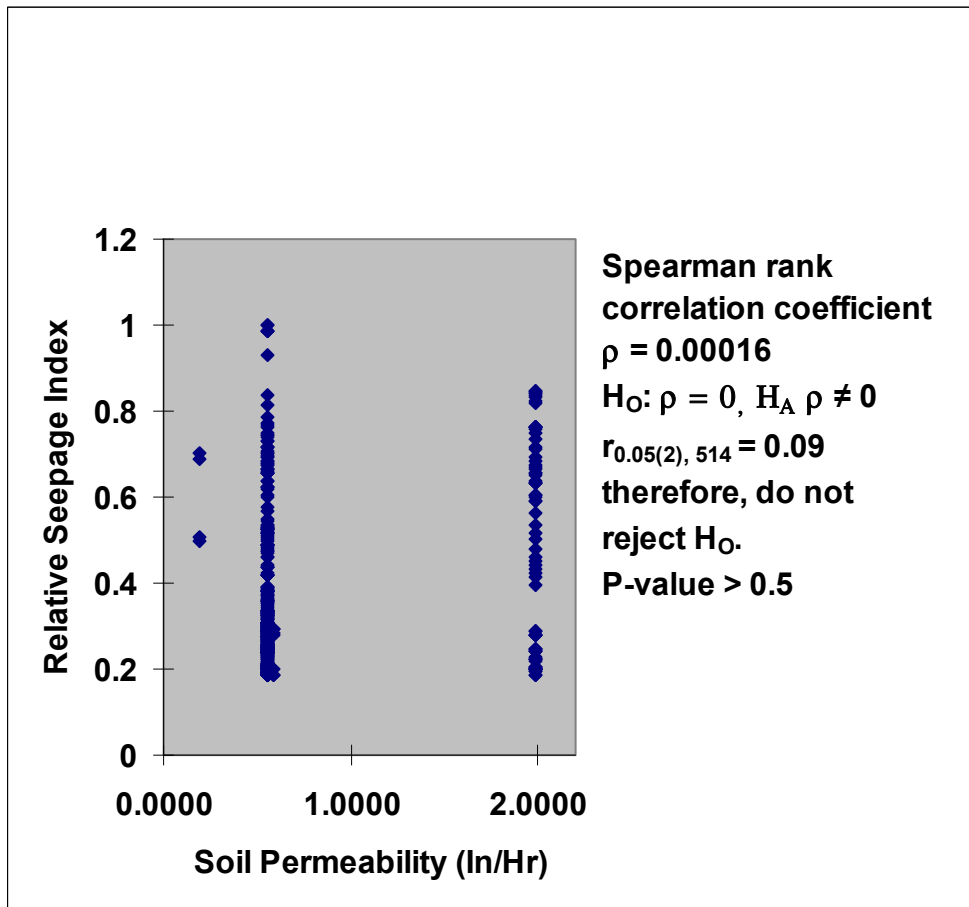


Figure 49. Rank correlation of relative seepage index versus soil permeability. The null hypothesis of no correlation can not be rejected.

Regardless of the form of the relationship, the comparison has implications relevant to management issues, for example, the impact of seepage over less permeable soils (implications for ponding, runoff control). Conversely, the implications would be different for issues related to recharge of the aquifer or return flow to the reservoir.

Chapter 5 CONCLUSIONS and RECOMMENDATIONS

This study focused on the issue of seepage losses from unlined earthen canals. This chapter provides a summary of the results, problems, knowledge gained and recommendations.

Summary

GIS techniques provide valuable means for investigating and analyzing complex real world problems. The technique developed in this study for ranking relative seepage has been shown to be practically feasible and could be refined with additional factors.

Historic seasonal well water elevation responses were compared with canal water elevation levels to estimate horizontal hydraulic gradients in the vicinity of a local canal system. These gradients, their seasonal rates of change and the well water elevation change over the irrigation season were modeled as a relative seepage index for the purpose of quantifying relative seepage loss along the canal system, by using Darcy's law and a simplified local water balance approach.

Such an approach can:

- a. Provide management with cost-saving insight into canal performance;
- b. Identify relative seepage losses in the canal system;
- c. Indicate where more data (ground water levels, well locations) are needed;
- d. Monitor changes in system behavior due to alterations or maintenance;
- e. Be incorporated into hydrological models of the regional aquifer.

Other key findings of this study were:

1. Seasonal responses of well water elevations to canal seepage show regular and repeatable trends.

2. At the scale of this study, the precision provided by the GPS locations gave more confidence in the model that was developed, but was probably more precise than necessary.

3. The assumption of canal water levels being the same between two check structures proved to be reasonable. More precise measurements could be obtained with intermediate GPS elevation measurements between check locations and by using more advanced GPS software and additional base stations.

4. An average annual response hydrograph was developed for each well to standardize the interpolation of historic water levels for further analysis and modeling.

5. A seepage index was calculated from the sum of three weighted factors determined along the entire length of the canal system: the inverse of the May gradient, the rate of change of gradient from May to August, and the change in ground water elevation from May to August.

6. Relative seepage is greatest at the upper and middle reaches of the lowline portion of the canal system.

A question to be considered is whether a single factor like water table rise would be more economical, easier to monitor and manage, and be as effective as a relative seepage index (Gill, 1984). Two of the three factors used in this study identified high seepage in the same general areas (Figure 40, 42, 43). It is possible that these two factors may be influenced similarly by internal errors that tend to cancel over the irrigation season and that do not similarly influence the determination of relative seepage based on the inverse of the hydraulic gradient at the beginning of the season. Regardless, the combined index identified all the canal reaches that were identified with the individual factors (Figure 44,

45, 46). This suggests that the seepage ranking index based on the combined factors is a better index than one based on an individual factor.

7. A sensitivity analysis performed by withholding ten random wells showed that ground water elevations could be adequately modeled with fewer wells. Similar methods could be used to determine the minimum number of required wells and/or their optimal spatial arrangement.

Recommendations

1. More frequent and uniform geographic coverage of well water-level monitoring would improve the precision of the relative seepage predictions.

2. Although the number of wells was shown to be adequate for this study, a different arrangement of locations might optimize kriging performance.

3. The calculations were based on two selected time periods but could be refined with more, shorter time periods.

4. Very early season gradients could not be reliably estimated because of the lack of canal water level data (e.g., dates of diversion of water into the canal system and the length of time needed to bring water up to normal operating levels in the canals). Because of the stepwise manner in which the checked water levels are gradually built up, the very early season canal water levels could not be estimated. The use of gradients calculated later in May or gradient changes calculated over shorter time periods should be investigated to determine if the seepage index can be refined.

5. The technique would benefit from uniform spatial and temporal data collection in wells (e.g., having wells in the vicinity of large changes in canal elevation, and ensuring that wells have measurements at all time periods).

6. It is recommended that water-level monitoring be more comprehensive, multi-purpose, and that data collection involves cost sharing. This could be achieved by installing transducer arrays and/or monitoring more wells monitored. An updated seepage model could then be tested and further refined to better manage the canal system as well as local ground water resources.

7. All monitoring wells should have their depths measured and the analysis should be restricted to only shallow wells.

8. The seepage index methodology could be incorporated in the numerical model(s) used to manage the ESRP aquifer.

LITERATURE CITED

- Agricultural Water Management Council. 2009. Monitoring and Verification. Canal Seepage. www.agwatercouncil.org/images/stories/monitoring_and_verification_canal_seepage.pdf. Last accessed 2.17.2009.
- Atmapoojya, S. L., and R. N. Ingle, 2001. Design of minimum seepage loss canal sections. *Journal of Irrigation and Drainage Engineering*, v. 127, p. 189-191.
- Badlands Journal Administrator's blog. 2005. Border canal seepage. November 18th. www.badlandsjournal.com/2005-11-18/009, p. 1-542. Last consulted 2.13.2009.
- Barnett, J. A., and D. A. Barnett. 2000. Report on the Recovery of Aberdeen-Springfield Project Water by Wells. Prepared for Aberdeen-Springfield Canal Company. Barnett Intermountain Water Consulting, Bountiful, Utah, 45p.
- Brown, G. 2009. Basics and More: Henry Darcy and His Law. Biosystems and Agricultural Engineering Oklahoma State University. <http://biosystems.okstate.edu/Darcy/LaLoi/basics.htm>. Last accessed 4.26.2009.
- Cassel, S. F., and J. R. Tischer. 2005. Development of a standardized procedure for rapid identification and quantification of canal seepage. A Research Proposal submitted to California Department of Water Resources, California Bay-Delta Water Use Efficiency Program, Section B. www.owue.water.ca.gov/docs/2004Apps/2004-056.pdf, p. 1-23. Last consulted 2.13.2009.
- Chowdary, V.M., N. H. Rao, and P.B.S. Sarma. 2003. GIS-based decision support system for groundwater assessment in large irrigation project areas. *Agricultural Water Management*, v. 62, p. 229-252.
- Contor, B. A. 2004. Irrigation Conveyance Loss. Idaho Water Resource Research Institute Technical Report 04-008, p. 1-12.
- Dawoud, M.A., M. M. Darwish, and M. M. El-Kady. 2005. GIS-Based Groundwater Management Model for Western Nile Delta. *Water Resources Management*, v. 19, p. 585-604.
- Einsiedl, F. 2005. Flow system dynamics and water storage of a fissured-porous karst aquifer characterized by artificial and environmental tracers. *Journal of Hydrology*, v. 312, p. 312-321.
- Englebert, P. J., R. J. Hotchkiss, and W. E. Kelly. 1997. Integrated Remote Sensing and Geophysical Techniques for Locating Canal Seepage in Nebraska. *J. Applied Geophysics*, v. 38. p. 143-154.
- Ersahin, S. 2003. Comparing Ordinary Kriging and Cokriging to Estimate Infiltration Rate. *Soil Sci. Soc. Am. J.*, v. 67, p. 1848-1855.

- Fortes, P.S., A.E. Platonov, and L.S. Pereira. 2005. GISAREG-A GIS based irrigation scheduling simulation model to support improved water use. *Agricultural Water Management*, v. 77, p. 159-179.
- Gill, M.A. 1984. Water-table rise due to infiltration from canals. *Journal of Hydrology*, v.70, p. 337-352.
- Haga, H., Y. Matsumoto, J. Matsutani, M. Fujita, K. Nishida, and Y. Sakamoto. 2005. Flow paths, rainfall properties, and antecedent soil moisture controlling lags to peak discharge in a granitic unchanneled catchment. *Water Resources Research*. v.41, p. W12410.1-W12410.14.
- Hersch, R.W., and R.W. Fairbridge (eds.), 1998. *Encyclopedia of Hydrology and Water Resources*, p. 777-778. Kluwer Academic, Dordrecht, The Netherlands.
- Hess, T., and C. Counsell, 2000. A water balance simulation model for teaching and learning – WaSim. Paper presented at the ICID British Section Irrigation and Drainage Research Day, 29 March 2000. HR Wallingford, Cranfield University, UK, p. 1-7. <https://dspace.lib.cranfield.ac.uk/bitstream/1826/2455/1/A%20water%20balance%20simulation%20model%20for%20teaching%20and%20learning.pdf>. Last consulted 2.13.2009.
- Holzbecher, E. 2005. Analytical solution for two-dimensional groundwater flow in presence of two isopotential lines. *Water Resources Research*. v.41, p. W12502.1-W12502.7.
- Hotchkiss, R.H., C.B. Wingert, and W.E. Kelly. 2001. Determining irrigation canal seepage with electrical resistivity. *Journal of Irrigation and Drainage Engineering*, v.127, p. 20-26.
- IDWR, hydro.online-gwl. 2009. Online ground water level database. <http://www.idwr.idaho.gov/hydro.online/gwl/default.html>. Last accessed 4.19.2009.
- Interagency Task Force on Irrigation Efficiencies. 1979. *Irrigation water use and management: an interagency task force report*. U.S. Dept. of the Interior. OCLC: 5745823, 133 p.
- Isaaks, H.E., and R.M. Srivastava. 1989. *An introduction to applied geostatistics*. Oxford Univ. Press, New York, 560 p.
- Kumar, C. P. (2004). "Groundwater Assessment Methodology". XXIII Annual Convention of AHI and National Seminar on Water Resources Management & People's Participation, 10-11 December 2004, Baroda. Electronic Proceedings (CD), p. 1-21. www.angelfire.com/nh/cpkumar/publication/Lgwa.pdf. Last accessed 2.17.2009.
- Leigh, E., and G. Fipps. 2003. Measured seepage losses of Canal 6.0 – La Feria Irrigation District, Cameron County No. 3, p.1-21. <http://idea.tamu.edu/documents/LaFeria%20Seepage.pdf>. Last accessed 2.17.2009.

- Limpert, E., W.A. Stahel, and M. Abbt. 2001. Log-normal distributions across the sciences: Keys and clues. *BioScience* v. 51, p. 341-352.
- Lin, G.F., and G.R. Chen. 2006. An improved neural network approach to the determination of aquifer parameters. *Journal of Hydrology*. v. 316, p. 281-289.
- Mesquita, M. G. B. F., S.O. Moraes, and J.E. Corrente. 2002. More adequate probability distributions to represent the saturated soil hydraulic conductivity. *Scientia Agricola*, v. 59, p. 789-793.
- Murray, J., A.T. O'Geen, and P.A. McDaniel. 2003. Development of a GIS database for ground-water recharge assessment of the Palouse Basin. *Soil Science*. v. 168, p. 759-768.
- Mustafa, S. 1987. Water table rise in a semi-confined aquifer due to surface infiltration and canal recharge. *Journal of Hydrology*. v. 95 p. 269-276.
- NAIP 2004. CCM County Selections. <http://inside.uidaho.edu/geodata/NAIP2004/NAIP2004CCMImageMap.htm>. Last accessed 4.19.2009.
- Pearce, F. 2006. When the rivers run dry: Water: the defining crisis of the twenty-first century. Beacon Press. Boston, MA.
- Rodgers, M., and J. Mulqueen. 2006. Field-saturated hydraulic conductivity of unsaturated soils from falling-head well tests. *Agricultural Water Management*. v. 79, p. 160-176.
- Shaffer, M. J. 1995. Fate and transport of nitrogen: what models can and cannot do. Working Paper No. 11 USDA, Agricultural Research Service, Great Plains Systems Research Unit, Fort Collins, Colorado. September. p. 1-9. www.nrcs.usda.gov/technical/NRI/pubs/wp11text.html. Last consulted 2.13.2009.
- Si, B.C., and R.G. Kachanoski. 2000. Estimating soil hydraulic properties during constant flux infiltration inverse procedures. *Soil Science Society of America Journal*. v.64, p. 439-449.
- Smith, R. P. 2004. Geologic Setting of the Snake River Plain Aquifer and Vadose Zone. *Vadose Zone Journal*, v.3, p.47-58.
- Sreekanth, S., S.O. Prasher, and C.C. Yang. 1997. Importance of choice of input parameters in artificial neural network simulation of water-table depths. *Canadian Water Resources Journal*, v.22, p. 19-31.
- Stergiou, C. and D. Siganos. 2007. Neural Networks, p. 1-18. http://www.doc.ic.ac.uk/~nd/surprise_96/journal/vol4/cs11/report.html. Last accessed 2.17.2009.
- Swamee, P.K., G.C. Mishra, and B.R. Chahar. 2000. Design of Minimum Seepage Loss Canal Sections. *Journal of Irrigation and Drainage Engineering*, v. 126, p.28-32.

Swihart, J. and J. Haynes. 2001. Cost-Benefit Analysis of Alternate Canal Linings. Water Operation and Maintenance Bulletin. No. 196, p. 1-12. www.usbr.gov/pps/WaterOandMBulletins/196jun2001.pdf. Last accessed 2.17.2009.

Swihart, J. and J. Haynes. 2002. Canal-Lining Demonstration Project Year 10 Final Report, 277 p. U.S. Department of the Interior, Bureau of Reclamation Pacific Northwest Region, Water Conservation Center, Technical Service Center, Civil Engineering Services, Materials Engineering Research Laboratory. www.usbr.gov/pn/programs/wat/pdf/finalcanal/ch1.pdf. Last accessed 2.17.2009.

Szilagyi, J. 2001. Modeled areal evaporation trends over the conterminous United States. *Journal of Irrigation and Drainage Engineering*, v. 127, p. 196-200.

Trimble, 2000. Mapping Systems General Reference, Part Number 24177-01, Revision C, Trimble Navigation Limited, Mapping & GIS Systems, p. 4-13 – 4-18.

van der Leeden, F., F.L. Troise, and D.K. Todd. 1990. *The Water Encyclopedia*. 2nd edition. Lewis Publishers, Chelsea, Michigan, 830 p.

Visser, A., R. Stuurman, and M.F.P. Bierkens. 2006. Real-time forecasting of water table depth and soil moisture profiles [electronic resource]. *Advances in Water Resources*, v. 29, p. 692-706.

Welhan, John. 2008. Sources of nitrate contamination in ground water of Pleasant Valley, Power County, Idaho. Final Report, DEQ Contract # C564, 66p.

Welhan, John. 2005. Statistical evaluation of kriging results. Class notes, Geostatistics, GEOL 606, Idaho State University, 21 p.

Xie, X., S. Norra, Z. Berner, and D. Stuben. 2005. A GIS-supported multivariate statistical analysis of relationships among stream water chemistry, geology and land use in Baden-Wurttemberg, Germany. *Water, Air, and Soil Pollution*. v. 167, p. 39-57.

Yang, C., S.O. Prasher, R. Lacroix, and A. Madani. 1997a. Application of artificial neural networks in subsurface drainage system design. *Canadian Water Resources Journal*, v. 22, p.1-12.

Yang, C., S.O. Prasher, R. Lacroix, S. Sreekanth, N. K. Patni, and L. Masse. 1997b. Artificial neural network model for subsurface-drained farmlands. *Journal of Irrigation and Drainage Engineering*, v. 123, p. 285-292.

APPENDIX A – Water Balance

1. Theory and Concepts of system water balance

The storage and movement of water is determined by the general hydrological cycle. In any local reservoir or system, the accounting of the inputs to, and outputs from, the reservoir is known as the system water balance. Kumar (2004) gives a theoretical overview of the factors to be considered as a water balance equation for a ground water reservoir (aquifer): $R_r + R_c + R_i + R_t + S_i + I_g = E_t + T_p + S_e + O_g + \Delta S$

where,

R_r = recharge from rainfall;

R_c = recharge from canal seepage;

R_i = recharge from field irrigation;

R_t = recharge from tanks;

S_i = influent seepage from rivers;

I_g = inflow from other basins;

E_t = evapotranspiration from groundwater;

T_p = pumping and other withdrawals;

S_e = effluent seepage from the aquifer to rivers;

O_g = subsurface outflow to other ground water basins; and

ΔS = change in groundwater storage.

As Kumar (2004) notes, “it is not always possible to compute all individual components of the water balance equation separately”. For example, the discrepancies in a water balance accounting can increase with increasing area, together with the corresponding difficulty in accurately computing the various water balance components.

In the study area the rainfall is generally negligible during the growing season, so recharge from rainfall was considered negligible. In the study area the recharge components from field irrigation and tanks are included with canal seepage. These were considered negligible as water for irrigation is usually intermittent and usually not much more than the crop needs with any excess running off in drainage. Influent seepage from rivers and other basins (as well as effluent seepage from the aquifer and subsurface outflow to other ground water basins) are considered negligible or masked as the water table data show the levels falling after the irrigation season ends and rising when it starts. Also the river and reservoir levels usually fall once the irrigation season has started. For some situations, the only feasible approach may be to consider combined or lumped water balance components rather than accounting for all individual components.

2. Evapotranspiration

Szilagy (2001) modeled long-term areal evapotranspiration (AE) using data from 210 stations of the Solar and Meteorological Surface Observation Network within the conterminous United States. Averaged over all stations, modeled AE has shown an overall increase of about 2–3% in the period 1961–1990, both on an annual basis and over the growing season (May–September). The rate of increase has differed among three geographic regions of the United States (eastern, central, and western), with the largest modeled increase in the east. In the western part of the continent, modeled AE remained constant. Of these trends, only the ones over the eastern part of the conterminous United States are statistically significant.

As Kumar (2004) notes, “it is not always possible to compute all individual

components of the water balance equation separately”. For example, the discrepancies in a water balance accounting can increase with increasing area, together with the corresponding difficulty in accurately computing the various water balance components. For some situations, the only feasible approach may be to consider combined or lumped water balance components rather than accounting for all individual components.

3. Seepage Losses.

Several means have been used to study canal seepage. Gill (1984) used water-table rise to estimate infiltration from canals and Mustafa (1987) examined the increase in hydraulic head in a semi-confined aquifer to estimate surface infiltration and canal recharge. Other researchers have looked at flow system dynamics and water storage (Einsiedl, 2005), rainfall, flow paths, and antecedent soil moisture conditions (Haga et al., 2005). The latter researchers found that hydrological properties in a catchment could be indexed by the lag time between peak rainfall and peak discharge. In an analogous way it was planned to index seepage by using lag times in well water elevation responses. They concluded that antecedent soil moisture, rainfall amount and intensity are necessary for understanding the regional characteristics of lag times and water percolation in granitic terrain. In the local situation there is an annual response in the water-table to the irrigation season and the average annual response hydrograph will be used to develop a seepage index for different reaches of the canal system.

APPENDIX B - Methods of Quantifying and Modeling Seepage

This appendix gives a survey of measurement methods developed, data analysis and evolving modeling techniques for seepage losses including artificial neural networks (ANNs).

Protocols have been developed for monitoring and verification of the estimated volume of water conserved by water use efficiency projects. These would be applicable to post-project assessments. Comprehensive quantification of the local water balance flow paths taking into consideration the spatial and temporal scales are prerequisites to successful projects (Agricultural Water Management Council, 2009). In reviewing the factors affecting seepage and methods of quantifying existing canal seepage, general and specific assumptions as well as measurement inaccuracies were considered. Infrared photography and inflow-outflow analysis has been used to identify potential high seepage sections of canals (Engelbert et al., 1997). They also compared several non-destructive testing methods to determine their applicability for pinpointing high seepage reaches. Electrical resistivity (ER) had the greatest potential (Engelbert et al., 1997).

1. Measurements

Various types of measurement have been used in the effort to monitor and manage seepage. Leigh and Fipps (2003) used the ponding method to measure seepage losses on canals with and without different lining materials. On the other hand, Rodgers and Mulqueen (2006) used falling-head well tests to obtain field-saturated hydraulic conductivity of unsaturated soils. Ersahin (2003) used double-ring infiltrometers until steady-state infiltration rates (IRs) were obtained. Si and Kachanoski (2000) note that estimation of soil hydraulic properties require accurate and cost-effective methods.

Previous measurements of a single hydraulic response did not necessarily result in unique and stable estimates of hydraulic parameters when there were more than two unknowns. Estimation is better performed when prior data on the parameters or additional measurements are available. However, accurate prior information is seldom available due to temporal and spatial variability of soil hydraulic properties. Procedures for quantifying seepage losses in unlined irrigation canals for reaches on the order of 100 ft. (30 m) were developed and tested by Hotchkiss et al. (2001). These are applicable to trapezoidal canal sections underlain by clay over a deeper layer of more permeable material. The ER of the underlying clay layer was measured while canals are in service. ER data were correlated to canal depth and seepage rate. The technique is suitable for estimates of seepage over short reaches in extensive conveyance systems. Similarly, use of electromagnetic inductance (EM) technology to identify locations of canal seepage and use of ponding tests to determine the rate of seepage at those locations was proposed by Cassel and Tischer (2005).

2. Data Analysis

Quantitative and qualitative assessment of spatial data variability in IR was done by Ersahin (2003) using semivariograms, kriging and cokriging. IR ranged from 1.92 to 8.88 cm h^{-1} , with a mean of 5.11 cm h^{-1} in field measurements. Significant correlation of subsoil bulk density and IR provided an auxiliary variable (for cokriging) to make estimations of IR values at unobserved sites, as discussed by Isaaks and Srivastava (1989). Ersahin (2003) found cokriging superior to kriging in estimating IR when available data was limited. The spatial information on **infiltration was used** for kriging, while the spatial information on **infiltration** along with spatial correlation between

infiltration and bulk density was used for cokriging.

3. Modeling

As research into systems develops, theories from portions of the system need to be integrated into workable models. Since these are simulations of the real world situation, the amount of detail would vary depending on the needs and objectives of their respective projects. Research situations involving integrated subsystems have not been adequately addressed studying isolated processes as in classical field research (Shaffer, 1995). Interpolation of field results, education as to how systems respond to environmental and managerial inputs, identification of knowledge gaps, long-term simulation studies and importance of parameters and state variables are potential benefits from modeling.

Valuable tools have been developed as models describing water infiltration and percolation through the soil. These analytical and numerical models for quantifying and integrating hydraulic processes in the unsaturated or saturated soil zone rely heavily on the quality of the model parameters (Si and Kachanoski, 2000). This is especially pertinent to the unsaturated hydraulic properties in application of these models to field-scale flow problems.

WaSim is an example of a teaching and learning water balance simulation model (Hess and Counsell, 2000). A more complex analytical solution for two-dimensional groundwater flow considering two isopotential lines is discussed by Holzbecher (2005). He examined the groundwater flow pattern in an idealized situation. He assumed that the aquifer is well connected to all surface water bodies and the flow field is constructed using superposition of analytical solutions and conformal mapping.

The literature has many analytic solutions to different boundary conditions for the problem of seepage from canals. Goyal, Rohit and Chawla (1997) present an analytic solution for seepage from a canal of variable width to symmetric drainages at variable distances. Such models provide an initial analysis and understanding, but get much more complex in the real life field situation. However, the water table and hydrogeologic environment interrelationship must be understood before designing a water-table management system (Yang et al., 1997b). They reviewed many conventional computer simulation models noting the large amount of input parameters and computational effort required. The great complexity of relationships between the numerous parameters involved in managing the water balance has stimulated a move toward models that do not require explicit relationships between inputs and outputs. ANNs are examples of such models.

4. Artificial Neural Networks

The various types of neural networks are explained and demonstrated with applications of neural networks and a detailed historical background (Stergiou and Siganos, 2007). The connection between the artificial and the real thing is also investigated and explained. Finally, the mathematical models involved are presented and demonstrated.

Training by field observations to map the implicit relationship between inputs and outputs, requiring fewer input parameters and quick execution on a microcomputer are advantages of ANNs (Yang et al., 1997a). Yang et al. (1997b) modeled the performance of a subsurface drainage system in Nova Scotia, Canada. An ANN model was built and trained by using measured data on midspan water-table depths and drain outflows from

an alfalfa field. Comparison of the ANN model results, the measured data, and the simulated results from a conventional mathematical model, DRAINMOD showed good simulation by the ANN model of midspan water-table fluctuations and drain outflows. The ANN model required significantly fewer inputs than DRAINMOD and ran significantly faster. Input data quality for both average and extreme conditions substantially affected the ANN simulations.

Thus, design and evaluation of subsurface drainage systems can be effectively done using an ANN model. Speed, accuracy, ease-of-use and flexibility are the advantages of ANNs. Lin and Chen (2006) discuss a method for improving an ANN approach that avoids inappropriate setting of a training range and requires less training time. On the other hand, ANN model performance excelled when the input variables mimicked the physical dependence of the output, as compared to other types of input variables, in simulations of water-table depths (Sreekanth et al., 1997).

APPENDIX C - Management of Seepage Loss

Sustainable management requires the control of losses. Major factors towards this end are discussed in this section as use of GIS, canal design optimization, maintenance and modernization and conveyance losses in the study area.

A substantial part of management is the capability of assessing future scenarios. With modern technology, this is fast moving from brainstormed “what if” scenarios to real-time interactive systems. Water table depth and soil moisture profile real-time forecasting is an example in this direction (Visser et al. 2006). Such systems become increasingly dependent on development of GIS based decision support systems.

1. Conveyance Losses in the Study Area

Canal maintenance programs largely eliminate most transpiration losses, in or near the large canals, but seepage losses can exceed 40% of diversion water, and in Idaho this loss is primarily associated with leakage to the aquifer (Contor, 2004). He accounts for canal leakage in a water budget by two approaches to the spatial distribution of losses. He uses the following equations: Field Delivery = Diversions – Canal Leakage – Return Flows

Net Recharge (surface water source) = (Field Delivery + Precipitation) – (ET x Adjustment Factor).

A simplified approach with assumption that all diverted water is applied to the intended place of use was proposed. Mixed model approaches are reviewed and conceptual treatment of leakage as a volume per time per length of canal, or as a depth per time applied to average wetted area is justified by factors (e.g. check structures) that produce an essentially constant water head. This approach is used in the Snake River

Basin Adjudication and in aquifer modeling. The paper illustrates the potential inaccuracy of treating leakage as a fixed rate per time and as a percentage of diversion volume with an example from Mexico.

2. Use of Geographic Information Science

As the intensity of competition for available water escalates, the need to develop sustainable management will increase the use of management scenarios evaluated on GIS-based models (Dawoud et al. 2005). When surface sources of water become marginalized by competition, the importance of the groundwater and its management increases as in the case of the Nile Delta and Valley (Dawoud et al. 2005). As they envisioned, situations like this stimulate the development of a comprehensive database that represents the characteristics of the aquifer system. This provides the foundation for efficient integrated and sustainable management of water resources by use of modeling tools to assess the impacts of decision alternatives.

Examples are use of selected soil characteristics to delineate and classify recharge mechanisms and classify recharge potentials. A database for mapping areas of relative recharge potential by indicators of deep percolation was obtained by linkage to Basin recharge mechanisms (Murray et al. 2003). Chowdary et al. (2003) also illustrate groundwater assessment in large irrigation project areas using a GIS-based decision support system, while Fortes et al. (2005) support improved water use by development of a GIS based irrigation scheduling simulation model (GISAREG). The necessity and capacity of being able to manage the complex interaction of factors due to geomorphic and anthropogenic influences is demonstrated by Xie et al. (2005). Stream water chemistry, geology and land use in Baden-Wurttemberg, Germany are analyzed with

their GIS-supported multivariate statistics.

3. Canal Design Optimization

According to Swamee et al. (2000), “The minimum area section is a thoroughly investigated problem in the hydraulics literature. However, because of the complexities of the analysis, the design of a minimum seepage loss section has not been attempted yet. In this investigation, using previously derived results, simplified algebraic equations for computation of seepage loss from triangular, rectangular, and trapezoidal canals have been presented, which replace accurately the cumbersome evaluation of complex integrals. Using these seepage loss equations and the general uniform flow equation, explicit equations for the design variables of minimum seepage loss canal sections have been obtained for each of the three canal shapes by applying nonlinear optimization technique. The optimal trapezoidal section has the least seepage loss and cross-sectional area among the three optimal sections. A step-by-step design procedure for rectangular and trapezoidal canal sections has been presented. The analysis also includes the sensitivity of the seepage loss to design variables around the optimum value”.

This stimulated substantial discussion by Atmapoojya and Ramesh (2001) and A. R. Kacimov (* same paper). The discussers congratulated the authors for adopting the concept of minimum seepage loss for optimum canal section design. They noted the use of equation (10) for calculation of resistance in uniform channel flow, which is applicable for partially as well as fully turbulent flows and hence can be considered more general in character. However, they point out that, Manning’s equation is more popular and generally adopted for design of canal section by practicing engineers. This is because the flow in canals is usually in the fully turbulent region and engineers are more

familiar with the values of Manning's coefficient of roughness n , due to its availability in literature for a wide range of lining materials.

Further, they noted the difficulty of estimating the value of e in situations where the canal lining is cracked or has uneven and irregular joints, because this type of information is not available in the literature. Therefore, the discussers suggested a simplified procedure for design of canal section following the authors' method and using Manning's equation (Atmapoojya and Ramesh 2001). Kacimov (* same paper) gave a five-point critique using a comprehensive literature review. Swamee et al. (* same paper) acknowledged the contributions and gave a five-point response in defense of their solutions for real situations.

In addition to the issues of canal design for minimum seepage, efficient water use depends on continued maintenance and modernization of the canal systems.

4. Canal Maintenance and Modernization

For sustainable systems in the context of increasing water demand, alternative canal-lining materials are continually being studied. These must be less expensive, easier to construct where access is limited, and compatible with severe rocky subgrades such as the fractured volcanic basalt typically found in the Pacific Northwest (Swihart, J. and J. Haynes. 2002).

On-going studies involving 11 irrigation districts (five irrigation districts on the Deschutes river in central Oregon, two in Idaho, three in Montana, and one in Oklahoma) have test sections ranging in age from 1 to 10 years. Combinations of geosynthetics, shotcrete, roller compacted concrete, grout mattresses, soil, elastomeric coatings, and sprayed-in-place foam are the lining materials being studied.

Cost-benefit ratios indicate that a geomembrane with a concrete cover would provide the best long-term performance (Swihart and Haynes, 2001).